

**The viability of poly(chlorotrifluoroethylene-*co*-  
vinylidene fluoride) as an oxidiser in extrudable  
pyrotechnic compositions**

By

**Andrew William Cowgill**

Dissertation submitted in partial fulfilment of the requirements for the degree of

**Master of Engineering  
(Chemical Engineering)**

In the Faculty of Engineering, Built Environment and Information Technology  
University of Pretoria

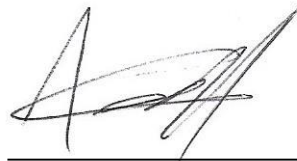
Pretoria

February 2017

## DECLARATION

I, **Andrew William Cowgill**, student No. **10280449**, do hereby declare that this research is my original work and that to the best of my knowledge and belief, it has not been previously in its entirety or in part been submitted and is not currently being submitted either in whole or in part at any university for a degree or diploma, and that all references are acknowledged.

**SIGNED** on this 27<sup>th</sup> day of February 2017.



---

**Andrew W. Cowgill**

# **The viability of poly(chlorotrifluoroethylene-co-vinylidene fluoride) as an oxidiser in extrudable pyrotechnic compositions**

Student: Andrew William Cowgill

Supervisor: Prof. Walter W. Focke

Department of Chemical Engineering

University of Pretoria

Degree: Master of Engineering (Chemical Engineering)

## **ABSTRACT**

In a push towards more environmentally friendly pyrotechnics, new greener pyrotechnic compositions need to be developed. A primary goal is to replace components such as lead, barium, and chromium in pyrotechnic compositions.

Fused Deposition Modelling (FDM) is a 3D printing/additive manufacturing method whereby a thin filament is passed through a heated nozzle, and extruded onto a substrate in successive layers. This method of manufacturing could be used to produce pyrotechnic time delays based on suitable “green” polymer/fuel mixtures.

Fluoropolymers are an attractive oxidising system for pyrotechnic use as fluorine is highly reactive and reacts relatively easily with common metallic fuels such as aluminium and magnesium to release a large amount of energy. Fluoropolymers are already in use as oxidisers and binders, especially in infrared decoy flares. PTFE has found wide use in the pyrotechnics industry, but is not melt-processible.

A similar fluoropolymer, poly(chloro-trifluoroethylene) (PCTFE) was considered instead. PCTFE differs from PTFE in that one of the fluorine atoms in the TFE monomer has

been replaced by a chlorine atom. The larger chlorine atom interferes with the packing of the polymer chains during polymerisation and, as such, may make it easier to process than PTFE. It was found that pure PCTFE degraded heavily during processing and was therefore precluded from any further study.

Melt-processible copolymers containing PCTFE are available from industry. These copolymers contain vinylidene fluoride (VDF) in addition to the CTFE i.e. poly(CTFE-*co*-VDF). Two grades of copolymer were obtained from 3M: FK-800<sup>®</sup> resin and Dyneon<sup>®</sup> 31508 resin. These two polymers contain different ratios of CTFE to VDF.

FK-800<sup>®</sup> resin was successfully extruded and showed minimal signs of degradation. Pyrotechnic films, containing aluminium powder as the fuel, were cast with both polymers using solvent techniques. Differential thermal analysis (DTA) was used to determine the ignition points of the compositions. All of the FK-800<sup>®</sup>-based compositions ignited at approximately 450 °C whilst all the Dyneon<sup>®</sup> 31508-based compositions ignited at approximately 400 °C. The energy output of the compositions was determined using bomb calorimetry. The experimental energy outputs of the FK-800<sup>®</sup>-based compositions correlated well with the predictions from the thermodynamic simulations. The maximum energy output, ~7.0 MJ·kg<sup>-1</sup>, occurred at a fuel loading between 30 – 35 wt.%. Except for one composition, the Dyneon<sup>®</sup> 31508-based compositions did not ignite in the bomb calorimeter.

FK-800<sup>®</sup> was successfully extruded into a filament and showed minimal signs of degradation. In order to assess the impact of adding a solid filler on the mechanical properties and extrudability of the polymer, magnesium hydroxide was used as inactive model compound in place of aluminium. A filament of FK-800<sup>®</sup> and Mg(OH)<sub>2</sub> was successfully compounded and produced using a filler loading of 30 wt.%. Compounding of the Dyneon 31508<sup>®</sup> with the magnesium hydroxide was unsuccessful. Addition of LFC-1<sup>®</sup> liquid fluoroelastomer improved the processibility of the Dyneon 31508<sup>®</sup> by lowering the melt viscosity.

**Keywords:** Poly(chloro-trifluoroethylene); Poly(vinylidene fluoride); Pyrotechnics; Additive manufacturing; Extrusion

## ACKNOWLEDGEMENTS

Firstly, to my parents, Craig and Cheryl, and sister, Kerry, who have supported me both financially and emotionally throughout the course of my studies. It is thanks to the three of you and your tremendous sacrifices that I have been able to get to this point in my life successfully. I can never say “thank you” enough.

To my supervisor, Prof. Walter Focke. Your support and guidance has been invaluable and I have learned so much from working with you.

Thank you to AEL Mining Services, and in particular Cheryl Kelly, George Labuschagne, Craig Rimmington and Kolela Ilunga, for financial and technical support for this project.

To all my colleagues at the Institute of Applied Materials at the University of Pretoria. Dr. Shepherd Tichapondwa, Marnes Grobler, Desania Govender, Stefan Endres, and Craig Sechel for the lengthy and, mostly, useful discussions.

I would like to extend a very special word of thanks to Suzette Seymore who always makes everyone feel like they’re the most important person in the department but we all know we’d fall apart without you.

Lastly, to all my family and friends who have stood by me throughout the course of this degree. Your love and support have kept me going through the toughest of times and I am truly grateful to have each and every one of you in my life.



## TABLE OF CONTENTS

ABSTRACT.....	i
ACKNOWLEDGEMENTS.....	iii
LIST OF FIGURES .....	vii
LIST OF TABLES.....	ix
ABBREVIATIONS .....	x
CHAPTER 1: INTRODUCTION.....	1
1.1 Introduction.....	1
1.2 Problem statement.....	1
1.3 Aim.....	2
CHAPTER 2: LITERATURE REVIEW .....	3
2.1 General pyrotechnics.....	3
2.1.1 Definition.....	3
2.1.2 Fuels.....	3
2.1.2.1 Metals .....	4
2.1.2.2 Non-metals.....	5
2.1.2.3 Organic fuels.....	5
2.1.3 Oxidisers .....	6
2.1.4 Ignition.....	6
2.1.5 Propagation .....	9
2.1.6 Factors affecting pyrotechnic reactions .....	12
2.2 Need for “Green” pyrotechnics .....	14
2.3 Fluoropolymers .....	16
2.3.1 Polytetrafluoroethylene.....	17
2.3.2 Poly(chloro-trifluoroethylene).....	18
2.3.3 Fluoropolymer copolymers.....	20
2.4 Applications in pyrotechnics.....	22



2.5	Additive manufacturing of pyrotechnics.....	23
CHAPTER 3: EXPERIMENTAL METHODS .....		25
3.1	Thermodynamic simulation.....	25
3.2	Solution casting .....	25
3.3	Open burn tests.....	26
3.4	Extrusion trials .....	26
3.5	Characterisation.....	28
CHAPTER 4: SOLIDS CHARACTERISATION .....		32
4.1	Aluminium .....	32
4.2	Magnesium hydroxide.....	34
4.3	Magnesium hydroxide as a model compound.....	37
CHAPTER 5: POLYMER CHARACTERISATION .....		38
5.1	Poly(chloro-trifluoroethylene) .....	38
5.2	FK-800® .....	40
5.3	Dyneon 31508® .....	43
5.4	LFC-1® .....	46
CHAPTER 6: PCTFE SIMULATION .....		50
6.1	Reducing agent selection.....	50
6.2	Stoichiometric determination of PCTFE/Al system .....	51
CHAPTER 7: PCTFE RESULTS AND DISCUSSION.....		52
7.1	Solution casting .....	52
7.2	Open burn tests.....	52
7.3	Extrusion trials .....	53
CHAPTER 8: COPOLYMER SIMULATION.....		55
CHAPTER 9: COPOLYMER RESULTS AND DISCUSSION .....		60
9.1	Solution casting .....	60
9.2	Energetics .....	60



9.2.1	Differential thermal analysis .....	60
9.2.2	Bomb calorimetry .....	63
9.2.2.1	FK-800® .....	63
9.2.2.2	Dyneon 31508® .....	64
9.2.3	Residue analysis .....	64
9.3	Extrusion trials .....	69
CHAPTER 10: CONCLUSIONS AND RECOMMENDATIONS .....		71
10.1	PCTFE .....	71
10.2	Copolymers.....	72
10.2.1	Energetics.....	72
10.2.2	Product analysis .....	73
10.2.3	Extrusion trials .....	73
10.3	Recommendations .....	74
REFERENCES .....		75



## LIST OF FIGURES

Figure 1: Schematic showing how solid fuel and oxidiser particles contact each other (Adapted from Kosanke et al. (2004)) .....	7
Figure 2: Schematic showing molten oxidiser covering solid fuel particles (Adapted from Kosanke et al. (2004)).....	7
Figure 3: Simplified model showing where ignition temperature occurs as a result of heat gains and losses (Akhavan, 2011) .....	8
Figure 4: Model showing the dependence of ignition temperature on sample size (Kosanke et al., 2004) .....	9
Figure 5: Simplified model for burning pyrotechnic composition (Kosanke et al., 2004).....	10
Figure 6: Model for steady-state propagation of burning (USAMC, 1968) .....	10
Figure 7: Reaction for production of PTFE from TFE monomer (Koch, 2007).....	17
Figure 8: Structure of PCTFE (Sigma-Aldrich, 2015).....	19
Figure 9: Schematic diagram of a pyrotechnic delay element (Tsang, 2005) .....	22
Figure 10: Schematic of the HAAKE Rheomix CTW5 microcompounder .....	27
Figure 11: Schematic of lab-scale single screw extruder setup used in extrusion trials.....	27
Figure 12: Cross-section of combustion vessel used for bomb calorimetry .....	30
Figure 13: XRD analysis result of aluminium powder used.....	32
Figure 14: Particle size distribution of aluminium powder .....	33
Figure 15: SEM image showing morphology of aluminium particles.....	34
Figure 16: XRD analysis of magnesium hydroxide powder used .....	35
Figure 17: Particle size analysis of magnesium hydroxide powder.....	36
Figure 18: SEM images of magnesium hydroxide powder .....	36
Figure 19: FTIR spectrum of PCTFE powder .....	38
Figure 20: TGA curve for PCTFE powder obtained from Sigma-Aldrich.....	39
Figure 21: DSC heating and cooling curves for PCTFE powder obtained from Sigma-Aldrich .....	39
Figure 22: FTIR spectrum for FK-800 <sup>®</sup> resin.....	40
Figure 23: TGA curve for FK-800 <sup>®</sup> resin .....	41
Figure 24: DSC curves for FK-800 <sup>®</sup> resin.....	42
Figure 25: Rheology results for FK-800 <sup>®</sup> resin .....	43
Figure 26: FTIR spectrum for Dyneon 31508 <sup>®</sup> resin.....	44
Figure 27: TGA curve for Dyneon 31508 <sup>®</sup> resin.....	45

Figure 28: DSC curves for Dyneon 31508 <sup>®</sup> resin.....	45
Figure 29: Rheology results for Dyneon 31508 <sup>®</sup> resin.....	46
Figure 30: FTIR spectrum for LFC-1 <sup>®</sup> fluoroelastomer resin .....	47
Figure 31: TGA curve for LFC-1 <sup>®</sup> resin.....	48
Figure 32: DSC curves for LFC-1 <sup>®</sup> fluoroelastomer .....	48
Figure 33: EKVI simulation results using PCTFE and various reducing agents.....	50
Figure 34: Simulated temperature and enthalpy results for PCTFE/Al compositions.....	51
Figure 35: Extruded PCTFE strand showing a large degree of degradation and porous structure .....	53
Figure 36: Simulated enthalpy releases for FK-800 <sup>®</sup> and Dyneon 31508 <sup>®</sup> compositions .....	55
Figure 37: Simulated temperatures for FK-800 <sup>®</sup> and Dyneon 31508 <sup>®</sup> compositions .....	55
Figure 38: Condensed product spectrum for FK-800 <sup>®</sup> compositions using aluminium as fuel .....	56
Figure 39: Gaseous product spectrum for FK-800 <sup>®</sup> compositions using aluminium as fuel ..	57
Figure 40: Condensed product spectrum for Dyneon 31508 <sup>®</sup> compositions using aluminium as fuel .....	57
Figure 41: Gaseous product spectrum for Dyneon 31508 <sup>®</sup> compositions using aluminium as fuel .....	58
Figure 42: DTA response curves for FK-800 <sup>®</sup> compositions at various fuel loadings .....	61
Figure 43: DTA response curves for Dyneon 31508 <sup>®</sup> compositions at various fuel loadings	61
Figure 44: Bomb calorimeter and simulated energy outputs for FK-800 <sup>®</sup> -based compositions .....	63
Figure 45: XRD analysis results for reaction products at various fuel loadings. Peaks are identified as follows: ● - Aluminium fluoride, ■ - Aluminium, ★ - Graphite, ▲ - Aluminium carbide.....	65
Figure 46: SEM mirographs of ashes collected from bomb calorimeter for FK-800 <sup>®</sup> -based compositions. (a-b) 20 wt.% fuel. (c-d) 40 wt.% fuel. (e-f) 60 wt.% fuel.....	66
Figure 47: SEM-EDS images showing (a) carbon covered aluminium fluoride (b) spherical aluminium fluoride (c) unreacted aluminium (d) cubic aluminium fluoride particles .....	68

## LIST OF TABLES

Table 1: Commonly used metal fuels and their heats of combustion (Adapted from Conkling, 1985) .....	4
Table 2: Commonly used non-metal fuels and their heats of combustion (Adapted from Conkling, 1985) .....	5
Table 3: Specific effects of controlling factors on pyrotechnic reactions (Adapted from Kosanke and Kosanke (2014)).....	13
Table 4: Examples of MTV compositions (Adapted from Christo (1999)).....	18
Table 5: PIR onset and continuous combustion onset temperatures for various metal/PTFE systems (Koch, 2007).....	18
Table 6: Suitable solvents for PCTFE and the temperatures required to achieve solubility (Adapted from [a] Barton (1990) and [b] Boschet and Ameduri (2013)).....	20
Table 7: Common copolymers of TFE and CTFE (Adapted from [a] Ebnesajjad (2003) and [b] Boschet and Ameduri (2013)).....	21
Table 8: Details of lab-scale single screw extruder used in extrusion trials .....	28
Table 9: Conditions used for extrusion trials .....	28
Table 10: XRF analysis results for Aluminium powder used.....	32
Table 11: Particle size analysis results for aluminium powder.....	33
Table 12: XRF analysis of magnesium hydroxide powder.....	35
Table 13: Particle size analysis results of magnesium hydroxide powder.....	35
Table 14: Summary of material properties of aluminium and magnesium hydroxide .....	37
Table 15: Characteristic bands from FTIR analysis of PCTFE powder .....	38
Table 16: DSC results for PCTFE powder .....	40
Table 17: Characteristic bands from FTIR analysis of FK-800.....	41
Table 18: Characteristic bands from FTIR analysis of Dyneon 31508 <sup>®</sup> .....	44
Table 19: DSC results for Dyneon 31508 <sup>®</sup> resin .....	46
Table 20: Characteristic bands from FTIR analysis of LFC-1 <sup>®</sup> fluoroelastomer .....	47
Table 21: DSC results for LFC-1 <sup>®</sup> resin .....	49
Table 22: Details of extrusion trials with PCTFE resin.....	53
Table 23: Active regions of reaction of copolymers with aluminium and indications thereof	59
Table 24: SEM-EDS results for reaction products .....	68

## ABBREVIATIONS

CTFE	Chloro-trifluoroethylene
DSC	Differential scanning calorimetry
DTA	Differential thermal analysis
EDS	Energy-dispersive X-ray spectroscopy
EKVI	Thermochemical code used for thermodynamic simulations
FTIR	Fourier transform infrared (spectroscopy)
HCl	Hydrochloric acid
HEM/s	High energy material/s
HF	Hydrofluoric acid
PCTFE	Poly(chloro-trifluoroethylene)
PTFE	Poly(tetrafluoroethylene)
PVDF	Poly(vinylidene fluoride)
SEM	Scanning electron microscopy
TFE	Tetrafluoroethylene
TGA	Thermo-gravimetric analysis
VDF	Vinylidene fluoride
XRD	X-ray diffraction
XRF	X-ray fluorescence

## CHAPTER 1: INTRODUCTION

### 1.1 Introduction

It is a well-documented fact that traditional pyrotechnic compositions containing lead, mercury, barium, and cadmium compounds are sources of pollution and contamination (Danali et al., 2010; Ilyushin et al., 2012; Steinhäuser et al., 2008). These components, which are released upon burning or explosion, are toxic and can cause harm to the environment in which they were reacted.

As such, an increasing amount of resources are devoted to finding ways to reduce the pollution potential of pyrotechnics. The primary method of making pyrotechnics greener is to replace the toxic heavy metal and oxidising components found in traditional pyrotechnic compositions. Fluorinated polymers are attractive alternatives for oxidisers such as the perchlorates that are traditionally used.

Fluorinated polymers are used as oxidisers in industry already. However, the most highly fluorinated polymer, PTFE, is not melt processible, and the others in use serve merely as binders for the active composition.

Extrusion is becoming more popular as a processing technique for energetic compounds, and advances in additive manufacturing technology are allowing this processing technique to be used for processing and manufacturing of energetic compositions.

Advances in additive manufacturing technology are making it possible to print energetic material-based devices. One such 3D printing method is fused deposition modelling (FDM). This technique involves the “printing” of successive layers of material onto a substrate. The material, provided in a filament form, is passed through a heated printing head that moves relative to the bed to produce the required shape. This manufacturing method facilitates the manufacture of very complex designs. It also eliminates much of the waste associated with traditional manufacturing techniques such as milling and cutting.

### 1.2 Problem statement

A major challenge faced by the pyrotechnics industry is the safe transport of energetic materials. Detonators contain very sensitive primary high explosives which are used to initiate

the main charge in blasting operations. They therefore need special transport and handling procedures which prevent the composition from igniting/reacting.

Many energetic compositions use polymers as binders. The fuel and oxidiser particles are compounded into the polymer. This raises the solids loading and makes the composition more difficult to process.

### **1.3 Aim**

The aim of this research is to investigate the viability of using a highly fluorinated polymer as the main oxidiser in a pyrotechnic composition which could be extruded, and subsequently processed using FDM. This will allow for safer transport of the material as it may be less sensitive than traditional primary explosives.

By using the polymer as the main oxidiser, oxidising particles will not have to be compounded in addition to the fuel particles. This will lower the overall solids loading and make the composition easier to process. It will also allow a more flexible manufacturing method that can be used on-site to adjust to varying spatial and energetic requirements.

## CHAPTER 2: LITERATURE REVIEW

### 2.1 General pyrotechnics

#### 2.1.1 Definition

The term “pyrotechnics” comes from the Greek words *pyr*, meaning fire, and *techne*, meaning art (Akhavan, 2011), so literally it is the art of fire. It is the field of technology that deals with the generation of heat from one or more self-contained and self-sustaining chemical reactions, and the use of that heat energy to generate pressure, smoke, light and loud noises for a variety of applications (Kosanke et al., 2012). Pyrotechnics are metastable mixtures of chemicals that react when initiated to produce one or more of the effects mentioned above (Steinhauser et al., 2008).

Energetic materials are generally classified as one of three categories: high explosives, propellants, and pyrolants. High explosives can undergo a detonation which produces a supersonic shock wave that is in turn supported by exothermic chemical reactions. Propellants and pyrolants produce reaction fronts that propagate at subsonic speeds. The difference between the two is that propellants yield mostly gaseous products whilst pyrolants yield mostly condensed products (Koch, 2007).

Pyrotechnic reactions are similar to combustion reactions in that they are exothermic oxidation reactions. However, the primary difference between the two is the fact that pyrotechnic reactions do not require atmospheric oxygen to burn due to the presence of oxidising chemicals in the reaction mixture (Ellern, 1968).

Pyrotechnic devices are always composed of at least one fuel and one oxidising agent combined in a physical mixture (as opposed to a chemical compound) (Kosanke et al., 2004). Compounds which contain both the oxidising agent and fuel in one molecule tend to be unstable and have explosive properties, such as TNT and nitroglycerine (Conkling, 1985; Steinhauser and Klapötke, 2008).

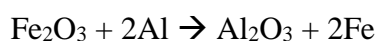
#### 2.1.2 Fuels

Fuels react with the oxidising agent in highly exothermic reactions in order to produce the heat necessary to make the pyrotechnic reaction self-sustaining. Many options for fuels exist and

the choice will depend on the intended application. Fuels are divided into three categories: metals, non-metallic elements, and organics (Conkling, 1985).

### 2.1.2.1 Metals

Metals are commonly used as fuels in pyrotechnic compositions where high temperatures are required as they produce a large amount of heat when burned, more so than non-metal fuels (Steinhauser and Klapötke, 2010). A widely known example of using metal fuels to produce a lot of heat is the thermite reaction described in Scheme I below. This reaction can reach a temperature well in excess of 2 000 °C and generates a heat of 3 975 MJ·kg<sup>-1</sup> (Conkling, 1985).



Scheme I: Thermite reaction between iron oxide and aluminium

The two most widely used metal fuels are aluminium and magnesium, but other metals are also used such as zinc, tungsten, and titanium. Group 1 and 2 metals such as sodium, barium, and calcium would theoretically make very good fuels for pyrotechnic use but they tend to be too reactive with moisture and atmospheric oxygen and, as such, the resulting pyrotechnic mixture would prove to be too unstable (Conkling, 1985). Table 1 details some commonly used metal fuels and their respective heats of combustion.

Table 1: Commonly used metal fuels and their heats of combustion (Adapted from Conkling, 1985)

Metal	Symbol	Heat of combustion
		/MJ·kg <sup>-1</sup>
Aluminium	Al	30.96
Iron	Fe	7.53
Magnesium	Mg	24.69
Titanium	Ti	19.66
Tungsten	W	4.60
Zinc	Zn	5.44
Zirconium	Zr	12.13



### 2.1.2.2 Non-metals

Various non-metallic fuels have been used for over one thousand years and are still in common use in pyrotechnics today. Common non-metallic fuels include sulphur, boron, silicon and phosphorus, and their properties are summarised in Table 2 (Conkling, 1985).

Table 2: Commonly used non-metal fuels and their heats of combustion (Adapted from Conkling, 1985)

Non-Metal fuel	Symbol	Heat of combustion
		/MJ·kg <sup>-1</sup>
Sulphur	S	9.20
Boron	B	58.58
Silicon	Si	30.96
Phosphorus (red)	P	24.69
Phosphorus (yellow)	P	24.69

Boron has a very low molecular mass and, as such, yields a very high heat of combustion per unit mass. It can, however prove difficult to ignite if used with an oxidiser with a high melting point. The boron oxide product that forms can also lower the reaction temperature achieved as it has a low melting point (Conkling, 1985). Silicon is similar to boron as a fuel (Conkling, 1985), but it can be used to raise the final flame temperature. It also forms glassy droplets that are effective heat transfer agents which make the propagation of the reaction easier (Kosanke et al., 2012).

### 2.1.2.3 Organic fuels

A number of organic fuels exist for pyrotechnic use. These fuels produce a lot of gas that generates high pressures due to the formation of carbon dioxide and, in the case of hydrocarbons, water vapour. Carbon monoxide and elemental carbon are formed if insufficient amounts of oxygen are available for combustion (Conkling, 1985). The production of these side-products tends to lower the flame temperature of the final composition. The use of oxygen-rich organic fuels will also tend to lower the flame temperature and lower the total energy

output (Conkling, 1985). Due to the nature of organic chemistry, the number of organic fuels is almost unlimited. Some commonly used organic materials are nitrocellulose, polyvinyl alcohol, stearic acid, shellac, and red gum (Conkling, 1985).

### 2.1.3 Oxidisers

Oxidising agents are essential in pyrotechnic compositions to make the reaction self-contained. They undergo thermal decomposition to release the oxidising chemical (normally oxygen but exceptions exist such as hydroxyl radicals or halogens, like chlorine) which allows it to react with the fuel (Conkling, 1985). This release of the oxidising agent is what allows pyrotechnic compositions to burn without the need for atmospheric oxygen and has allowed them to find use in extreme environments such as underwater and in space.

Typically the oxidisers are metal salts containing anions with high energy N-O and Cl-O bonds, e.g. nitrate ion ( $\text{NO}_3^-$ ), chlorate ion ( $\text{ClO}_3^-$ ), perchlorate ion ( $\text{ClO}_4^-$ ), and chromate ion ( $\text{CrO}_4^{2-}$ ) (Conkling, 1985).

Group I and II metals are generally preferred for use as the cation as they are good electron donors and will not react with the metal fuel used. The lighter metals in these groups ( $\text{Na}^+$  and  $\text{K}^+$ ) are generally preferred over the heavier metals ( $\text{Pb}^{2+}$  and  $\text{Ba}^{2+}$ ) as these increase the active oxygen content of the final compound. The final compound should have a low hygroscopy (it should not attract water) and should have a heat of reaction that is neither too high nor too low for the application. Too high could lead to an explosion while too low could make ignition and propagation very difficult (Conkling, 1985).

### 2.1.4 Ignition

For any chemical reaction to take place, the atoms of the reacting species need to be able to come into contact with each other. Due to the fact that most pyrotechnic reactions involve the use of solid powders, these reactions are therefore initially limited to the atoms near the surfaces of the particles. A 25  $\mu\text{m}$  diameter particle consists of  $10^{15}$  atoms, of which only 1 in 30 000 is located on the surface of the particle (Kosanke et al., 2004). In addition to this problem, the particles are not in intimate contact throughout the sample as shown schematically in Figure 1.

The fraction of fuel and oxidiser surfaces which are in contact and are therefore immediately available to react upon is, according to Kosanke et al. (2004), approximately 1 in 20.

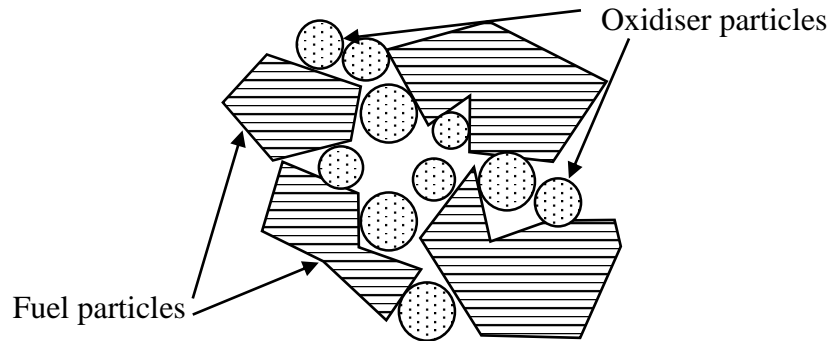


Figure 1: Schematic showing how solid fuel and oxidiser particles contact each other (Adapted from Kosanke et al. (2004))

If the temperature increases sufficiently, the oxidiser will tend to melt before the fuel and therefore cover the fuel particles as shown in the schematic in Figure 2. This molten oxidiser allows more atoms to come into intimate contact. Therefore a relatively low melting oxidiser is generally preferred as this would allow a more reliable, faster reaction to occur.

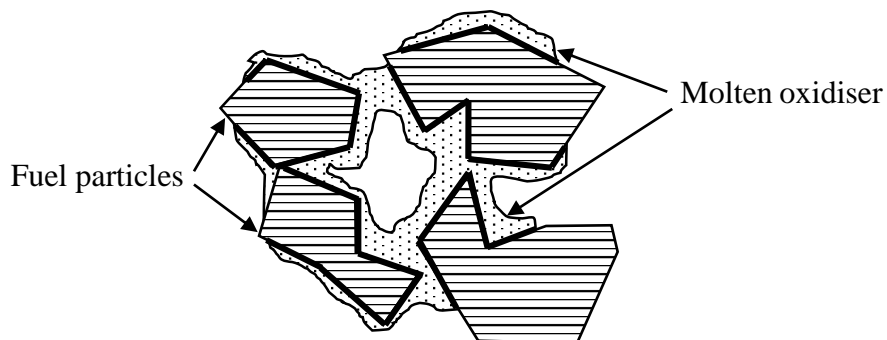


Figure 2: Schematic showing molten oxidiser covering solid fuel particles (Adapted from Kosanke et al. (2004))

Generally ignition will occur when one of the components reaches its melting temperature for the reasons detailed above. The ignition temperature of a composition is the minimum

temperature required to allow the initiation process to be self-sustaining (Akhavan, 2011). Ignition of a pyrotechnic mixture will occur when the heat generated by the system exceeds the heat loss to the environment, as shown in Figure 3. As the composition begins to burn, the rate of heat gain will increase exponentially while the rate of heat loss will increase linearly.

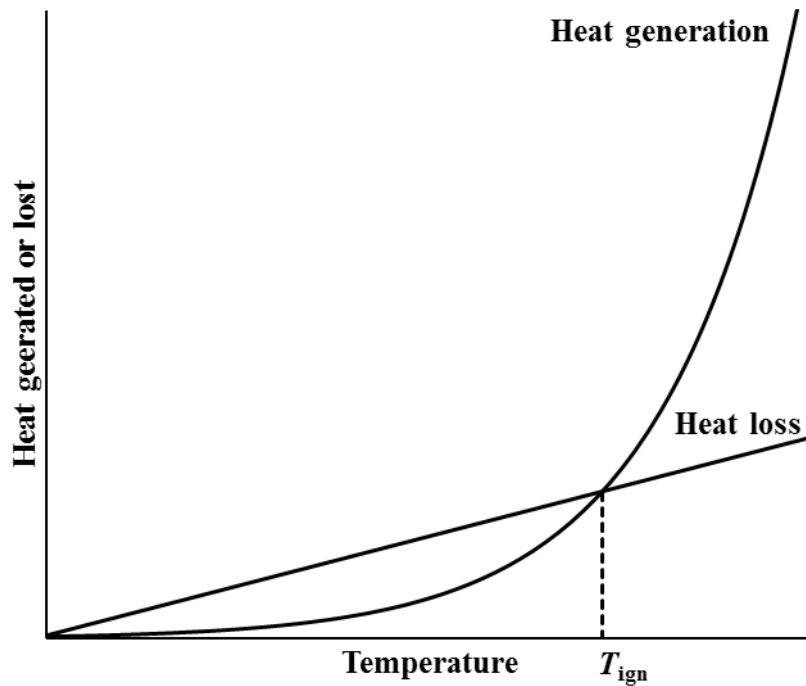


Figure 3: Simplified model showing where ignition temperature occurs as a result of heat gains and losses (Akhavan, 2011)

The rate of heat loss to the environment is dependent on the size of the sample, as well as on the ambient temperature of the environment (Kosanke et al., 2004). As particles get smaller, the ratio of surface area to volume increases. Therefore, small isolated particles will lose heat quicker than larger particles. Thus, the gradient of the straight line will increase. Figure 4 presents a set of scenarios where varying the sample size affects when, or if, ignition of the pyrotechnic composition occurs.

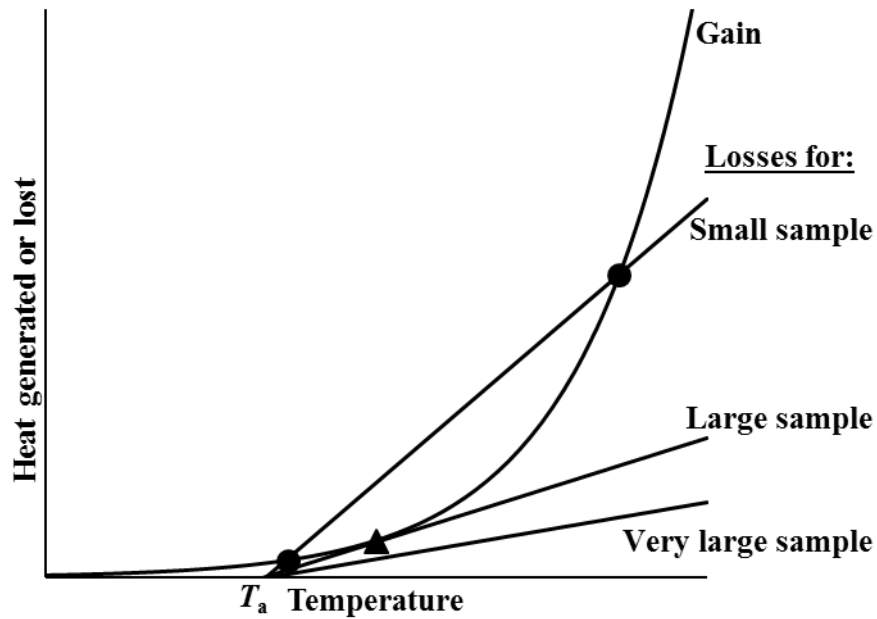


Figure 4: Model showing the dependence of ignition temperature on sample size (Kosanke et al., 2004)

From this it can be seen that a very small sample of pyrotechnic composition needs to be heated to a higher temperature than a larger sample in order for ignition to occur. This is due to the much higher surface area to volume ratio of smaller sample when compared to the larger sample. Additionally, if a large enough sample of pyrotechnic composition is available, spontaneous ignition can definitely occur (Kosanke et al., 2004). However, the required size of sample for this to occur may be enormously large, or the time to ignition may be very long.

From Figure 4 it can also be deduced that there is a practical limit to how small a sample can be. As the sample gets smaller, the temperature required increases until it is impractically large. As such, FDM is determined to be a viable manufacturing technique as one can adjust the thickness of the layers very easily to make the composition easier or more difficult to ignite.

### 2.1.5 Propagation

The burning process of pyrotechnic, propellant, and explosive compositions can be described as “self-sustaining, exothermic, rapid-oxidising reactions” (Akhavan, 2011). The term “self-sustaining” refers to the ability of the composition to continue to burn without the need for any

added external stimulus. A simple model for the propagation of a pyrotechnic reaction is presented in Figure 5.

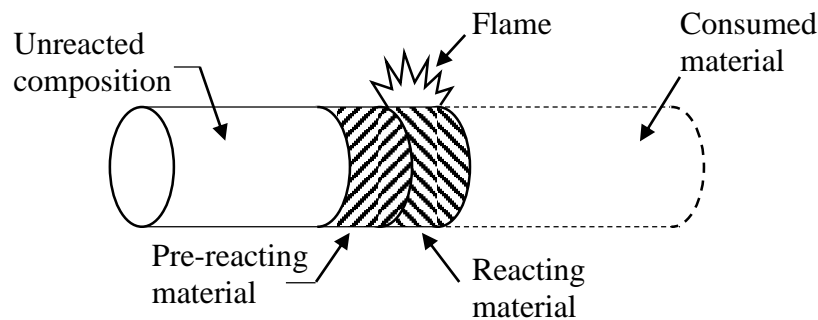


Figure 5: Simplified model for burning pyrotechnic composition (Kosanke et al., 2004)

In the model above, the flame is propagating to the left. In order for the burning process to be self-sustaining and to propagate, the reacting material needs to be able to transfer enough heat to the pre-reacting material to raise it to its ignition temperature and thus allow it to react sequentially. If the rate of heat loss to the environment is greater than the rate of heat gained from the reaction, the reaction will terminate and the composition will cease to burn.

A more in-depth model is presented in Figure 6. This model breaks the pre-ignition zone from the model in Figure 5 into three separate zones; Zones 2, 3 and 4 in Figure 6.

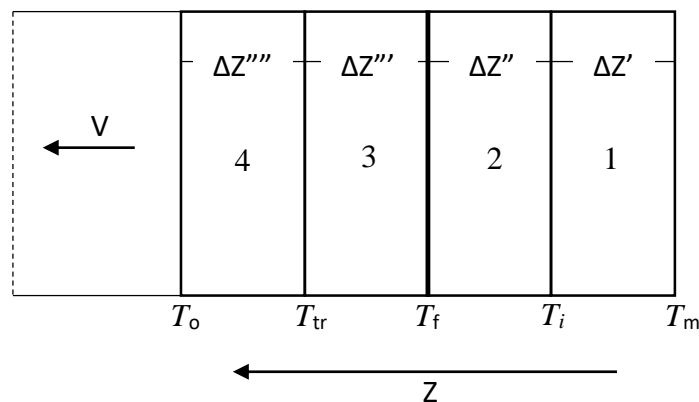


Figure 6: Model for steady-state propagation of burning (USAMC, 1968)

here:  $T_m$  = Maximum reaction temperature  
 $T_i$  = Minimum ignition temperature  
 $T_f$  = Fusion temperature  
 $T_{tr}$  = Transition temperature

$T_0$  = Ambient temperature  
 $\Delta Z', \Delta Z'', \Delta Z''', \Delta Z''''$  = Length of zones  
 1 = Reaction zone  
 2 = Zone of fusion  
 3 = Zone of crystalline transition  
 4 = Heat conduction zone  
 $Z$  = Direction of burning  
 $V$  = Velocity of burning

The assumption of steady state burning implies that the position of the zones changes linearly with time (USAMC, 1968). Pre-ignition reactions take place in zones 2 and 3. Once enough heat has been transferred to the unreacted material in zone 4, it initiates physical transitions in the crystal structure of the composition (zone 3) which occurs in the solid state. Now more heat is transferred to the solids due to the increasing nearness of the reacting material until enough heat has been transferred to the material to cause one of the components to melt as described in the previous section which will allow the composition in this zone to continue the reaction.

For the determination of burning rate, two extreme cases can be defined. Purely homogeneous reaction (kinetics limited) and purely heterogeneous (diffusion limited) (Margolis, 1993).

Equation 1 describes the linear burning rate of a composition for the kinetics-limited case for an  $n^{\text{th}}$  order gasless, exothermic, solid-state reaction. This equation assumes that the physical properties of the mixture are independent of the composition and temperature of the mixture, that there are no phase transitions and that the reaction zone is very thin compared to the length of the burning column. It also assumes that an Arrhenius-type temperature dependence holds true for the rate constant (Khaikin and Merzhanov, 1966).

$$u^2 = \frac{g(n)RT_c^2}{E_a(T_c - T_0)} (\alpha k_0) e^{-E_a/RT_c} \quad (1)$$

here:  $u$  = Burning velocity /m·s<sup>-1</sup>  
 $g(n)$  = Dimensionless function of reaction order  $n$ :  $0.5 < g(n) < 2$   
 $R$  = Universal gas constant /8.314 J·mol<sup>-1</sup>·K<sup>-1</sup>  
 $T_c$  = Maximum burning temperature /K  
 $T_0$  = Initial temperature /K  
 $\alpha$  = Thermal diffusivity /m<sup>2</sup>·s<sup>-1</sup>

$k_o$  = Arrhenius pre-exponential factor /s<sup>-1</sup>

$E_a$  = Activation energy /J·mol<sup>-1</sup>

In the heterogeneous case, described by Equation 2, the burning rate is determined by heat and mass transfer through a thin boundary layer. The determination of the burning rate for this situation require detailed information about particle geometry and packing. If this is approximated by alternating layers of components, with the thicknesses being determined by the stoichiometry and densities of the components, then the burning rate can be described as below (Aldushin and Khaikin, 1974).

$$u^2 = \frac{6RT_c^2}{E_D(T_c - T_0)} \left( \frac{\alpha D_o}{d^2} \right) e^{E_D/RT_c} \quad (2)$$

here:  $D_o$  = Pre-exponential factor for the diffusion coefficient /m<sup>2</sup>·s<sup>-1</sup>

$E_D$  = Activation energy for the diffusion coefficient /J·mol<sup>-1</sup>

$d$  = Measure of the particle size distribution of reactants /m

All other variables are as described for Equation 1.

A strong dependence can be seen on the particle size in Equation 2. This term implies that the burning rate will increase linearly with a decrease in particle size. Having a wider particle size distribution will increase the packing density of the mixture. This factor will also increase the burning rate, as well as decrease the effective ignition temperature and time (Dugam et al., 1999). Again, this is due to the increased contact area between the particles with a higher packing density.

Equations 1 and 2 were derived under the assumption that no phase transitions occur. However, as seen in Figure 6, phase transitions do occur in reality. This effect only appears as a reduction in the burning temperature and may be accounted for by considering the heat capacity of the mixture (Aldushin et al., 1987).

#### 2.1.6 Factors affecting pyrotechnic reactions

A number of factors may affect both the rate of reaction of pyrotechnic reactions as well as the heat released during the reaction. Berger (2005) summarises these parameters as follows:

- Type of chemicals



- Oxygen balance
- Particle size/active surface
- Binder type/content
- Mixing process

Table 3 summarises the specific parameter that each of these, and other, variables affect in the reaction.

Table 3: Specific effects of controlling factors on pyrotechnic reactions (Adapted from Kosanke and Kosanke (2014))

<b>Controlling Factor</b>	$E_a$	$\Delta H_r$	$F_{fb}^*$
Choice of fuel and oxidiser	X	X	X
Fuel-oxidiser ratio (Stoichiometry)		X	
Degree of mixing		X	
Particle size	X		
Particle shape	X		
Presence of additives	X	X	X
Presence of catalysts	X		
Ambient temperature	X		
Local pressure			X
Degree of confinement			X
Physical form			X
Degree of consolidation			X
Geometry			X
Crystal effects	X		X
Environmental effects	X	X	X

\*  $F_{fb}$  refers to the efficiency of energy feedback, in other words, how effectively the reaction occurring in the reaction zone heats up the unreacted material in the pre-reaction zone.

In general, an increase in reaction (burn) rate will occur when the activation energy ( $E_a$ ) is decreased and the heat of reaction ( $\Delta H_r$ ) and energy feedback efficiency ( $F_{fb}$ ) are increased. Examples of these effects include the increased reaction rates demonstrated by Poret et al. (2012) when pyrotechnic compositions were burned inside aluminium tubes as opposed to stainless steel tubes, and the decrease in ignition times and temperatures when nano-sized

aluminium particles were compared to micro-sized particles as described by Pantoya and Granier (2005).

The effect observed by Poret et al. (2012) can be attributed to an increase in the feedback efficiency ( $F_{fb}$ ) due to the higher heat conductivity of aluminium. Nanoparticles generally have a higher surface energy than micron particles (Nanda et al., 2003) and, as such, the activation energy ( $E_a$ ) for the nanoparticle composition is lower than for the micron composition which leads to the observed decrease in ignition time and temperature.

## 2.2 Need for “Green” pyrotechnics

It is a well-documented fact that traditional pyrotechnic compositions containing lead, mercury, barium, and cadmium compounds are sources of pollution and contamination (Danali et al., 2010; Ilyushin et al., 2012; Steinhauser et al., 2008). These components, which are released upon burning or explosion, are toxic and can cause damage to the environment in which they were reacted.

As such, there has been an increasing amount of resources devoted to finding ways to reduce the pollution potential of pyrotechnics. One of the primary ways of making pyrotechnics greener is to replace the heavy metal components found in traditional pyrotechnic compositions (Klapötke, 2015). Steinhauser and Klapötke (2010) specify that green pyrotechnics for either military or civil use should avoid the use of heavy metals and perchlorates. Ding and Inagaki (2003) propose a more general set of conditions for high energy density materials (HEDMs) as follows:

- i. They need to have a high energy density
- ii. They need to have excellent kinetic stability. i.e. they need to have a high activation energy
- iii. Production of environmentally friendly products should be favoured over products that could harm the environment
- iv. They should be easy to manufacture on a large enough scale for industrial use

Perchlorates such as ammonium perchlorate and potassium perchlorate are used as common oxidisers in pyrotechnic formulations (Conkling, 1985). Burning of chlorinated organic materials (such as PVC), or mixtures of hydrocarbons and perchlorates, have the potential to form highly carcinogenic compounds such as polychlorinated dibenzodioxins

(PCDDs), polychlorinated dibenzofuranes (PCDFs) and polychlorinated biphenyls (PCBs) (Sabatini et al., 2015). Although the amounts of these polychlorinated compounds produced from pyrotechnic devices have been debated (Fleischer et al., 1999; Dyke et al., 1997), the potential for releasing these compounds into the environment remains.

The toxicity of lead and lead-containing compounds is well known. Lead azide and lead styphnate are two widely used primary explosives (Ilyushin et al., 2012), the use of which has led to contamination of various practice and artillery ranges (Huynh et al., 2006). In addition, lead compounds are used as oxidants in many time delay formulations such as the silicon-red lead system which is widely used (Jakubko, 1999). Some barium salts are soluble in water and are very poisonous (Steinhauser and Klapötke, 2008). Many efforts have been made over the years to find suitable replacement formulations that do not include heavy metals such as mercury, lead or barium (Fronabarger et al., 2011).

Some chromium and strontium compounds are highly toxic with strontium chromate being a very powerful carcinogen (Steinhauser and Klapötke, 2008).

The challenge in developing green pyrotechnic compositions lies in trying to find new compositions and/or compounds that have comparable or better energetic performance than these traditional heavy metal containing formulations as well as having similar stabilities and sensitivities to stimuli such as heat, shear, impact and electrostatic discharge (ESD). Another problem arises in that these greener compositions may be more expensive to produce than the traditional formulations and thus the development and implementation of green solutions is hindered due to financial pressure (Steinhauser and Klapötke, 2008).

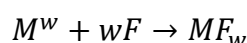
The majority of current research into green pyrotechnics is centred on high energy materials (HEMs) with a high nitrogen content (Talawar et al., 2009). These materials derive their energies, not from the oxidation of a carbon backbone as in traditional pyrotechnics (Badgujar et al., 2008), but from the proximity of the constituent nitrogen atoms which are poised to form molecular nitrogen ( $N_2$ ) (Talawar et al., 2009). These materials have a very high positive heat of formation which is associated with the breaking of the existing single or double bonds between nitrogen and other atoms and the forming of the triple bonded  $N_2$ .

The primary product from the combustion of these materials is molecular nitrogen which is environmentally benign (Ebespacher et al., 2009). In addition, the combustion products of these nitrogen-based materials are halogen- and heavy metal free, and produce very little smoke (Liu et al., 2015). The large amount of gas released by these materials make them ideally suited

to use as propellants and explosives but not for uses where condensed products are preferred, such as time delays.

### 2.3 Fluoropolymers

As mentioned in Section 2.1.3, the oxidiser in a pyrotechnic reaction does not necessarily have to be oxygen, but can also be a halogen with a high oxidation potential. Thus pyrotechnic reactions can essentially be viewed as reduction-oxidation (redox) reactions (Steinhauser and Klapötke, 2010). When metals with strong reducing potentials are used as fuels with halogen-containing compounds, especially fluorine, the mixtures demonstrate high exothermicity which is associated with the formation of the metal-halogen bond ( $M - X$ ) (Koch, 2007). Generally fluorine is the preferred halogen over others such as chlorine as the heat of formation of the metal-fluorine bond, as shown in Scheme II, is higher than any other combination with each specific metal (Koch, 2007).



Scheme II: General reaction of fluorine with a metal. Here  $w$  is the valence of the metal.

The use of non-energetic binders (such as hydroxyl-terminated polybutadiene (HTPB)) severely limits the performance of a system. To counter this, very high solid loadings, including both the fuel and oxidiser powders, are employed. Unfortunately, the higher solids loadings can limit the processibility of the composite (Colclough et al., 1994). At a given solids loading, superior performance can be achieved with a more energetic polymer (Colclough et al., 1994). Alternatively, an equivalent performance is possible at a lower solids loading, when compared to a non-energetic binder. The solids loading parameter is important as an increasing filler loading negatively affects the mechanical properties of the resultant composition (Potgieter et al., 2016).

By choosing a polymeric binder with sufficiently high fluorine content, the traditional oxidiser powder can be replaced and the polymer itself used as the oxidiser rather than just a binder. This would allow the total solids loading to be reduced while still maintaining system performance. The most common polymeric binders used in high energy applications are poly(ester urethane) block copolymers, vinylidene fluoride-hexafluoropropylene (VDF-HFP)

copolymers, and vinylidene fluoride-chlorotrifluoroethylene (VDF-CTFE) copolymers (Singh et al., 2013).

### 2.3.1 Polytetrafluoroethylene

Arguably the most well-known fluoropolymer is polytetrafluoroethylene (PTFE), more commonly known by the DuPont trademark Teflon<sup>®</sup> (Ebnesajjad, 2003). PTFE is the most chemically resistant and thermally stable polymer ever made (Koch, 2007). It is produced from the polymerisation of tetrafluoroethylene (TFE) as shown schematically in Figure 7.

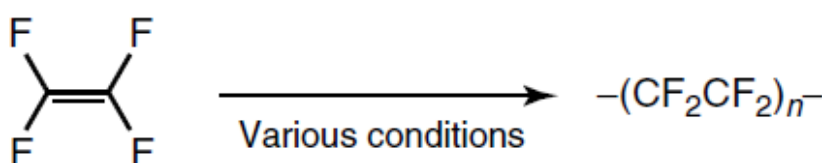


Figure 7: Reaction for production of PTFE from TFE monomer (Koch, 2007)

Virgin PTFE has a very high degree of crystallinity, around 92 – 98% (Ebnesajjad, 2003). As such it is not melt processible. It can be processed using ram extrusion, paste extrusion, and compression moulding (Ebnesajjad, 2003).

Teflon has found extensive use in the pyrotechnics industry (primarily in combination with magnesium and Viton<sup>®</sup>) as an oxidiser in infrared decoys and igniter compositions (De Yong and Smit, 1991). These Magnesium/Teflon<sup>®</sup>/Viton<sup>®</sup> (MTV) compositions have an exceptional energy output compared with other pyrotechnic compositions, are relatively safe to handle and store, and have a high degree of reliability in variable conditions (Christo, 1999; De Yong and Smit, 1991).

A number of possible MTV compositions are shown in Table 4, along with their specific applications. Shaw et al. (2015) use PTFE as an energetic binder in hand-held flare delay system containing boron carbide and sodium periodate at various compositions. In this system, PTFE is not the primary oxidant but due to its oxidising nature it robs very little, if any, energy from the primary reaction as would be the case with a non-energetic binder.

Table 4: Examples of MTV compositions (Adapted from Christo (1999))

<b>M:T:V ratio /wt.%</b>	<b>Application</b>
54:30:16	US flare composition
55:40:5	UK flare composition
61:34:5	US igniter composition

Although PTFE is primarily used with magnesium as the fuel, it can be used in conjunction with other metals as well. Table 5 details the pre-ignition reaction (PIR), where fluoride ions are adsorbed onto the outer shell of the fuel (Osborne, 2006), and continuous combustion onset temperatures for various metal/PTFE systems.

Table 5: PIR onset and continuous combustion onset temperatures for various metal/PTFE systems (Koch, 2007)

<b>System</b>	<b>PIR /°C</b>	<b>Combustion /°C</b>
Mg/PTFE	477	589
Al/PTFE	550	580
Zn/PTFE	270	420
Ti/PTFE	564	580
Zr/PTFE	510	570

As mentioned previously, PTFE is not melt processible. This precludes it from being considered as an oxidiser by itself in extrusion and FDM processes. However, its extensive use in the pyrotechnics industry means that it forms a good baseline to compare newly developed systems' performances.

### 2.3.2 Poly(chloro-trifluoroethylene)

Poly(chloro-trifluoroethylene) (PCTFE) is very similar to PTFE in many respects. The only difference between the repeat units of the two polymers is that one of the fluorine atoms has been replaced by a chlorine atom as shown in the schematic in Figure 8. The substitution of the single fluorine atom with chlorine interferes with the packing structure of the polymer chains, leading to a polymer with a much lower degree of crystallinity than PTFE, ranging from

30 % - 70 % (Boschet and Ameduri, 2013). Some grades are melt processible (Ebnesajjad, 2003).

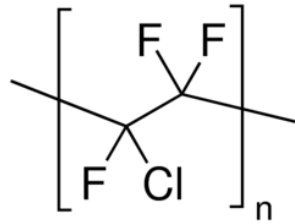


Figure 8: Structure of PCTFE (Sigma-Aldrich, 2015)

PCTFE was the first fluoropolymer to be discovered (Boschet and Ameduri, 2013) in 1934, and was the first perfluorinated polymer to be used as an oxidiser in a flare composition in 1956 (Cadwallader, 1964). The introduction of the chlorine atom leads to a slightly lower energetic performance than with PTFE as the formation of the metal-chlorine bond is not as exothermic as the metal-fluorine bond.

PCTFE exhibits excellent resistance to most common solvents at room temperature, and high temperatures (>120 °C) are required to allow the polymer to dissolve (Boschet and Ameduri, 2013). Table 6 presents some possible solvents for PCTFE and the temperatures required to allow the PCTFE to dissolve in them. This information is important as processing pyrotechnic compositions by solvent methods allows the fuel to be integrated into the polymer matrix without the extreme heat required to melt and compound the polymer as encountered in processing equipment such as extruders.

Table 6: Suitable solvents for PCTFE and the temperatures required to achieve solubility  
 (Adapted from [a] Barton (1990) and [b] Boschet and Ameduri (2013))

Solvent	Temperature /°C
Cyclohexane <sup>a</sup>	235 <sup>a</sup>
Benzene <sup>a</sup>	200 <sup>a</sup>
Toluene <sup>a</sup>	142 <sup>a</sup>
<i>p</i> -Xylene <sup>a</sup>	140 <sup>a</sup>
1,1,1-trichloroethane <sup>a</sup>	120 <sup>a</sup>
Tetrachloromethane <sup>a</sup>	114 <sup>a</sup>
1,2,3-trifluoropentachloropropane <sup>a</sup>	-
1,2,3-trifluoropentachloropentane <sup>a</sup>	-
1,1,2,2-tetrafluoro-3,3,4,4-tetrachlorocyclobutane <sup>a</sup>	-
1,2-dichlorotrifluorobenzene <sup>a</sup>	130 <sup>b</sup>
2,5-dinitrotrifluorobenzene <sup>a</sup>	130 <sup>a</sup>
Mesitylene <sup>a</sup>	140 <sup>a</sup>
Hexamethyltrisphosphoramidate <sup>a</sup>	-
2,5-dichlorotrifluoromethylbenzene <sup>b</sup>	130 <sup>b</sup>

The heat sensitivity of the pyrotechnic compositions is unknown before samples have been tested so solvent methods are preferred for initial manufacturing and testing in order to avoid accidental ignition. Singh et al. (2013) go so far as to say that “the solubility of polymeric binders in low molecular weight organic solvent is a primary requirement for the formulation of HEMs composites”. It should be noted that, with the exception of mesitylene, the temperatures required for solubility are above the normal boiling points of all the respective solvents.

### 2.3.3 Fluoropolymer copolymers

There are a number of commercially available fluoropolymer copolymers. Some common types of cofluoropolymers of both tetrafluoroethylene and chlorotrifluoroethylene are shown in Table 7. The copolymers mentioned in Table 7 are not the only cofluoropolymers available but are some of the more common ones.



One other fluoro-*co*-polymer worth mentioning is Viton<sup>®</sup>. Viton is a registered trademark of DuPont and, depending on the grade, is either a copolymer of hexafluoropropylene and vinylidene fluoride, or a terpolymer of tetrafluoroethylene, hexafluoropropylene and vinylidene fluoride (DuPont<sup>™</sup>, 2010). As mentioned previously, Viton finds extensive use in the pyrotechnics industry as a binder in MTV formulations (De Yong and Smit, 1991).

Table 7: Common copolymers of TFE and CTFE (Adapted from [a] Ebnesajjad (2003) and [b] Boschet and Ameduri (2013))

Monomer	Co-monomer	Copolymer resin
TFE	Hexafluoropropylene <sup>a</sup>	FEP <sup>a</sup>
	Perfluorovinylether <sup>a</sup>	PFA <sup>a</sup>
	Ethylene <sup>a</sup>	ETFE <sup>a</sup>
CTFE	Ethylene <sup>a</sup>	ECTFE <sup>a</sup>
	Vinylidene fluoride <sup>b</sup>	Poly(CTFE- <i>co</i> -VDF) <sup>b</sup>

Copolymers of both TFE and CTFE exhibit lower melting temperatures and can introduce varying degrees of solubility in conventional solvents which the homopolymers do not exhibit (Nielson et al., 2005). As mentioned previously, the solubility of the polymers in solvents is a very important characteristic.

Using a copolymer of TFE or CTFE with a lower melting point and higher solubility in common organic solvents may allow pyrotechnic compositions to be more easily processed or manufactured. Mention should be made, however, of the potential products from the burning of these composites. Many of the copolymers mentioned above (containing VDF or ethylene) contain hydrogen in their structure. This poses a problem as large amounts of hydrofluoric acid (HF) and/or hydrochloric acid (HCl) are produced upon burning (Huang et al., 2015; McCollum et al., 2015; Boschet and Ameduri, 2013; Martinez et al., 2012) which can cause problems for any surrounding equipment should these highly corrosive gasses come into contact with it.

## 2.4 Applications in pyrotechnics

A time delay is a device used to introduce a delay in the time taken for the main explosive to initiate. Examples of this effect can be seen in the operation of grenades in military applications (Wilson and Hancox, 2014) and initiation of sequential blasting in commercial mining operations (Beck et al., 1984).

A key property of time delay elements is that the majority of the products formed from burning remain in the condensed phase with little or no gaseous products forming (Koch, 2007). Primary explosives, or primers, are found at the end of the delay column as shown in the schematic in Figure 9. Primaries are generally fairly sensitive to ignition stimuli and are used in small amounts to provide the input energy to detonate the main charge of secondary explosive (Huynh et al., 2006).

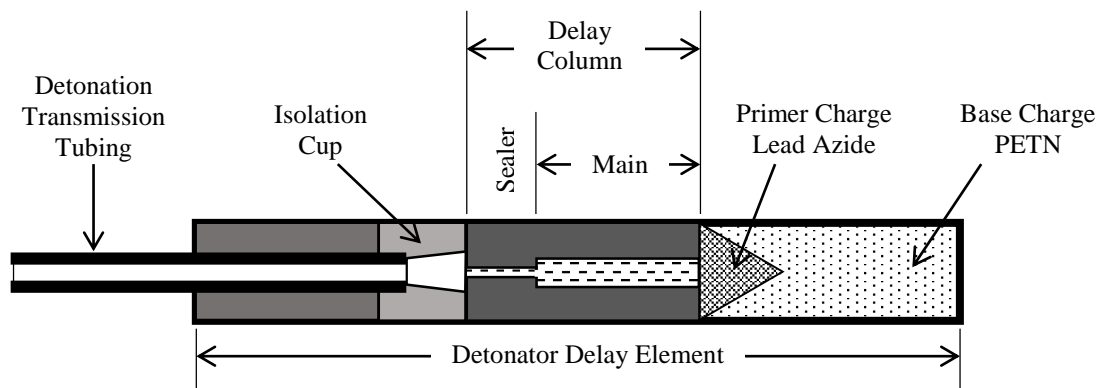


Figure 9: Schematic diagram of a pyrotechnic delay element (Tsang, 2005)

Traditional pyrotechnic mixing includes both wet (Morgan and Rimmington, 2012; Teipel, 1999; Chan et al., 1998) and dry (Teipel, 1999) mixing of the fuel and oxidiser powder. The latter works for the most part but does not ensure homogeneity of the mixture or ensure batch consistency (Blair et al., 2015). Wet processing is preferred over dry processing for safety reasons as a significant amount of static charge can build up between dry powders which may be enough to ignite the composition (Puszynski et al., 2007; Teipel, 1999).

As mentioned previously, by increasing the contact area between the fuel and oxidiser, the probability of two atoms interacting and reacting is increased. This can be accomplished in two ways; adding a polymeric binder to the composition or reducing the particle size.

Polymeric binders act by wetting the surface of the pyrotechnic particles, improving the contact area available for reaction by providing a void-free matrix for the particles, and giving

improved safety and mechanical properties (Colclough et al., 1994). Reducing the average particle size to the nanometer ( $< 100$  nm) region greatly improves the surface area to volume ratio of the particles (Pantoya and Granier, 2005). A typical nanoparticle may contain 1 000 or fewer atoms, with around 100 of those on the surface (Pantoya and Granier, 2005). This ratio of 1 in 10 atoms on the surface of a particle is far more desirable than the 1 in 30 000 mentioned previously for a 25  $\mu\text{m}$  diameter particle. Reducing the size of aluminium fuel particles to nanometer range can have drastic effects on aspects such as burn speed and ignition delay time (Francis, 2007). Nanotechnology is still relatively new and nanoparticles are appreciably more expensive than the more traditional micron-sized particles.

If a melt-processible energetic binder is used as the oxidant in a pyrotechnic composition, then the composition would be able to be processed and mixed in the polymer melt without the need for organic solvents, thus eliminating waste in the production. These components could be time delay compositions or primary explosives, depending on the products produced, but would more likely take the form of primaries due to the large amount of gas released when using both fluorinated and nitrated polymers (Glavier et al., 2015; Kappagantula, 2014; Talawar et al., 2009; Watson, 2007; Agrawal, 1998). The amount of gas produced and the rate at which it is produced could induce a pressure wave strong enough to detonate the main secondary explosive.

## **2.5 Additive manufacturing of pyrotechnics**

Although certain continuous processing techniques have been used for processing energetic materials, production is still largely limited to batch technology (Kowalczyk et al., 2007). Extrusion is becoming a more attractive method of processing of energetic materials as it offers several advantages over conventional batch processing (Dombe et al., 2015). These advantages include, but are not limited to (Dombe et al., 2015):

- i. Much smaller quantities of materials in the hazardous mixing zone at any given time when compared to batch processing
- ii. Flexible systems which can produce a variety of energetic materials
- iii. Less material wastage
- iv. Improved quality control
- v. Increase in production capacity

Advances in additive manufacturing technology are also allowing it to become more popular as a processing technique for energetic materials (Clark, 2016; Whitmore, 2015; Segó, 2015). One of the constraints that pyrotechnic elements must conform to is a volume constraint imposed by the available space inside of existing detonator shells (Rose et al., 2011). By using modern additive manufacturing techniques, such as fused deposition modelling, polymeric pyrotechnic compositions could be manufactured to varying spatial requirements on site. These shapes could also enhance burn properties and make the burning more efficient (Whitmore, 2015).

Conventional approaches to additive manufacturing of energetic materials have focused on using the common thermoplastic, acrylonitrile butadiene styrene (ABS), as the polymeric carrier. Whitmore et al. (2013) demonstrate the use of 3D-printed ABS as an attractive alternative rocket fuel to the thermosetting hydroxyl-terminated polybutadiene (HTPB). Clark (2016) used ABS as a binder for an Al/MoO<sub>3</sub>/KClO<sub>4</sub> nanothermite system due to its established use as a 3D printing material.

Very little has been published in the open literature on using an oxidising thermoplastic polymer as the primary oxidiser in an additively manufactured system, and not simply as a binder. By using an oxidising polymer, oxidiser particles will not need to be added to the composition in addition to the fuel particles. This will lower the overall fuel loading of the composition and make it easier to process.

## CHAPTER 3: EXPERIMENTAL METHODS

### 3.1 Thermodynamic simulation

EKVI thermodynamic software was used to perform simulations of the reactions before any physical experiments were performed. This was done in order to assess the compositions' viability for use in energetic compositions. The software contains a database of various chemicals and their thermodynamic properties. No additions or modifications to this database were made.

The software solves a given reaction iteratively by minimising the Gibbs free energy of the reaction. The software also selects possible products from the database based on the elemental analysis of the reagents given. Probable products are then calculated during the simulation using the activity coefficients of the list of possible products (Noläng, 2007).

All simulations were performed by varying the fuel ratio from 1 – 99 wt.% in increments of 1 wt.%. Expected temperature, enthalpy and product profiles were generated.

### 3.2 Solution casting

In order to obtain compositions that could be used to evaluate the energetic performance of the compositions, pyrotechnic films were cast using solvent techniques. This is a much safer method of mixing polymer-based pyrotechnics than other compounding techniques, such as extrusion, as it eliminates many of the stimuli to which the composition may be sensitive, such as heat, electrostatic discharge (ESD), and friction.

Firstly, a suitable solvent is selected. The solvent should effectively dissolve the polymer but the reducing agent should remain insoluble in the solvent. 10 wt.% solutions were prepared. The polymer was left to dissolve in the solvent for 24 hours to ensure complete dissolution.

After 24 hours, aluminium powder was added to the solution. The solution was then stirred to obtain a homogeneous mixture. The mixture was stirred for at least an hour to ensure homogeneity, and then quickly emptied into a Teflon<sup>®</sup>-lined baking pan. The pans were then left to allow the solvents to evaporate.

As the solvent evaporates, the polymer comes out of solution and the aluminium particles are effectively trapped in the polymer matrix, creating an even distribution of fuel particles in the pyrotechnic composition. Compositions with fuel loadings of 15 – 60 wt.% were prepared.

Mesitylene was used as the solvent for the PCTFE, THF for the FK-800<sup>®</sup> and NMP for the Dyneon 31508<sup>®</sup>.

10 wt.% solutions of the PCTFE and FK-800<sup>®</sup> were prepared. 5 wt.% solutions of Dyneon<sup>®</sup> 31508 were prepared as a 10 wt.% solution was found to be too viscous for easy pouring. The polymers were left to dissolve in the solvents for 24 hours to ensure complete dissolution (Yang, 2014).

### 3.3 Open burn tests

In order to determine if the composition is ignitable and whether or not it will sustain burning, open burn tests were performed. A small amount of material was laid in a line and exposed to an open flame produced by a commercial butane torch.

### 3.4 Extrusion trials

Extrusion trials were performed using the unfilled polymer. Once a polymer contains a solid filler, the viscosity increases and processing generally becomes harder. So initial trials were performed using the unfilled polymer and, if successful, the filler would be added in later trials.

Trials were performed on a HAAKE Rheomix CTW5 – Minilab II microcompounder. This is a twin-screw compounder using conical screws that can be run in a co-rotating or counter-rotating configuration. A schematic of the system is shown in Figure 10. Only one temperature can be set for the entire system, rather than the conventional temperature zones found in most extruders. The compounder also allows a circulating option where the valve at (a) is pneumatically actuated to allow the polymer to flow either into the recirculating channel back toward the screws or out through the die at (b). This allows for very good mixing to be achieved during compounding. The minimum and maximum screw diameters are 5 mm and 14 mm, and the screw length is 109.5 mm.

Due to the expected shear sensitivity of the material, the compounder was run in a counter-rotating configuration and without the circulating option and at a low RPM at 230 °C.

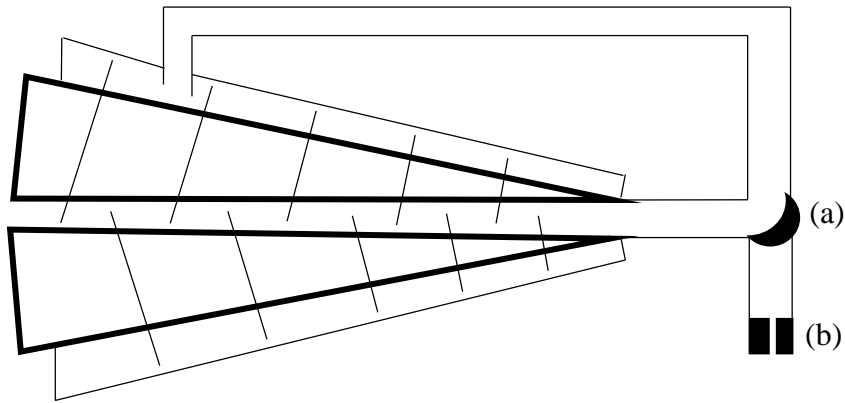


Figure 10: Schematic of the HAAKE Rheomix CTW5 microcompounder

Experiments were then scaled up to obtain larger sample sizes. The polymer and magnesium hydroxide powder were first compounded in a TX28P co-rotating twin screw extruder with intermeshing kneader elements with a forward transport action. The extruder had a barrel diameter of 28 mm and an L/D ratio of 18:1.

The compounded sample was pelletised and then fed through a lab-scale single screw extruder which was able to control the diameter of the resultant filament. A schematic of this single screw extruder is shown in Figure 11 and the details are summarised in Table 8.

Conditions used for the extrusion trials are summarised in Table 9.

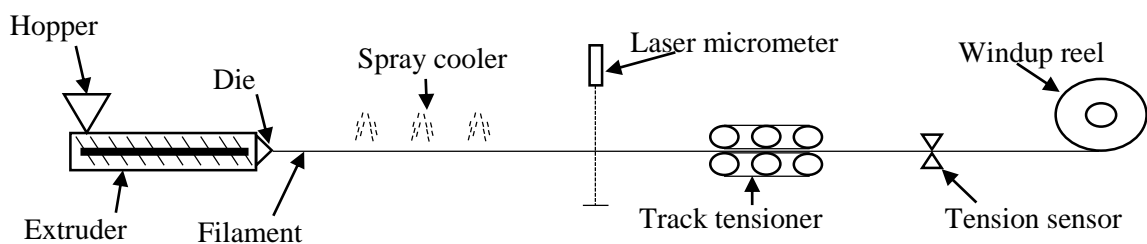


Figure 11: Schematic of lab-scale single screw extruder setup used in extrusion trials

Table 8: Details of lab-scale single screw extruder used in extrusion trials

Property	Value
Barrel internal diameter /mm	17.8
L/D	23:1
Max. linear draw speed /cm·s <sup>-1</sup>	18.7
Max temperature at die /°C	400

The conditions used during extrusion and compounding trials are shown in Table 9.

Table 9: Conditions used for extrusion trials

Property	Twin screw compounding	Single screw extrusion
Screw speed /rpm	20	46
T <sub>Feed</sub> /°C	190	190
T <sub>Zone 1</sub> /°C	210	210
T <sub>Zone 2</sub> /°C	220	220
T <sub>Zone 3</sub> /°C	230	-
T <sub>Die</sub> /°C	230	230
Cooling	Water bath	Spray cooling

### 3.5 Characterisation

FTIR analyses were performed using a PerkinElmer Spectrum 100 FTIR spectrometer with a Universal ATR sampling accessory. Samples were analysed in the wavenumber range of 4000 – 650 cm<sup>-1</sup>. 16 runs were performed for each sample in order to obtain an average reading. Spectrum software was then used for baseline correction and smoothing of the resultant spectra.

TGA analyses were performed using a PerkinElmer TGA 4000 Thermogravimetric Analyzer. Approximately 10 – 15 mg of sample was placed in an alumina cup and placed in the furnace. The temperature was ramped up from ambient conditions to 600 °C at a rate of 10 °C·min<sup>-1</sup>. Analyses were performed in air.



DSC analyses were performed using a PerkinElmer DSC 4000 Differential Scanning Calorimeter. Approximately 10 – 15 mg of sample was weighed into an aluminium tin and placed in the furnace. The temperature was ramped up from ambient conditions to (a) 350 °C for PCTFE, (b) 300 °C for the FK-800<sup>®</sup> and Dyneon 31508<sup>®</sup> resins, and (c) 250 °C for the LFC-1<sup>®</sup> fluoroelastomer, at a rate of 10 °C·min<sup>-1</sup>. The temperature was then brought back down to 30 °C at a rate of 10 °C·min<sup>-1</sup>. This cycle was repeated once more for each sample in order to ensure the thermal history of the polymer was negated. Analyses were performed in air. Pyris Series software was used to perform the analysis of the DSC curves.

XRF measurements were performed using an ARL Perform'X Sequential XRF instrument and Uniquant software was used for the analyses. The software analyses for all elements in the periodic table between Na and U, but only elements found above the detection limits were reported. The aluminium sample was prepared as boric acid powder briquettes. All other samples were prepared as pressed powders.

XRD measurements were performed on a Bruker D8 Advance diffractometer with 2.2 kW CuK $\alpha$  radiation ( $\lambda=1.5406$  nm) fitted with a LynxEye detector with a 3.7° active area. Samples were scanned in reflection mode in the angular range 5° to 90° 2 $\theta$ . Bruker Diffrac<sup>Plus</sup> EVA software was used for data analysis.

Particle size distributions were measured using a Mastersizer Hydrosizer 2000 machine with water as the dispersant. The water was continuously stirred and ultrasound was used to prevent agglomeration as much as possible. Two sets of five measurements each were run for each sample in order to obtain an average value.

BET analyses were performed using a Micromeritics Tristar II surface and porosity BET analyser using liquid nitrogen and a nitrogen atmosphere. Samples were first degassed at 150 °C for 12 hours using a Micromeritics VacPrep 061 Sample Degas System. Tristar II 3020 software was used to perform the analysis.

SEM analyses were performed using a ZEISS Gemini ULTRA Plus field emission scanning electron microscope (SEM) at 1.00 kV. The samples were coated five times with carbon from different angles. A SEM auto-coating unit E2500 (Polaron Equipment Ltd) sputter coater was used for the coating.

Rheology measurements were conducted at 230 °C at the Council for Scientific and Industrial Research (CSIR) using a SmartRheo capillary rheometer. The piston used was type 8.09 PT. The capillary diameter was 1 mm and the L/D ratio was 5.

Differential thermal analysis (DTA) was performed on the solution-cast samples using a Shimadzu Differential Thermal Analyzer DTA-50. Approximately 10 – 15 mg of sample was weighed into an alumina pan and an equal mass of aluminium oxide (Al<sub>2</sub>O<sub>3</sub>) DTA standard weighed into a separate pan. The temperature was increased from 30 °C to 600 °C at a rate of 50 °C·min<sup>-1</sup>.

Bomb calorimetry was performed using a Parr 6200 calorimeter utilising a 1104B 240 mL high-strength bomb. The tests were carried out in a 3.0 MPa helium atmosphere. Approximately 500 – 700 mg of sample was weighed into the pan and then ignited using an electrically heated 30 gauge nichrome wire. A cross-section of the calorimeter combustion vessel is shown in Figure 12.

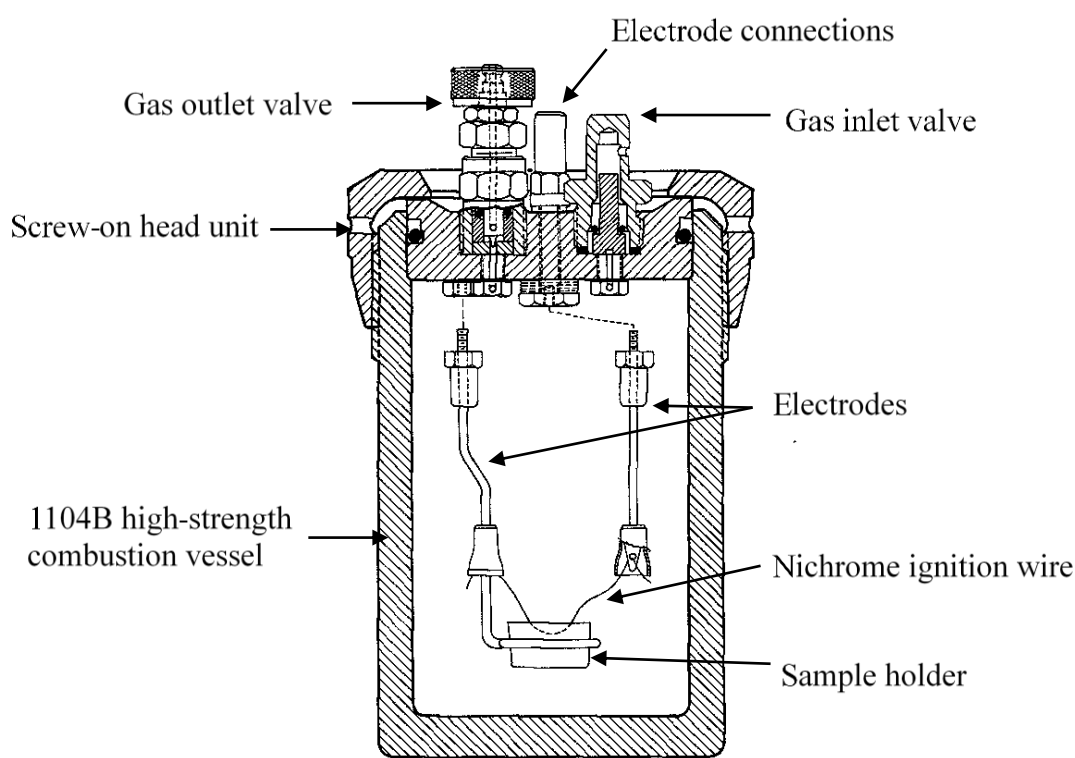


Figure 12: Cross-section of combustion vessel used for bomb calorimetry

The condensed combustion products were collected from the combustion vessel after the test runs and also subjected to XRD and SEM analyses.

In addition to the regular SEM analysis, SEM-EDS was also performed on the products collected. This analysis was performed with the aforementioned ZEISS microscope, and AZtec software was used to perform the EDS analysis. Samples were cast in an epoxy resin. The hardened resin was then polished with progressively finer sand paper in order to get a smooth surface which allows for a higher accuracy when using the EDS software.

The clean resin was analysed with the EDS software and found to contain 78 wt.% carbon, 13 wt.% oxygen and 9 wt.% chlorine. It should be noted that the software does not detect the hydrogen content of the sample. These values were used when correcting for resin content in the final analysis.

## CHAPTER 4: SOLIDS CHARACTERISATION

### 4.1 Aluminium

Atomised aluminium powder was obtained from Grinman (Pty) Ltd. The powder was sieved through a 25  $\mu\text{m}$  screen prior to use. Otherwise, the powder was used as delivered. The XRF and XRD results for the aluminium are detailed in Table 10 and Figure 13.

Table 10: XRF analysis results for Aluminium powder used

Element	Al	Mg	Fe	Si	Na	V
Wt. %	99.57	0.19	0.11	0.05	0.03	0.01

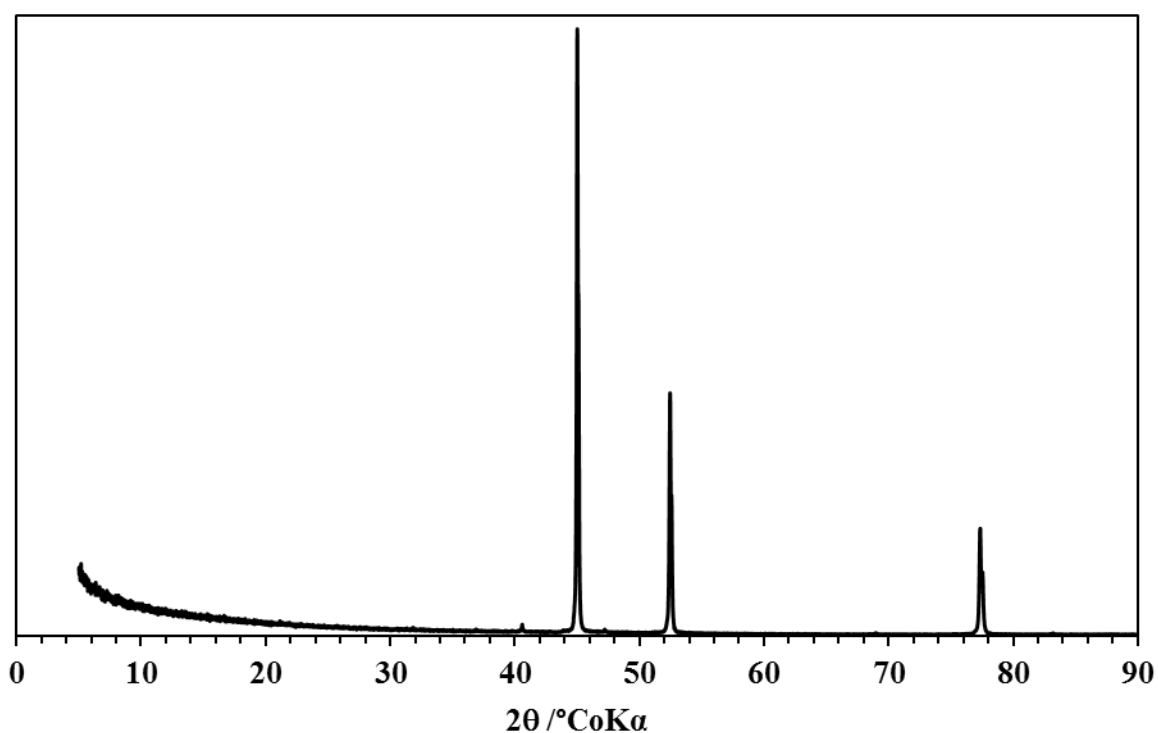


Figure 13: XRD analysis result of aluminium powder used

The XRD and XRF analyses both show that the aluminium used was pure, with only trace amounts of other metals present. All other metallic elements that were identified in the XRF analysis made up less than 0.01 wt. % of the sample.

The aluminium powder was sieved through a 25  $\mu\text{m}$  sieve, and the resultant particle size analysis as obtained from the Mastersizer is shown in Table 11 and Figure 14.

Table 11: Particle size analysis results for aluminium powder

<b>D<sub>10</sub></b>	<b>D<sub>50</sub></b>	<b>D<sub>90</sub></b>
6.91 $\mu\text{m}$	15.9 $\mu\text{m}$	32.7 $\mu\text{m}$

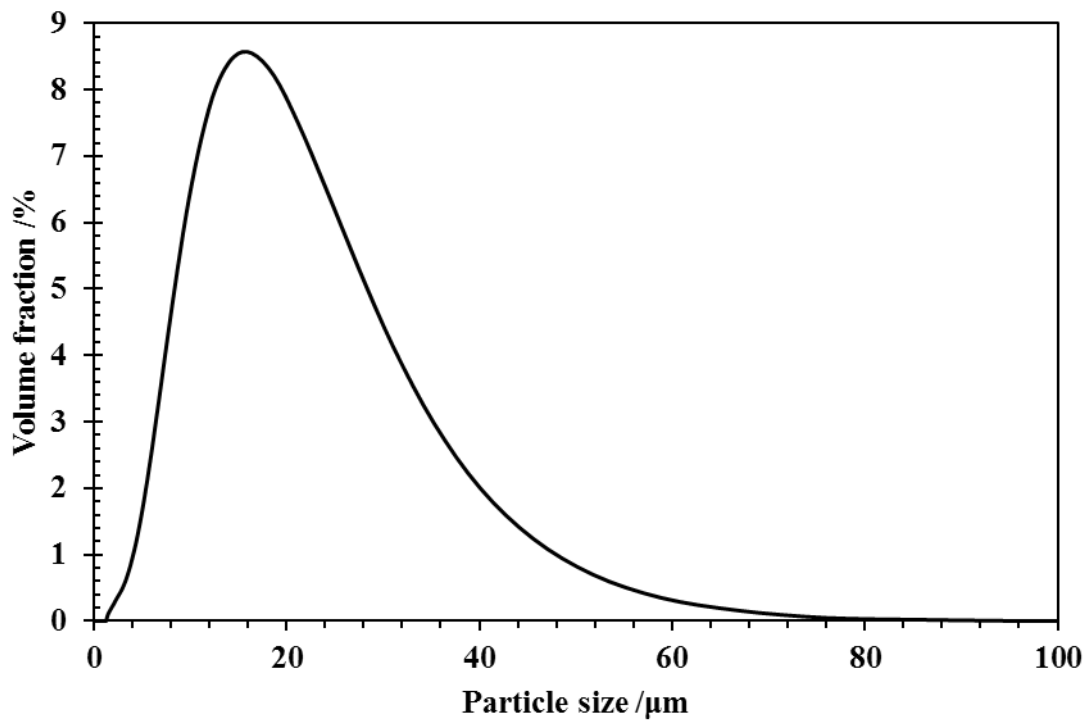


Figure 14: Particle size distribution of aluminium powder

According to the particle size analysis shown above, a fraction of the particles appears to be bigger than 25  $\mu\text{m}$ , however 88 vol.% of the particles are smaller than 25  $\mu\text{m}$ . This larger fraction is attributed to agglomeration of the particles.

The specific surface area of the aluminium particles was determined using BET analysis and found to be 40  $\text{m}^2\cdot\text{g}^{-1}$ .

SEM analysis was performed in order to determine the morphology of the particles. Result is shown in Figure 15.

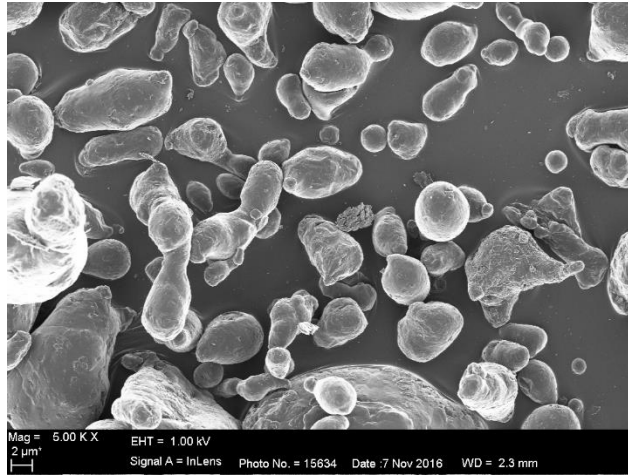


Figure 15: SEM image showing morphology of aluminium particles

The SEM results show that the aluminium particles are relatively spherical or elongated spheres. This morphology is important to consider when one considers the final application as a filler in a polymer as well as a reducing agent in a pyrotechnic composition. For optimal energetic properties, a higher surface area to volume ratio, such as flakes, would be preferred as this would mass transfer and kinetic properties of the reaction. However, this particle shape has an adverse effect on the mechanical properties of the final product (Potgieter et al., 2016). Therefore, in order to preserve the mechanical properties of the parent polymer for extrusion, spherical particles were used.

## 4.2 Magnesium hydroxide

In order to safely test the extrudability and printability of the final compound, magnesium hydroxide was used as a model filler. Magnesium hydroxide is a well-known flame retardant in the polymer industry and using this would ensure that there would be no reaction of the compound from the intense conditions that occur during extrusion. Lab-grade magnesium hydroxide powder from Merck was used. The magnesium hydroxide powder was sieved through a 25  $\mu\text{m}$  screen prior to use but otherwise was used as delivered.

The XRD and XRF analyses of the magnesium hydroxide powder are shown in Figure 16 and Table 12. Particle size analysis results are shown in Table 13 and Figure 17.

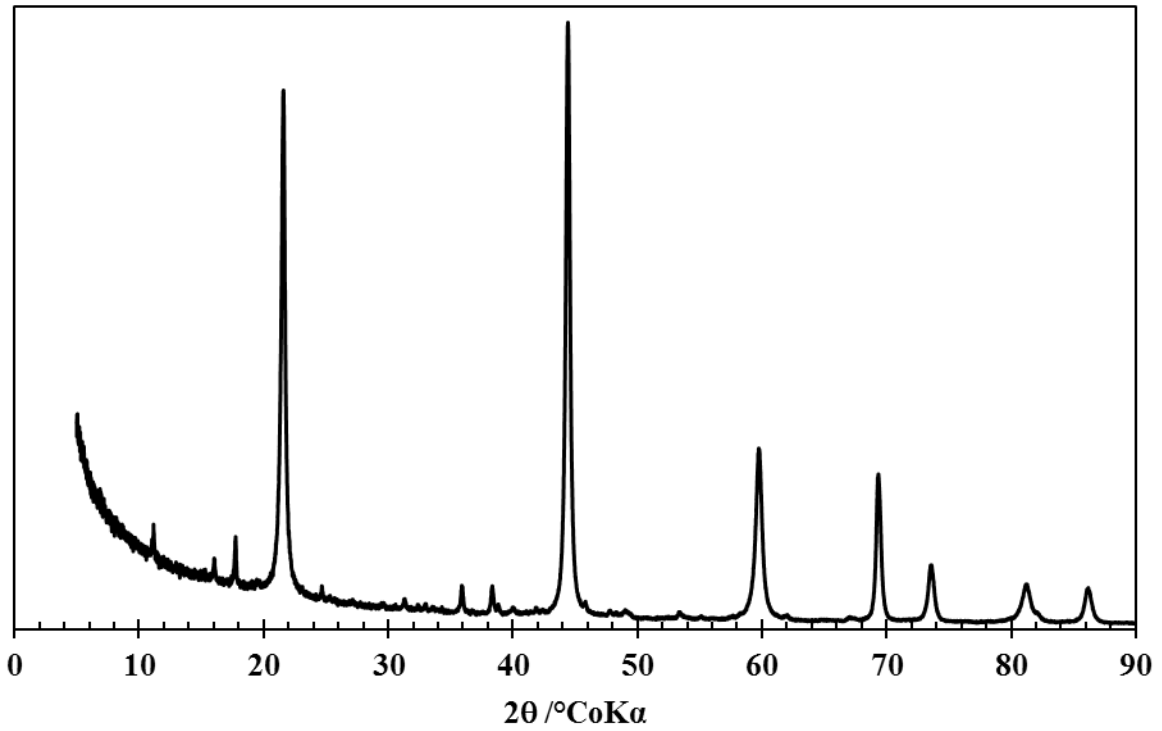


Figure 16: XRD analysis of magnesium hydroxide powder used

Table 12: XRF analysis of magnesium hydroxide powder

Element	Mg	Fe	Si	Ca	Ba	I
Wt. %	98.82	0.01	0.12	0.32	0.32	0.15

Table 13: Particle size analysis results of magnesium hydroxide powder

D <sub>10</sub>	D <sub>50</sub>	D <sub>90</sub>
2.4 μm	20.2 μm	47.7 μm

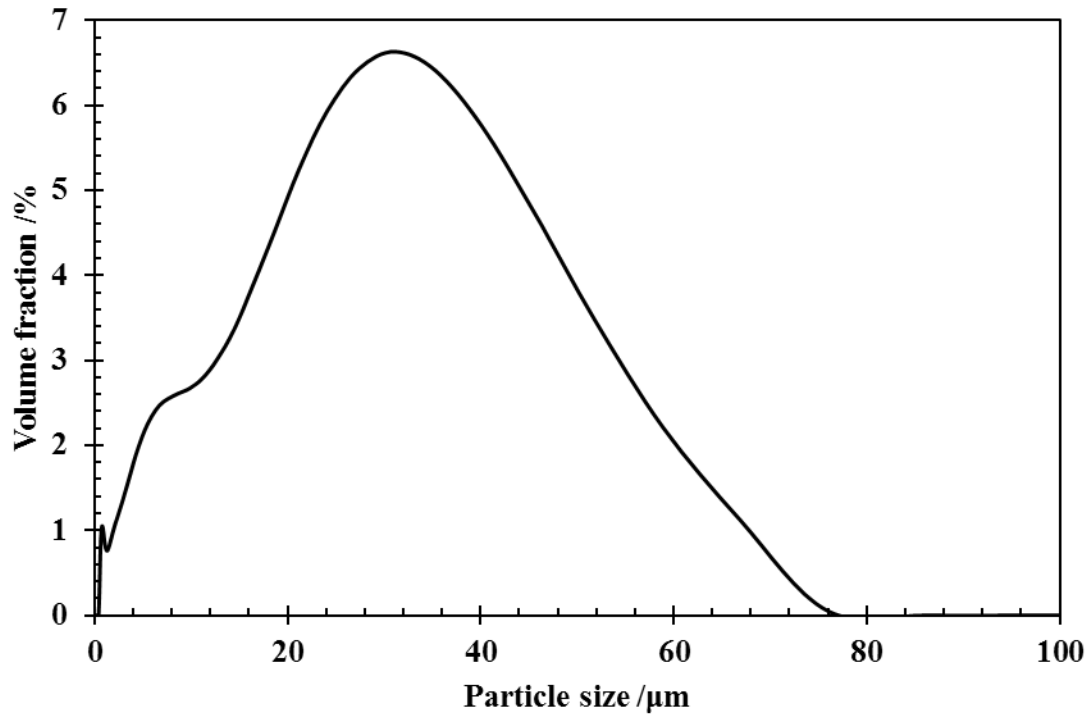


Figure 17: Particle size analysis of magnesium hydroxide powder

SEM analysis was performed to see the morphology of the magnesium hydroxide powder. The result is shown in Figure 18.

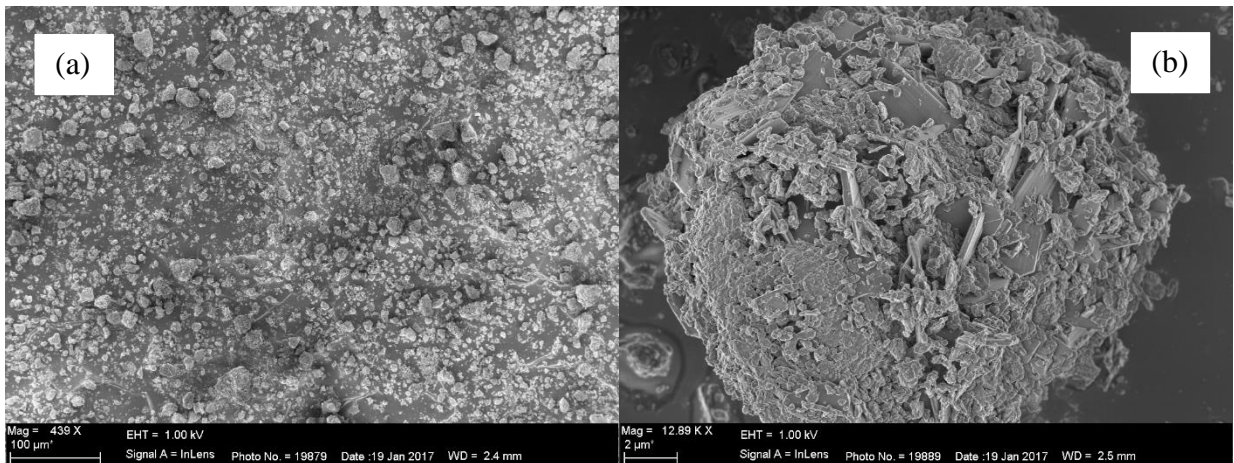


Figure 18: SEM images of magnesium hydroxide powder



The SEM analysis shows that the magnesium hydroxide powder is composed almost entirely of polygonal nano-platelets agglomerated into rough spheres. Figure 18(a) shows a field view of the magnesium hydroxide powder, showing the macro-spheres that have formed throughout the volume of the powder. Figure 18(b) is zoomed in on one of the spheres showing how it is composed of agglomerated nano-platelets. This explains the sharp peak seen on the extreme left side of the curve in Figure 17 as a small fraction of the platelets may have not agglomerated or become detached from the agglomerates.

### 4.3 Magnesium hydroxide as a model compound

A comparison between the aluminium and magnesium hydroxide powders is shown in Table 14.

Table 14: Summary of material properties of aluminium and magnesium hydroxide

Property	Aluminium	Magnesium hydroxide
Density /g·cm <sup>-3</sup>	2.7	2.34
Particle size (D <sub>50</sub> ) /μm	15.9	20.2
Mohs hardness	2.75	2.5
Morphology	Imperfect solid spheres	Spherical agglomerates of nano-platelets

Based on the summary shown above, it can be seen that the magnesium hydroxide powder used would act as a suitable model compound in place of the aluminium powder. The densities and particle size distributions are similar enough. The morphologies are slightly different. As mentioned previously, flake-like particles have an adverse effect on the mechanical strength of the final compound. Therefore, it was decided that if the compound could be processed successfully using magnesium hydroxide, then it should be possible to process the composition using the aluminium powder.

## CHAPTER 5: POLYMER CHARACTERISATION

### 5.1 Poly(chloro-trifluoroethylene)

Poly(chloro-trifluoroethylene) resin was obtained from Sigma-Aldrich. This resin comes in powder form. The resin was used as delivered without further chemical or physical manipulation.

FTIR analysis of the product was conducted and the result shown in Figure 19. The characteristic bands identified in Figure 19 are described in Table 15.

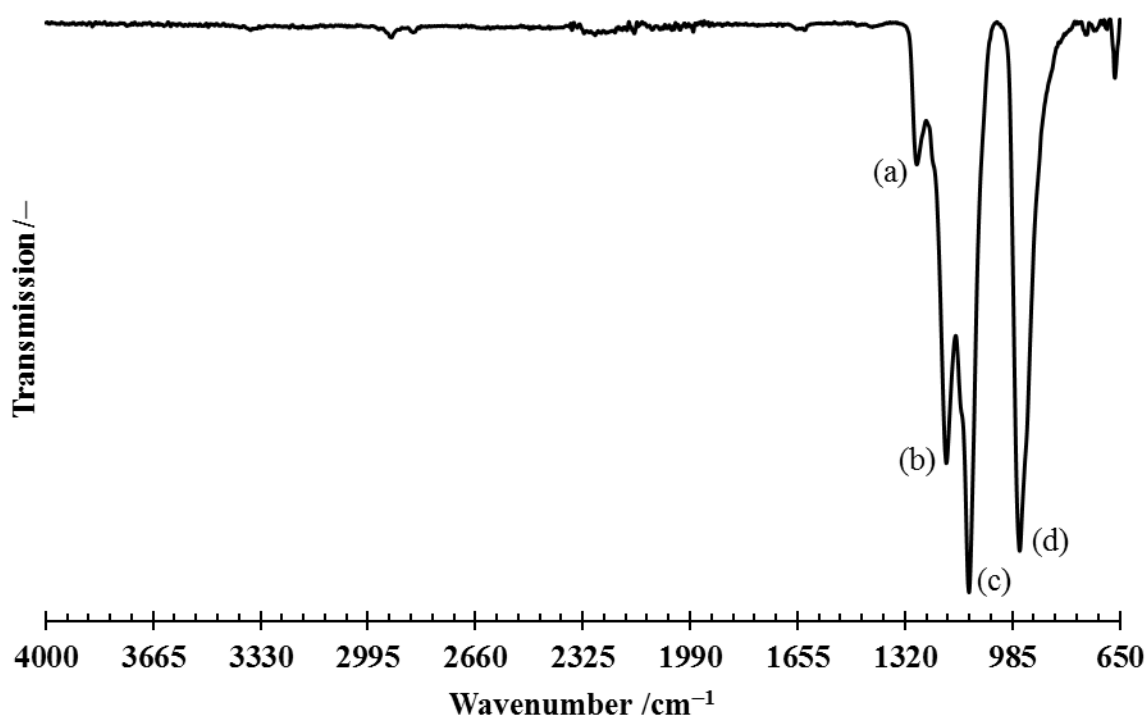


Figure 19: FTIR spectrum of PCTFE powder

Table 15: Characteristic bands from FTIR analysis of PCTFE powder

Band	Functional group vibration	Wavenumber /cm <sup>-1</sup>
(a)	C-F stretching	1000 – 1400
(b)	C-F stretching	1000 – 1400
(c)	C-F stretching	1000 – 1400
(d)	C-Cl stretching	600 – 800

This is as expected when compared to the structure of PCTFE which contains only C-F and C-Cl bonds.

TGA and DSC results are shown in Figure 20 and Figure 21. The results from the DSC are summarised in Table 16.

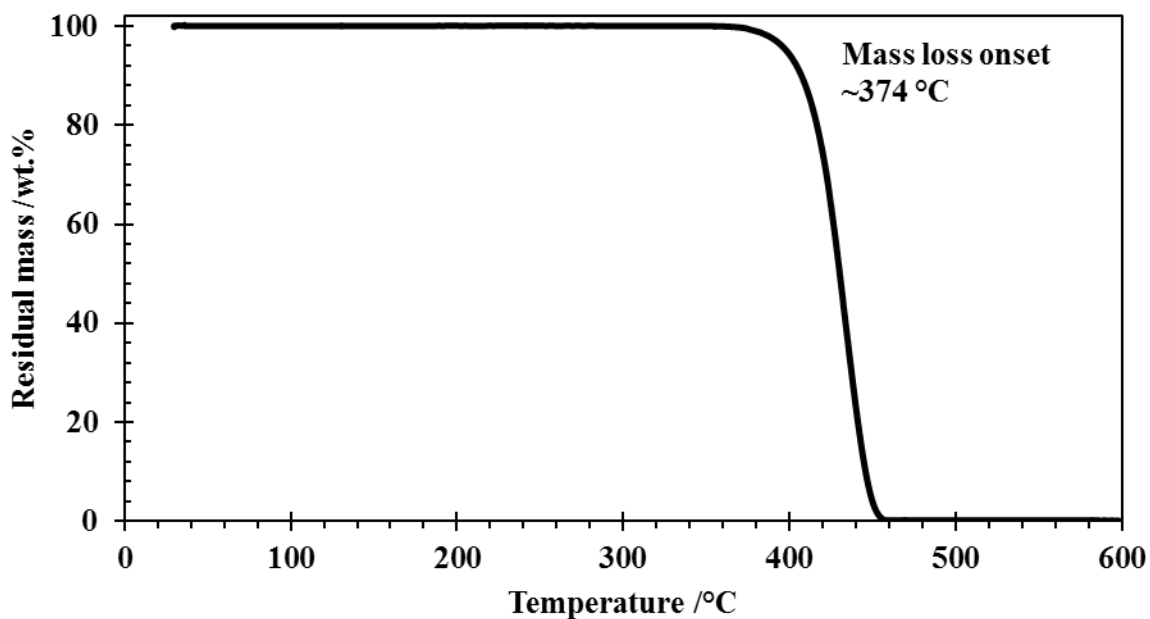


Figure 20: TGA curve for PCTFE powder obtained from Sigma-Aldrich

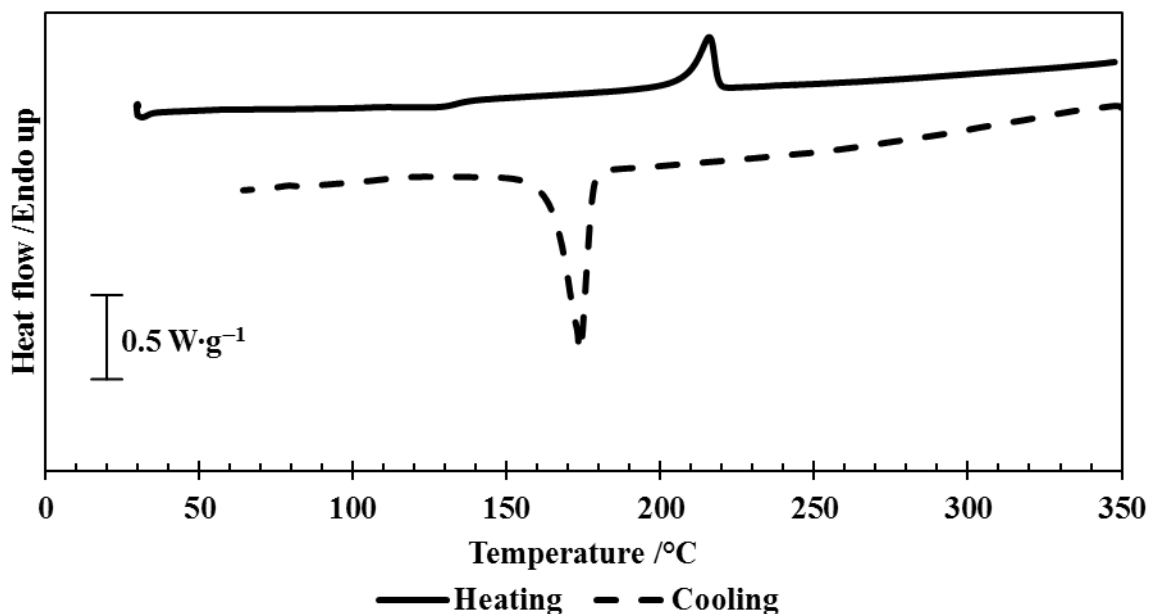


Figure 21: DSC heating and cooling curves for PCTFE powder obtained from Sigma-Aldrich

Table 16: DSC results for PCTFE powder

Property	$T_g$	$\Delta H_{\text{Melting}}$	$\Delta H_{\text{Crystallisation}}$
Value	133 °C	16.7 J·g <sup>-1</sup>	21.0 J·g <sup>-1</sup>

## 5.2 FK-800<sup>®</sup>

FK-800<sup>®</sup> resin was obtained from 3M. This resin is a copolymer containing 83,7 wt. % CTFE and 16,3 wt. % vinylidene fluoride (VDF).

Results of the FTIR analysis of the FK-800<sup>®</sup> resin are shown and discussed in Figure 22 and Table 17.

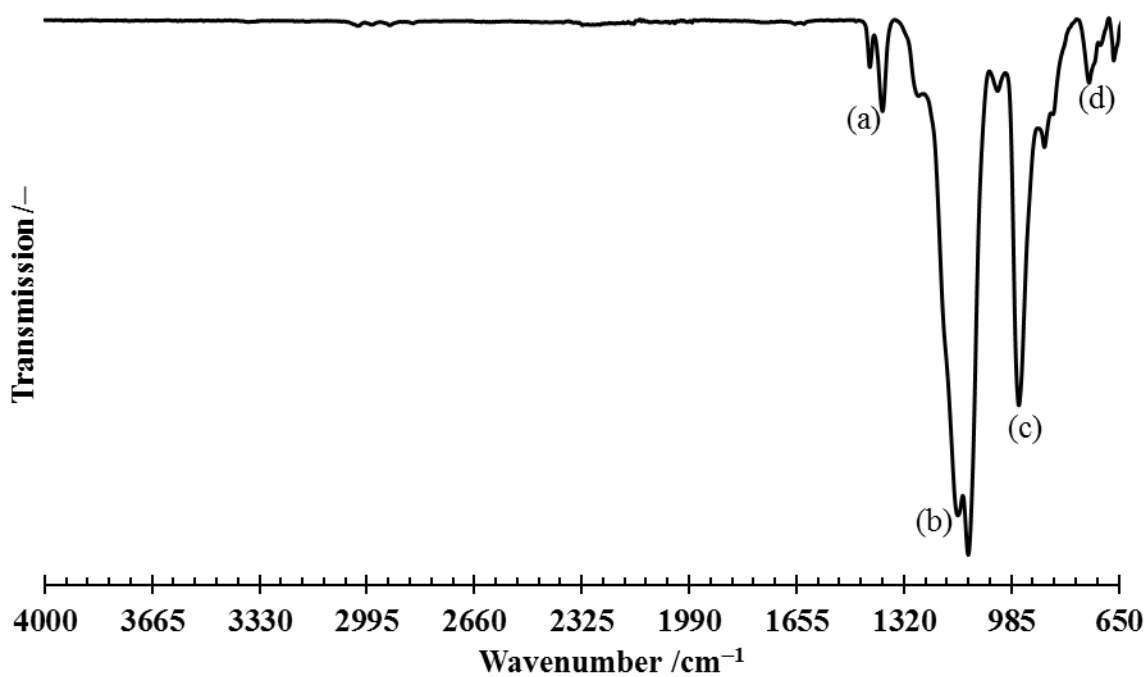


Figure 22: FTIR spectrum for FK-800<sup>®</sup> resin

Table 17: Characteristic bands from FTIR analysis of FK-800

Band	Functional group vibration	Wavenumber /cm <sup>-1</sup>
(a)	-C-H bending	1350 – 1480
(b)	C-F stretching	1000 – 1400
(c)	C-Cl stretching	600 – 800
(d)	C-Cl stretching	600 – 800

TGA and DSC results for the FK-800® resin are shown in Figure 23 and Figure 24.

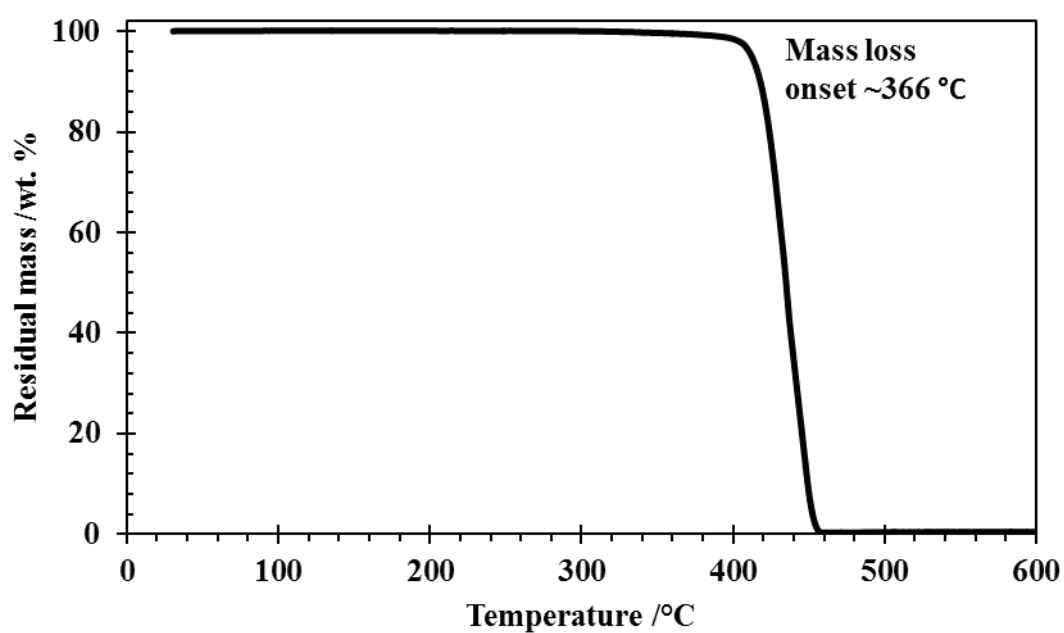


Figure 23: TGA curve for FK-800® resin

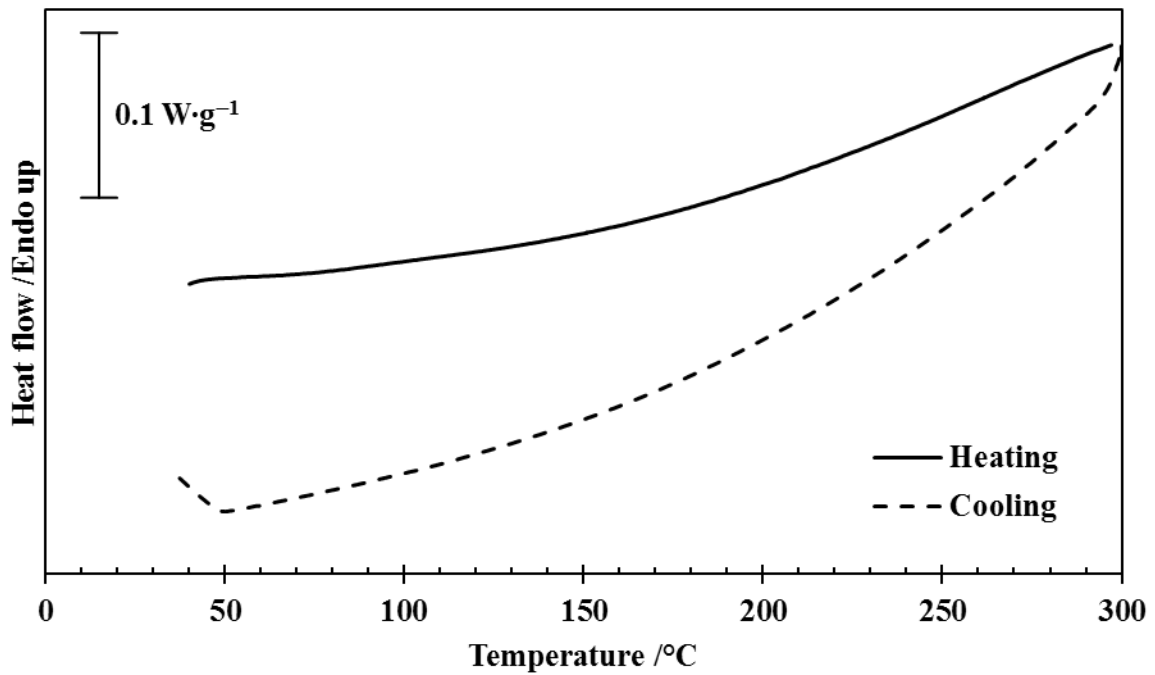


Figure 24: DSC curves for FK-800<sup>®</sup> resin

The DSC results of the FK-800<sup>®</sup> resin point to a completely amorphous polymer as indicated by the absence of any melting or crystallisation peaks during the heating and cooling cycles. Although the polymer feels hard at room temperature, it is also clearly above its  $T_g$  as the characteristic step shape is also not noticed in the DSC results. Rheology results of the FK-800<sup>®</sup> resin are presented in Figure 25.

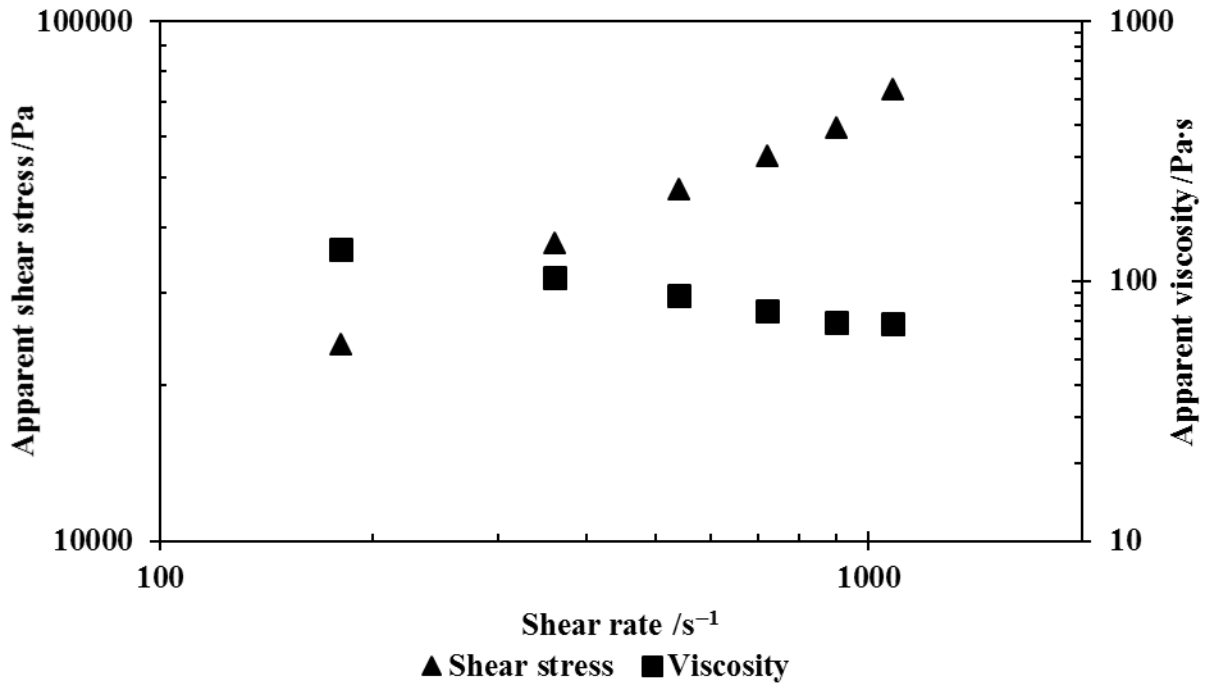


Figure 25: Rheology results for FK-800<sup>®</sup> resin

### 5.3 Dyneon 31508<sup>®</sup>

Dyneon 31508<sup>®</sup> resin was obtained from 3M. This resin is a copolymer containing 18.6 wt. % CTFE and 81.4 wt. % VDF.

Results of the FTIR analysis of the Dyneon 31508<sup>®</sup> resin are shown and discussed in Figure 26 and Table 18.

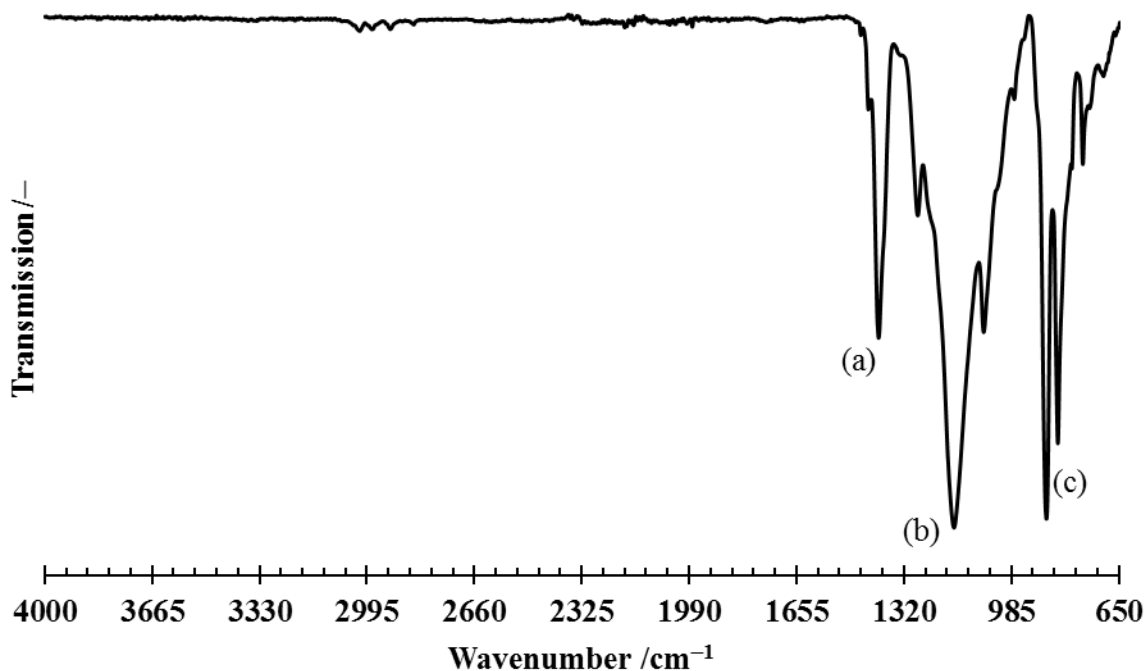


Figure 26: FTIR spectrum for Dyneon 31508<sup>®</sup> resin

Table 18: Characteristic bands from FTIR analysis of Dyneon 31508<sup>®</sup>

Band	Functional group vibration	Wavenumber /cm <sup>-1</sup>
(a)	-C-H bending	1350 – 1480
(b)	C-F stretching	1000 – 1400
(c)	C-Cl stretching	600 – 800

TGA and DSC results for the Dyneon 31508<sup>®</sup> resin are shown in Figure 27 and Figure 28. DSC results are shown in Table 19.



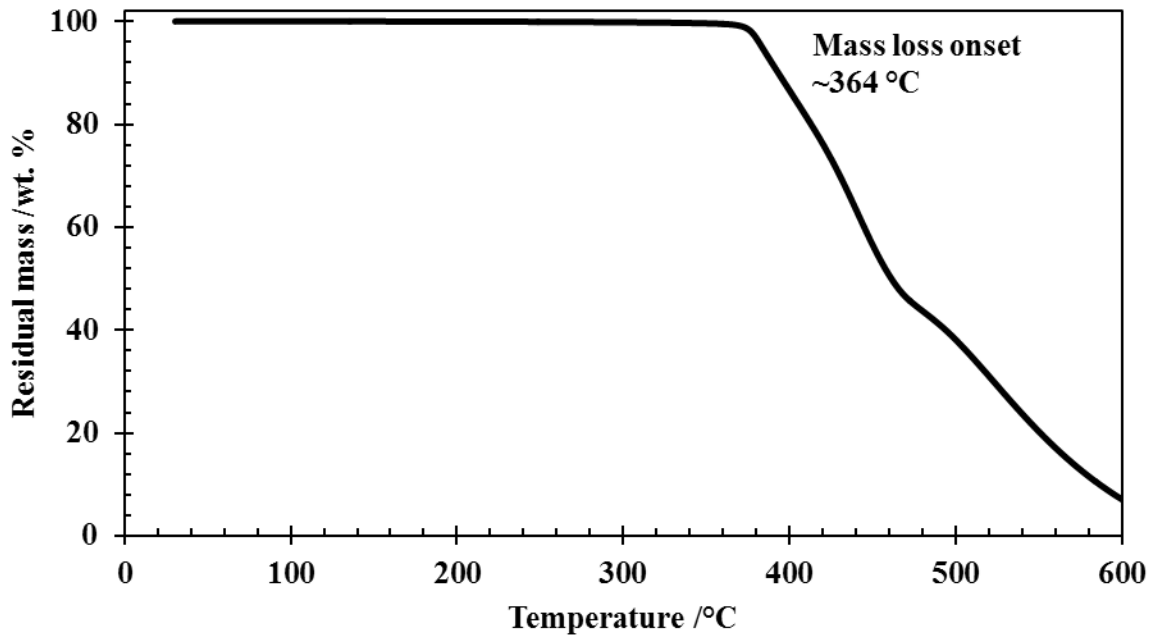


Figure 27: TGA curve for Dyneon 31508<sup>®</sup> resin

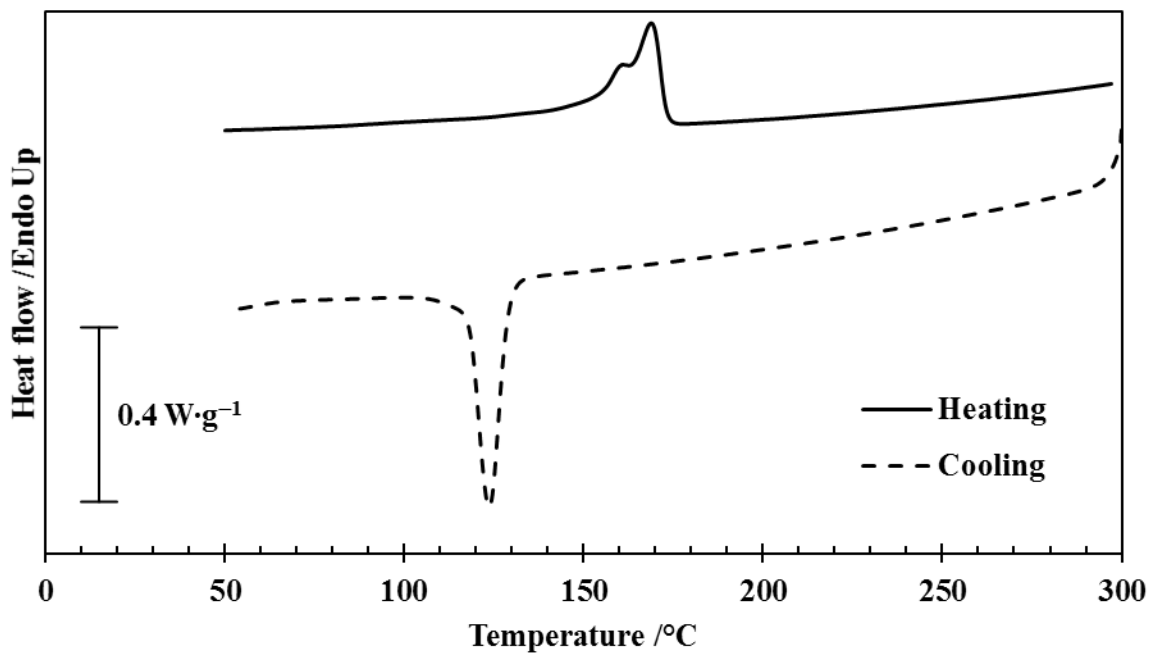


Figure 28: DSC curves for Dyneon 31508<sup>®</sup> resin

Table 19: DSC results for Dyneon 31508<sup>®</sup> resin

Property	$\Delta H_{\text{Melting}}$	$\Delta H_{\text{Crystallisation}}$
Value /J·g <sup>-1</sup>	22.4	25.6

The DSC results for the Dyneon 31508<sup>®</sup> resin show that it is a semi-crystalline polymer as there are definite melting and crystallisation peaks seen in Figure 28. This could have an effect on the maximum solids loading that the polymer can handle before becoming unprocessable. Viscosity results for the Dyneon 31508<sup>®</sup> resin are shown in Figure 29.

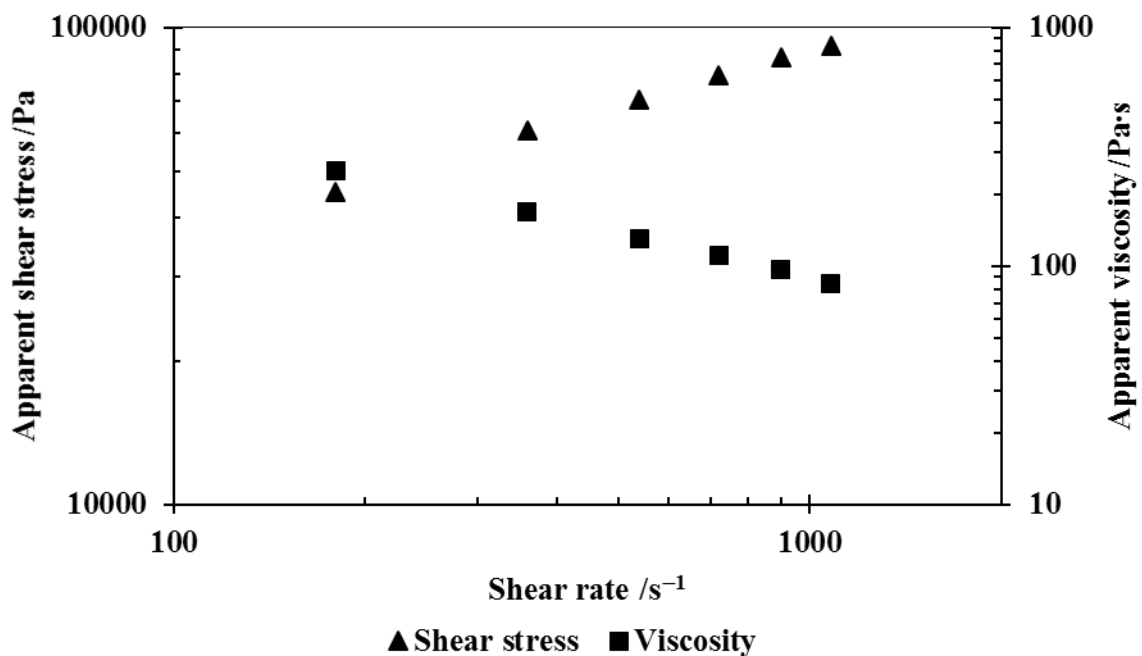


Figure 29: Rheology results for Dyneon 31508<sup>®</sup> resin

#### 5.4 LFC-1<sup>®</sup>

LFC-1<sup>®</sup> is an ultra-low molecular weight liquid fluoroelastomer obtained from 3M. This polymer was obtained with the intention of using it as a viscosity-reducing additive for the extrusion of the above copolymers if necessary. This liquid fluoroelastomer is made up of “1,1,2,3,3,3-hexafluoro-1-propene polymer with 1,1-difluoroethene” (3M<sup>(TM)</sup>, 2005)

The results of the FTIR analysis for the LFC-1<sup>®</sup> resin are shown in Figure 30 and Table 20.

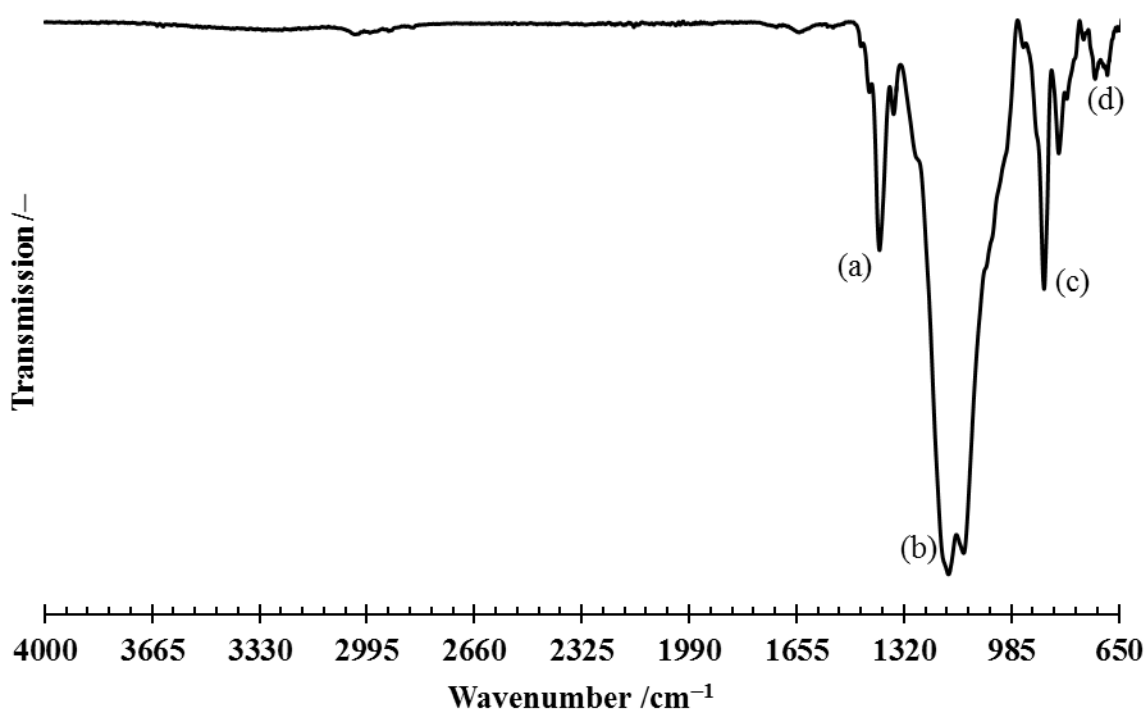


Figure 30: FTIR spectrum for LFC-1<sup>®</sup> fluoroelastomer resin

Table 20: Characteristic bands from FTIR analysis of LFC-1<sup>®</sup> fluoroelastomer

Band	Functional group vibration	Wavenumber /cm <sup>-1</sup>
(a)	-C-H bending	1350 – 1480
(b)	C-F stretching	1000 – 1400
(c)	=C-H bending	675 – 1000
(d)	=C-H bending	675 – 1000

TGA and DSC results for the LFC-1<sup>®</sup> resin are shown in Figure 31 and. DSC results are shown in Figure 32 and Table 21.

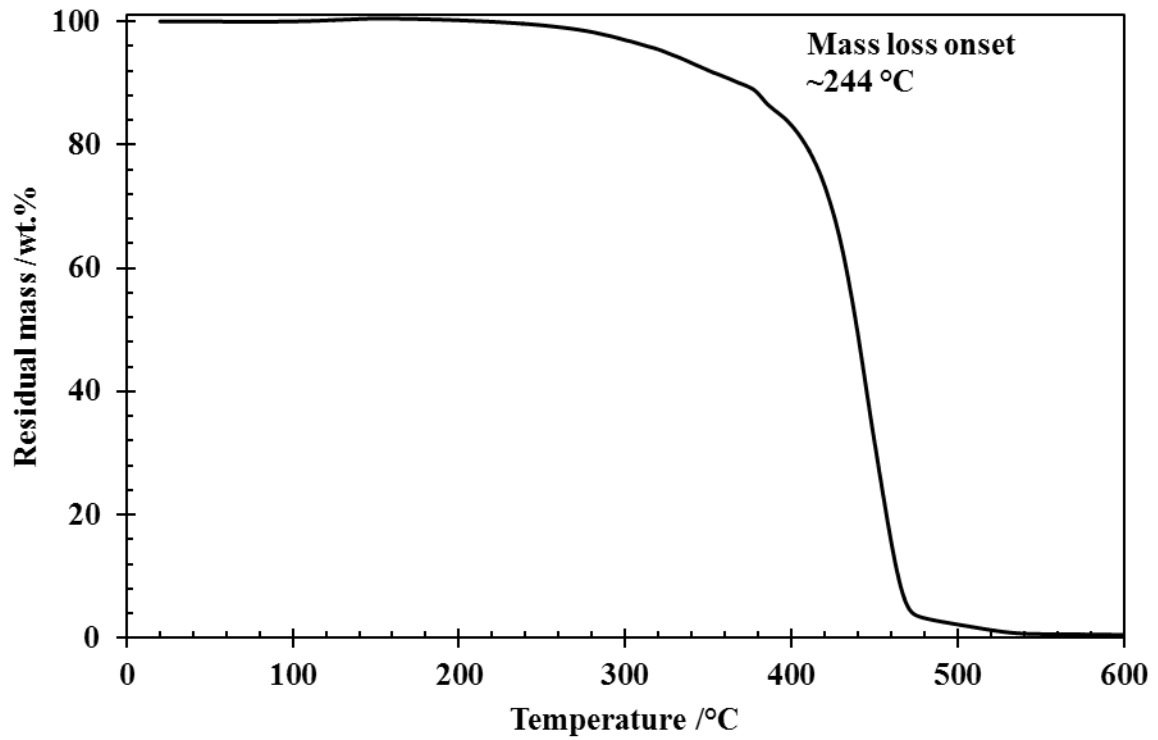


Figure 31: TGA curve for LFC-1<sup>®</sup> resin

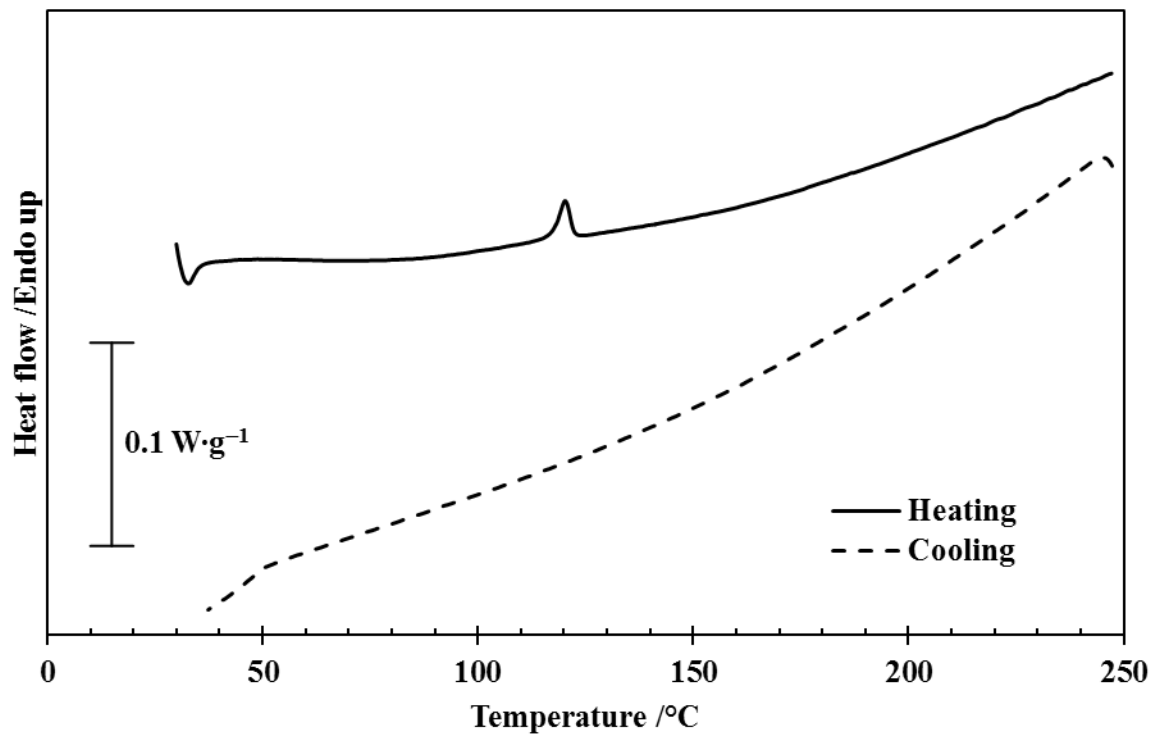


Figure 32: DSC curves for LFC-1<sup>®</sup> fluoroelastomer

Table 21: DSC results for LFC-1<sup>®</sup> resin

<b>Property</b>	$\Delta H_{\text{Melting}}$	$\Delta H_{\text{Crystallisation}}$
<b>Value /J·g<sup>-1</sup></b>	0.31	0.34

## CHAPTER 6: PCTFE SIMULATION

As mentioned previously, PTFE is not suitable for this investigation due to its inability to be melt processed and PCTFE was chosen instead as the oxidising polymer. Thermodynamic simulations were run using EKVI thermodynamic software in order to screen potential compositions.

### 6.1 Reducing agent selection

Simulations were run using PCTFE as the oxidising agent, and various metal fuels were tested. The maximum temperature and energy outputs were compared to determine energetic effectiveness of the compositions. All simulations were performed using the conditions expected in the bomb calorimeter described in section 3.5. These conditions lead to lower temperatures and higher energy outputs being experienced than would be during an open burn, as the limited volume and high pressure in the bomb suppresses gas formation. In an open burn (i.e. free volume for gas expansion), some of the energy would be utilised to evaporate certain products which remain condensed in the bomb calorimeter and so the energy output of the composition in an open burn would be slightly lower. Figure 33 shows the results of the simulations.

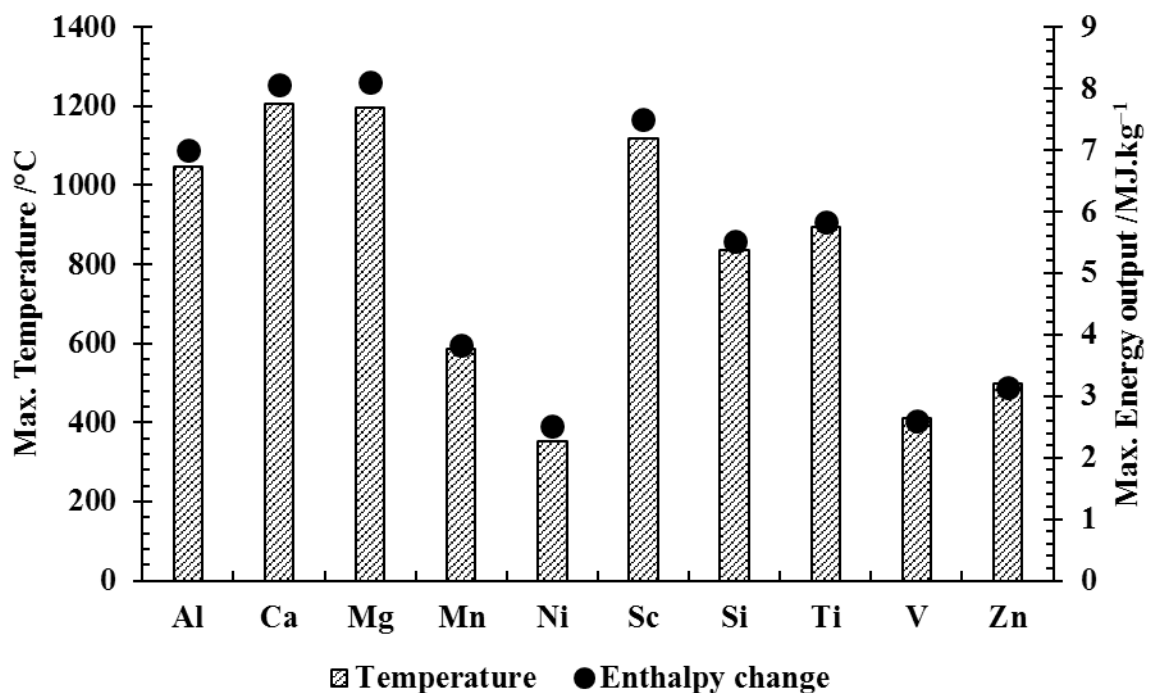


Figure 33: EKVI simulation results using PCTFE and various reducing agents

The results shown in Figure 33 show that there are four viable reducing agents which could be used with PCTFE as the oxidising agent, namely aluminium, calcium, magnesium, and scandium. Due to the prohibitively high cost of scandium metal and the relatively high sensitivities of calcium and magnesium, it was decided to use aluminium metal and, as such, all further simulations were performed using aluminium as the reducing agent.

## 6.2 Stoichiometric determination of PCTFE/Al system

In order to evaluate the thermodynamic performance of the PCTFE/Al system, the energy outputs and temperatures for compositions using varying fuel-oxidiser ratios were simulated. The results can be seen in Figure 34.

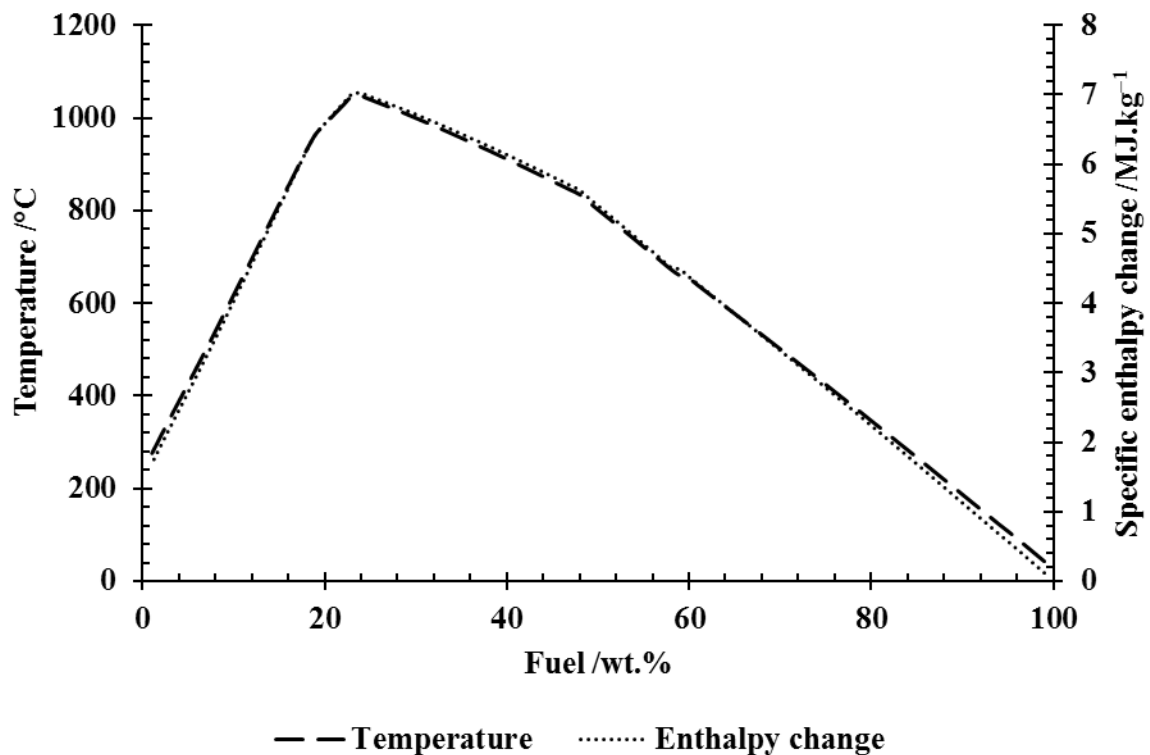


Figure 34: Simulated temperature and enthalpy results for PCTFE/Al compositions

The stoichiometric ratio between two components will occur where the energy output of the system is at a maximum. This point can be seen clearly on the chart above to occur at a fuel loading of 24 wt.%. This equates to a molar ratio of aluminium to CTFE monomer of approximately 1.4.

## CHAPTER 7: PCTFE RESULTS AND DISCUSSION

### 7.1 Solution casting

Mesitylene was selected as the solvent for PCTFE. This solvent is only effective at dissolving PCTFE at a temperature of over 140 °C. It is the only solvent that is able to dissolve PCTFE at a temperature below its normal boiling point (164 °C) (Barton, 1990).

It should be noted that, even at a temperature of 148 °C, the PCTFE did not completely dissolve in the mesitylene. The low molecular weight fraction effectively dissolved whereas the higher molecular weight fraction swelled substantially but did not dissolve. There was also substantial solvent loss during the process due to the “effective” dissolution temperature being so close to the boiling point of mesitylene.

When the solution was poured out the polymer came out of solution almost immediately due to the high evaporation rate of the solvent at the elevated dissolution temperature, as well as the rapid cooling experienced once the solution was removed from the oil bath.

Due to the fact that the polymer did not completely dissolve in the solution, a thin film was not formed as anticipated but rather a two distinct fractions formed. A thin, flimsy film formed from the low molecular weight fraction that did dissolve successfully and a larger solid mass from the high molecular fraction which swelled. Due to the large amount of swelling, the aluminium particles were able to be incorporated into the polymer bulk, resulting in a mixed composition.

### 7.2 Open burn tests

During the open burn tests, all samples ignited easily. The lower molecular weight fraction that had dissolved struggled to maintain burning. This is attributed to the fact that this fraction may be below the lower molecular weight limit which is required to maintain burning as explained by Rider et al. (2013). If the molecular weight of the polymer is too low, it will tend to evaporate before ignition occurs and the burning front will not propagate.

The higher molecular weight fractions all maintained burning more readily than the lower molecular weight fractions for all fuel loadings and all burned with a bright white light. The composition containing 60 wt.% fuel appeared to maintain burning less readily than the other compositions.



### 7.3 Extrusion trials

A number of extrusion trials were performed with the PCTFE resin. Details of the extrusion trials performed are shown in Table 22. After two unsuccessful runs with pure PCTFE, it was decided to attempt to extrude with a liquid fluoroelastomer, LFC-1<sup>®</sup>, obtained from 3M. It was theorised that the addition of this very low molecular weight elastomer should lower the melt viscosity and make it easier to process.

Table 22: Details of extrusion trials with PCTFE resin

Wt.% PCTFE	Wt.% LFC-1	Temperature /°C	Screw speed /RPM
100	-	290	11
100	-	280	20
90	10	240	50
99	1	290	20

The first three runs were unsuccessful. The polymer completely degraded to a dark brown, liquid state and was unable to successfully exit the extruder. The higher content of LFC-1<sup>®</sup> lowered the viscosity too much and the polymer was unable to maintain melt strength.

The final run was more successful with the polymer maintaining enough melt strength to be able to be pulled from the extruder. However, it still showed signs of heavy degradation, being a very dark brown colour. The strand also became extremely brittle on cooling and has a very porous final structure. This strand is shown in Figure 35.



Figure 35: Extruded PCTFE strand showing a large degree of degradation and porous structure

Based on these results, it was determined that the PCTFE homopolymer was unsuitable for extrusion and, by extension, 3D printing purposes. It was therefore decided to abandon any further investigation into the PCTFE homopolymer.

After further investigation, two industrially available copolymers were found which contain CTFE and vinylidene fluoride (VDF). FK-800<sup>®</sup>, containing ~83 wt.% CTFE, and Dyneon 31508<sup>®</sup>, containing ~18 wt.% CTFE. Both of these copolymers are marketed as more processable than the PCTFE homopolymer. Further investigations focussed on these two copolymers.

## CHAPTER 8: COPOLYMER SIMULATION

As with the PCTFE in Chapter 3, EKVI simulations were performed using the two copolymers and aluminium as the fuel. The energy and temperature profiles can be seen in Figure 36 and Figure 37. Once again, the conditions expected in the bomb calorimeter were simulated.

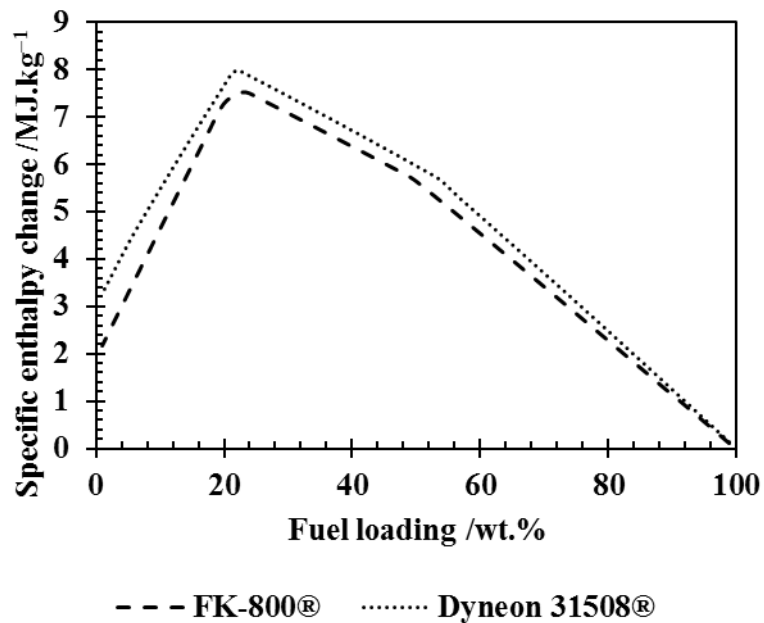


Figure 36: Simulated enthalpy releases for FK-800<sup>®</sup> and Dyneon 31508<sup>®</sup> compositions

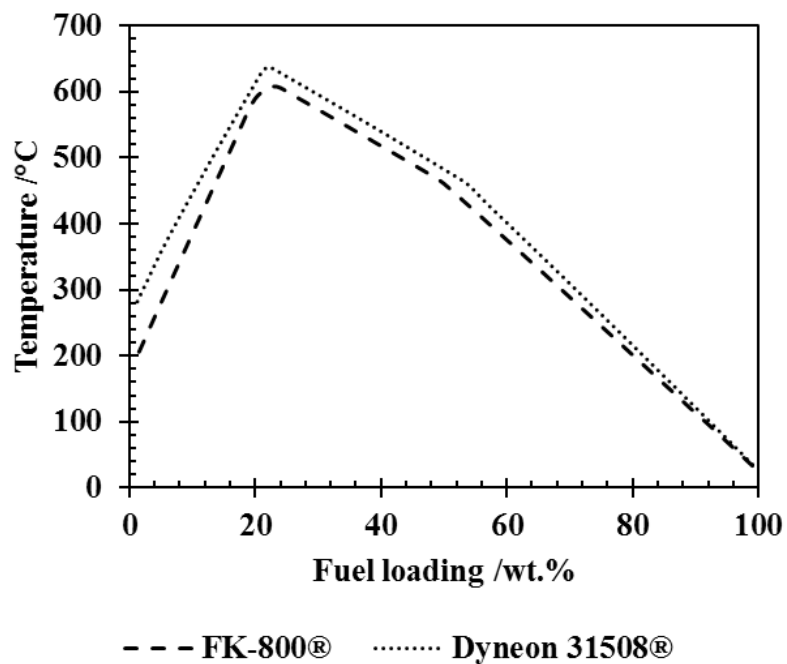


Figure 37: Simulated temperatures for FK-800<sup>®</sup> and Dyneon 31508<sup>®</sup> compositions

A problem expected by replacing the PCTFE homopolymer with a copolymer containing PVDF is the introduction of hydrogen into the system. This hydrogen content is expected to react preferentially with the fluorine and chlorine atoms liberated from the polymer to form hydrofluoric and hydrochloric acids. The product spectrum for the compositions are shown in Figure 38, Figure 39, Figure 40 and Figure 41. The specific enthalpy change curve for the reactions has been added to the figures to show the correlation between energy output and product formation.

The simulation software recognises a number of products based on the elemental composition of the reactants and determines whether or not these products might be formed during reaction through an iterative process which takes into account the activity coefficients of the product molecules. As such, the products shown in the figures below are only some of the primary products predicted to be formed upon reaction and not the full complex range of products that the software calculated.

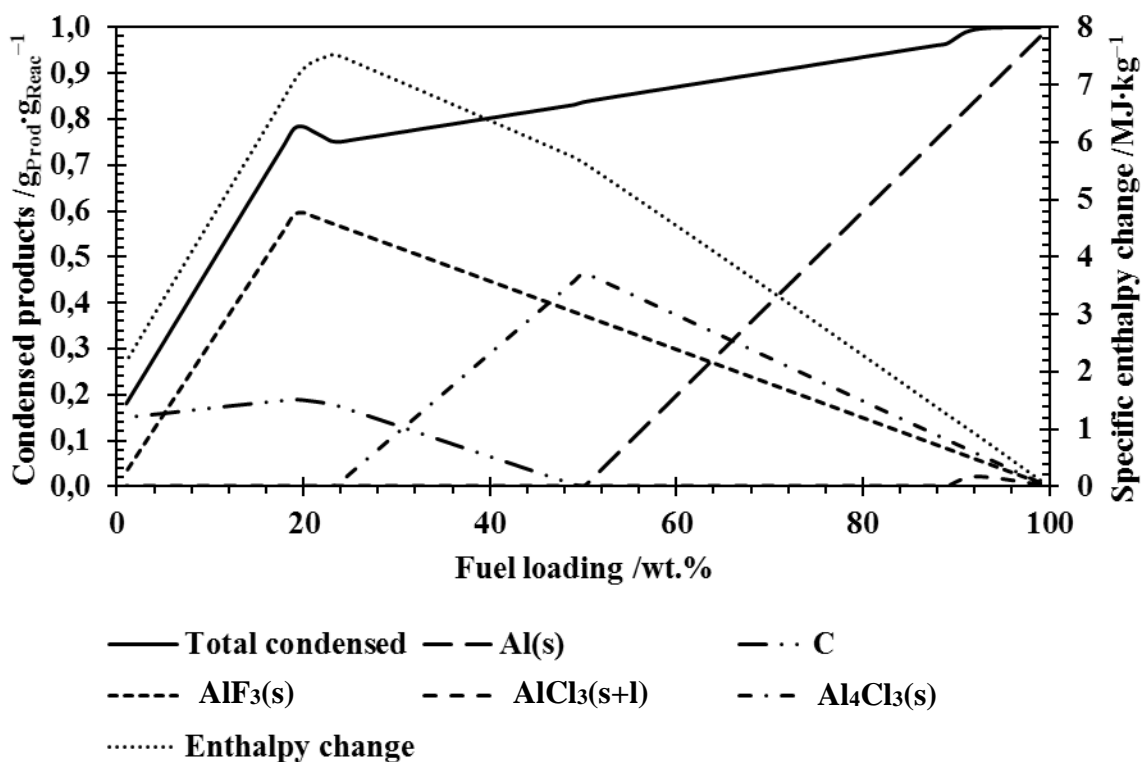


Figure 38: Condensed product spectrum for FK-800<sup>®</sup> compositions using aluminium as fuel

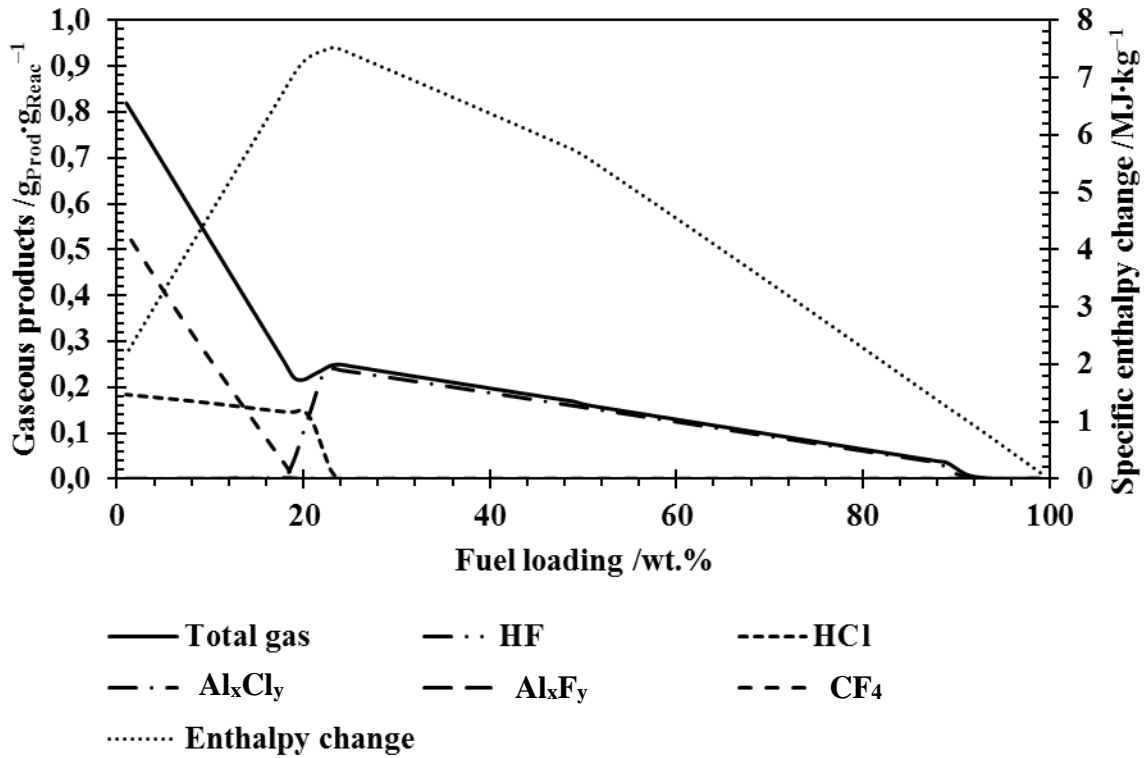


Figure 39: Gaseous product spectrum for FK-800<sup>®</sup> compositions using aluminium as fuel

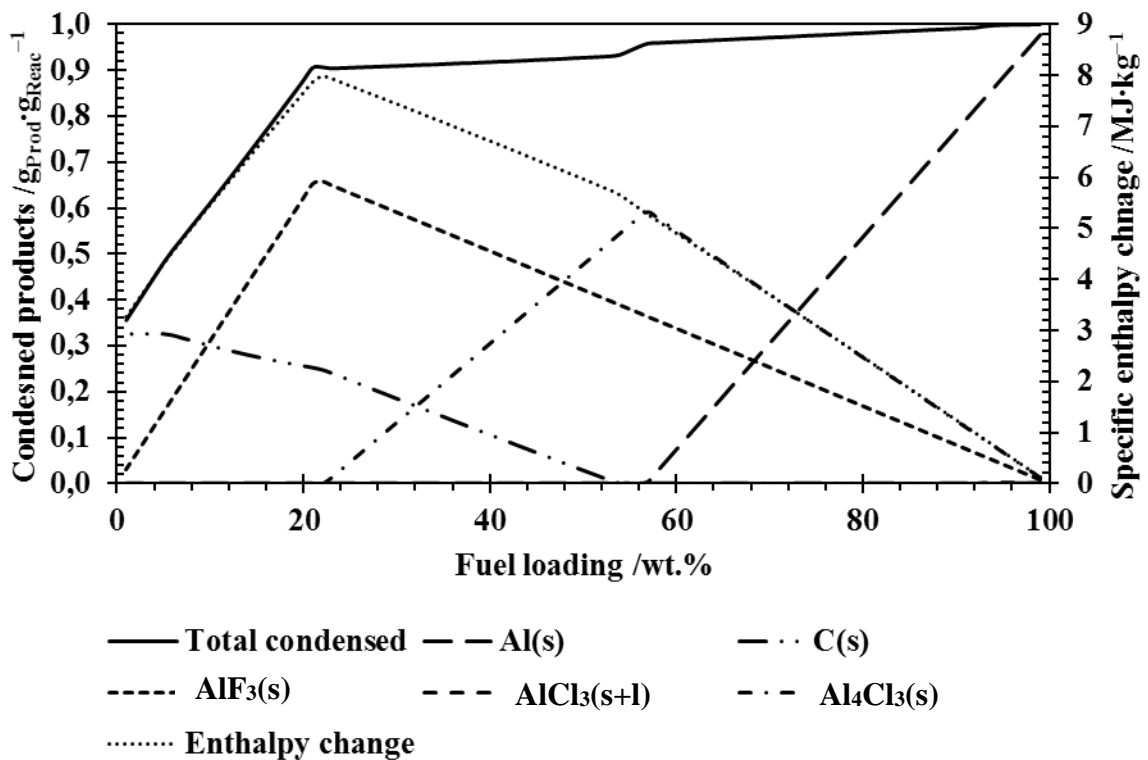


Figure 40: Condensed product spectrum for Dyneon 31508<sup>®</sup> compositions using aluminium as fuel

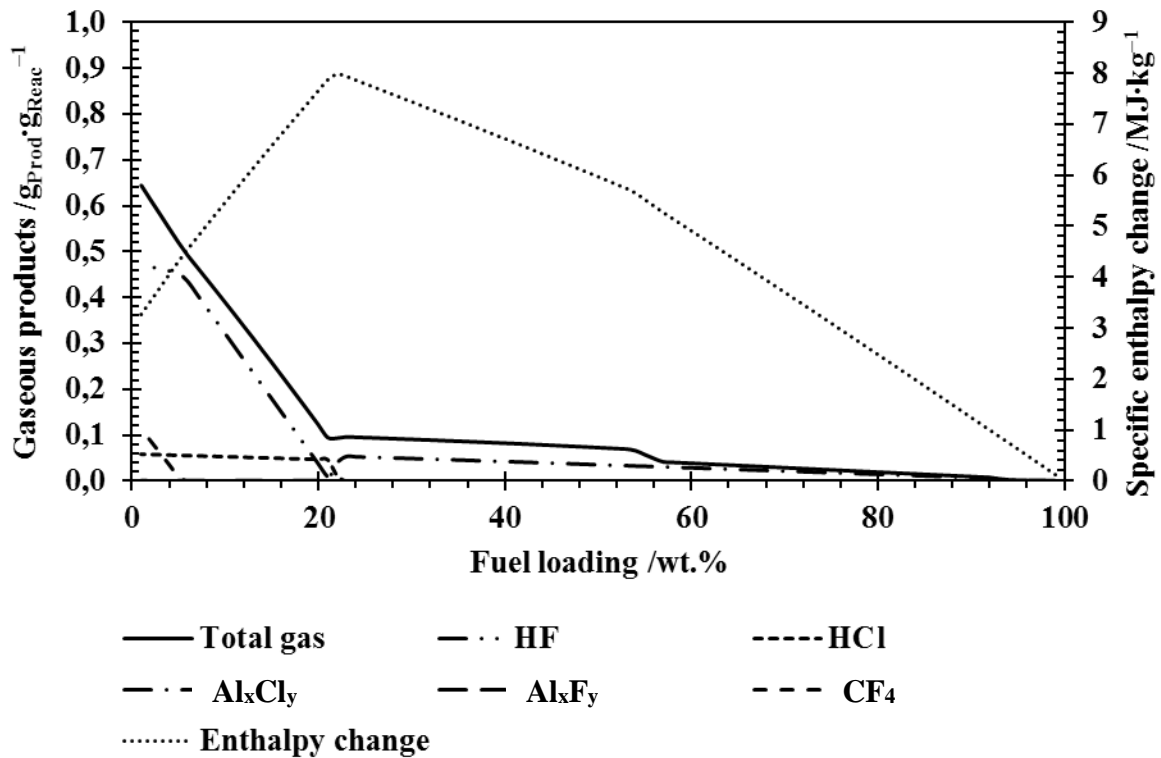


Figure 41: Gaseous product spectrum for Dyneon 31508<sup>®</sup> compositions using aluminium as fuel

It can be seen in Figure 38 and Figure 40 that the maximum energy output of the reactions is associated with the maximum production of solid aluminium fluoride (AlF<sub>3</sub>(s)). In both cases the formation of aluminium chloride (AlCl<sub>3</sub>(s) and AlCl<sub>3</sub>(l)) is negligible across all but the highest fuel loadings (>90 wt.% fuel).

The region immediately following the stoichiometric ratio is associated in both cases with a decrease in the production of aluminium fluoride and carbon and a marked increase in the production of aluminium carbide (Al<sub>4</sub>C<sub>3</sub>).

In both cases, a strong correlation is also shown when the aluminium is present in excess and starts appearing in the product spectrum (>50 wt.% for FK-800<sup>®</sup> and >56 wt.% for Dyneon 31508<sup>®</sup>). This is the point where the composition moves from simply being “fuel-rich” to having aluminium in excess.

As seen in Figure 39, the formation of HF when using FK-800<sup>®</sup> resin and aluminium is negligible for the full range of fuel loadings. However, when using Dyneon 31508<sup>®</sup> at low fuel loadings the formation of HF is much more substantial, but becomes negligible at fuel loadings in excess of the stoichiometric ratio.

For both polymers, the formation of HCl is expected to be a problem at lower fuel loadings, however, the formation of this acid also becomes negligible at fuel loadings in excess of the stoichiometric ratio.

Tetrafluoromethane (CF<sub>4</sub>) is a potent greenhouse gas with a global warming potential of ~6600 (Jubb et al., 2015) (CO<sub>2</sub> is rated at 1) and, with an atmospheric lifetime of approximately 50 000 years, it is the most persistent greenhouse gas (Forster et al., 2007). As such, the production of CF<sub>4</sub> should be limited as much as possible. Once again, it can be seen in Figure 39 and Figure 41 that the formation of CF<sub>4</sub> is only noticeable at low fuel loadings and becomes negligible at fuel loadings in excess of the stoichiometric ratio.

Table 23 shows a brief summary of the four regions shown in the figures above as well as the associated compounds that are indicative of the active region.

Table 23: Active regions of reaction of copolymers with aluminium and indications thereof

<b>Region</b>	<b>Indications</b>
<b>Fuel-lean</b>	<ul style="list-style-type: none"> <li>• HF, HCl and CF<sub>4</sub> gas production</li> <li>• Peak in energy output</li> </ul>
<b>Stoichiometric</b>	<ul style="list-style-type: none"> <li>• No HF or CF<sub>4</sub> produced</li> <li>• Minimal HCl produced</li> </ul>
<b>Fuel-rich</b>	<ul style="list-style-type: none"> <li>• No HF, HCl or CF<sub>4</sub> produced</li> <li>• Aluminium chloride gases produced</li> <li>• Decrease in solid aluminium fluoride production</li> <li>• Increase in aluminium carbide production</li> </ul>
<b>Excess fuel</b>	<ul style="list-style-type: none"> <li>• Decrease in aluminium carbide production</li> <li>• Unreacted aluminium appears in the product spectrum</li> </ul>

Based on the above observations, it was decided that both copolymers were worthy of further investigation due to the fact that many of the undesirable compounds thought to be produced are produced only in a fuel-lean mixture. Therefore a stoichiometric or fuel-rich mixture (without going into the excess fuel region) would be suitable for pyrotechnic applications.

## CHAPTER 9: COPOLYMER RESULTS AND DISCUSSION

### 9.1 Solution casting

Uniform pyrotechnic films were successfully cast using solvent methods as both copolymers were able to completely dissolve in the selected solvents. All films were approximately 200  $\mu\text{m}$  thick. These films were cut into smaller sections for further analysis.

It should be noted that, due to the low volatility of the NMP used to dissolve the Dyneon 31508<sup>®</sup> resin, these films needed to be heated in order to evaporate the solvent quickly enough to prevent the aluminium particles settling too much and creating a film with two distinct volumes of mixed composition and clean polymer, whereas the THF used for the FK-800<sup>®</sup> is volatile enough to evaporate at room temperature.

### 9.2 Energetics

#### 9.2.1 Differential thermal analysis

In order to assess the viability of the compositions for pyrotechnic use, the energetics of the compounds was tested. Differential thermal analysis (DTA) was used to assess the compositions' sensitivities to heat and to get an idea of the ignition temperature of the compositions in order to determine if they would be safe to process in an extruder. Due to the much more intense conditions found in an extruder as opposed to a 3D printer, it was assumed that if the compositions could be safely extruded then they would be safe for 3D printing applications as well. The DTA results for the FK-800<sup>®</sup>-based compositions are shown in Figure 42 and for the Dyneon 31508<sup>®</sup>-based compositions in Figure 43.



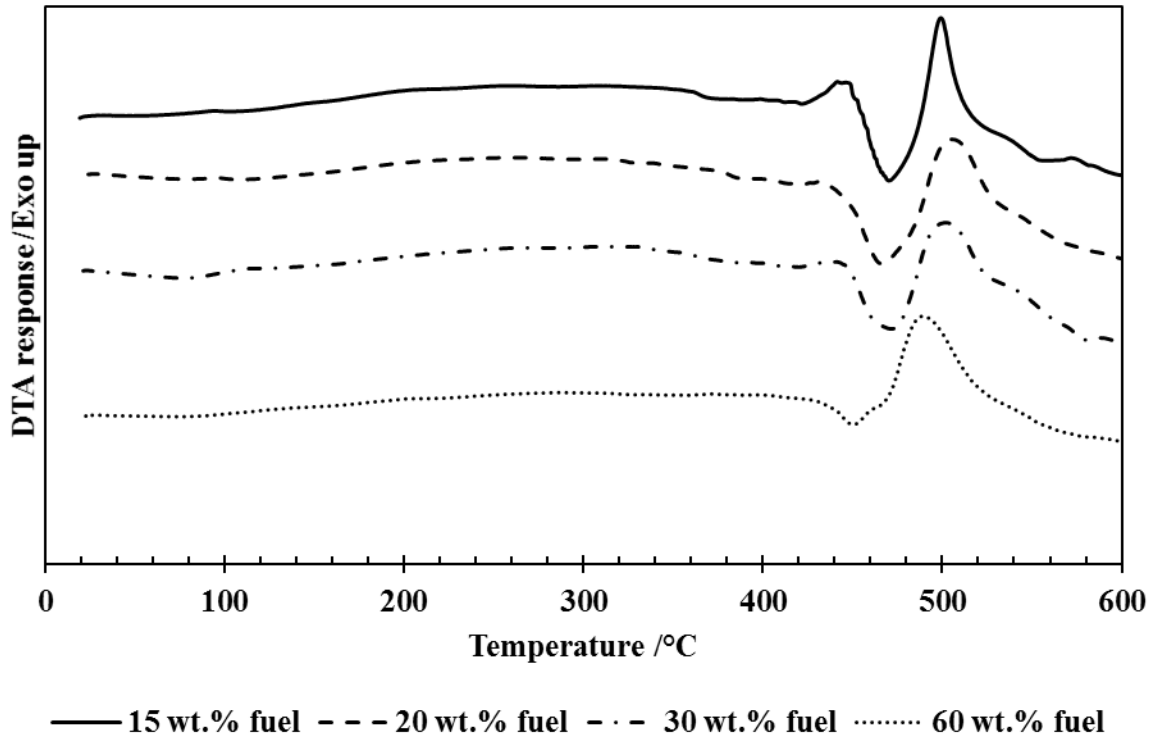


Figure 42: DTA response curves for FK-800<sup>®</sup> compositions at various fuel loadings

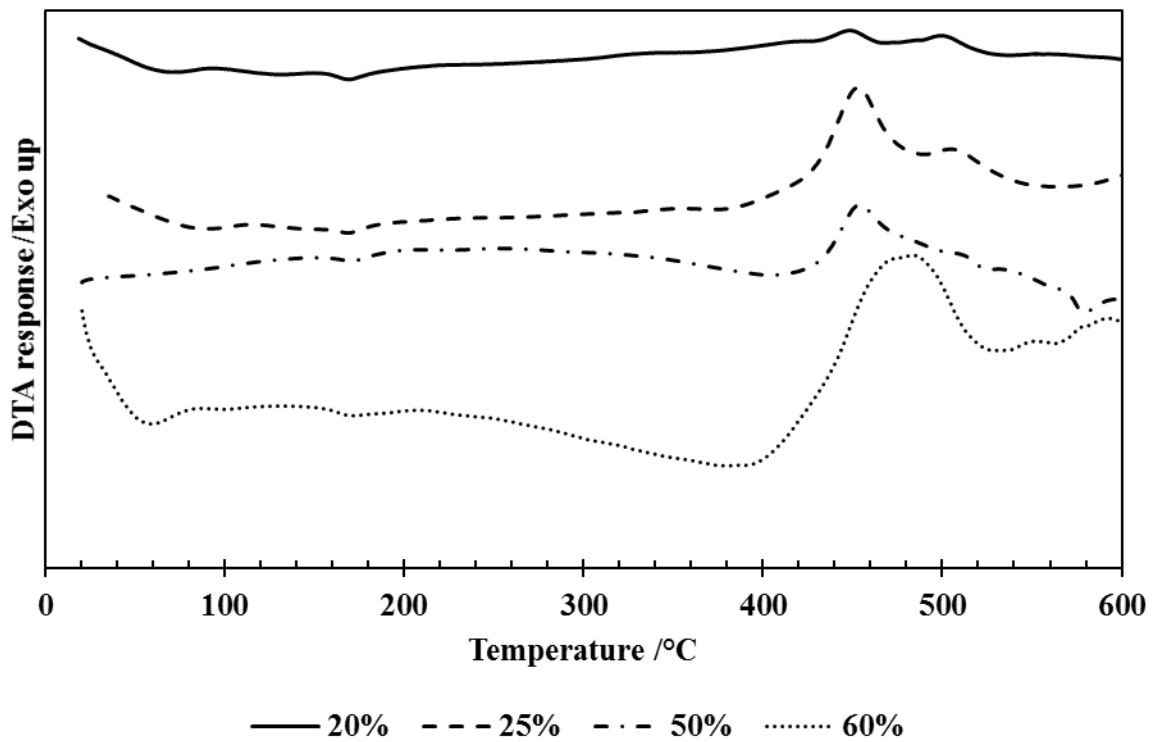


Figure 43: DTA response curves for Dyneon 31508<sup>®</sup> compositions at various fuel loadings

For all FK-800<sup>®</sup>-based compositions, a very clear endotherm occurs at approximately 450 °C for all the samples, followed immediately by a very strong exothermic peak. This implies that the ignition temperature for the FK-800<sup>®</sup>-based compositions is approximately 450 °C and is independent of the fuel loading.

From Figure 23, the degradation temperature for FK-800<sup>®</sup> resin is approximately 366 °C. It was expected that the composition would begin reacting as the polymer degraded and the fluorine, chlorine and hydrogen atoms were liberated from the polymer. The fact that an endothermic peak appears at 450 °C in Figure 42 shows that the composition is absorbing energy before burning occurs. Thus it is theorised that the aluminium had a heat-stabilising effect on the polymer due to the high thermal conductivity of the aluminium. This would mean that the heat was dissipated into the bulk of the polymer by the aluminium reducing the formation of hot spots.

A similar trend appears in Figure 43 for the Dyneon 31508<sup>®</sup>-based compositions. The degradation temperature from the TGA curve in Figure 27 is approximately 364 °C, yet the compositions all appear to ignite at approximately 420 °C from the DTA response in Figure 43.

An important consideration is the fact that the temperature in a polymer melt in an extruder is not the same as the temperature of the barrel wall, which is controlled. Due to the high viscosity of polymer melts, there is a significant amount of viscous heating that takes place in the extruder. Temperature profiles presented by Kelly et al. (2006) demonstrate this fact, with the temperature at the centre of the flow being up to 30 °C hotter than at the wall. This temperature differential is dependent on many factors such as screw and die geometry, as well as polymer rheology.

Based on these considerations, even if one considers a safety factor of 100 °C between the ignition and processing temperatures, it was decided that processing of both resins' compositions would be safe as the processing temperature of the compositions, 230 °C, is much lower than the ignition temperatures of 420 °C (for Dyneon 31508<sup>®</sup>) and 450 °C (for FK-800<sup>®</sup>).

## 9.2.2 Bomb calorimetry

### 9.2.2.1 FK-800<sup>®</sup>

In order to assess the energetic output of the compositions and decide whether or not they may be viable for use in pyrotechnic applications, as well as to determine the accuracy of the simulation results obtained in Chapter 8, enthalpy measurements were performed using bomb calorimetry. The results of the bomb calorimeter runs for the FK-800<sup>®</sup>-based compositions are shown in Figure 44, as well as the simulated energy output curve from Figure 36. The maximum experimental energy output was 7.0 MJ·kg<sup>-1</sup> and occurred at a fuel loading of 30 wt.%.

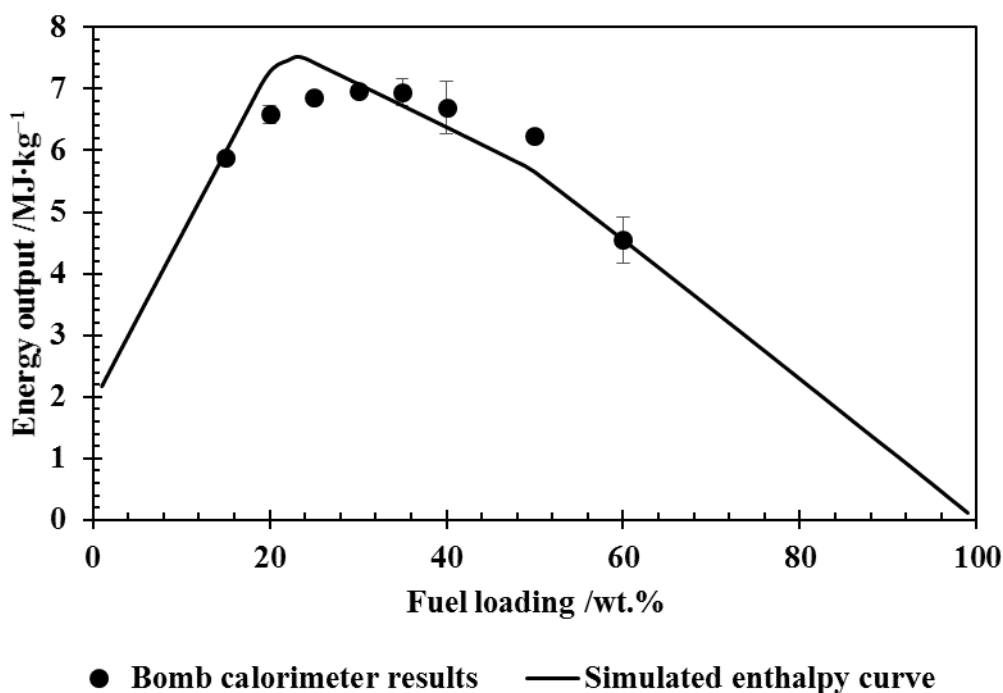


Figure 44: Bomb calorimeter and simulated energy outputs for FK-800<sup>®</sup>-based compositions

Another reason for the lower energy output may be due to the fact that the software does not recognise polymers or take into account the heats of polymerisation. As such, the system was modelled with the monomer gases. Realistically, the polymer requires energy to dissociate in order for the reaction to begin and thus the real energy output is slightly lower than that predicted by the software. However, this is a minimal difference when compared to the total heat release.

The bomb calorimeter trend also appears to be shifted slightly to the right of the predicted curve with the maximum energy output occurring at a fuel loading of 30 wt.% as opposed to the 25 wt.% predicted in the simulation. Once again this may be due to the fact that the software works in an ideal scenario whilst realistically slightly more fuel may be required to give the extent of reaction necessary to obtain the energy outputs predicted by the software.

All compositions were ignited successfully, however, during both runs with the 15 wt.% composition there was a misfire and the bomb needed to be re-prepped. When the bomb was opened in both cases, the composition showed signs of charring where the nichrome wire was in contact with it. This indicates that a composition of approximately 15 wt.% fuel is approaching the lower limit for successful burning of the composition. It is very insensitive to ignition and, with a lower fuel content, may not ignite at all. In both cases, the composition ignited successfully on the second attempt.

#### 9.2.2.2 Dyneon 31508<sup>®</sup>

The same bomb calorimeter runs were attempted with the Dyneon 31508<sup>®</sup>-based compositions, however, none were able to be ignited with one exception. All compositions (two samples of each composition) were put through two runs in the bomb calorimeter before being declared failures. When the bomb was opened in all cases the compositions showed signs of charring indicating that the nichrome wire had maintained contact with the composition throughout the packing process. In some cases, the polymer had melted onto the nichrome wire.

This shows an extreme insensitivity to ignition by heat, which is surprising when one considers that the ignition temperature of the Dyneon 31508<sup>®</sup>-based compositions is approximately 30 °C lower than that of the FK-800<sup>®</sup>-based compositions (See Section 9.2.1). This may indicate that the Dyneon 31508<sup>®</sup> has a higher heat capacity than the FK-800<sup>®</sup> and therefore requires more time in contact with the heat source in order to ignite.

#### 9.2.3 Residue analysis

When the bomb was opened after the burning of the compositions above 35 wt.% fuel, yellow particles were noticed amongst the ashes along with a strong foul-smelling odour. This was assumed to be the aluminium carbide crystals which are yellow in colour and decompose

on contact with water to release methane (Eagleson, 1993), which explains the foul smell in the bomb. The reaction products were collected after the runs and analysed.

XRD analysis results for the residues of compositions containing fuel loadings of 20 wt.%, 40 wt.% and 60 wt.% are shown in Figure 45. SEM images of the ashes collected from the bomb calorimeter are shown in Figure 46.

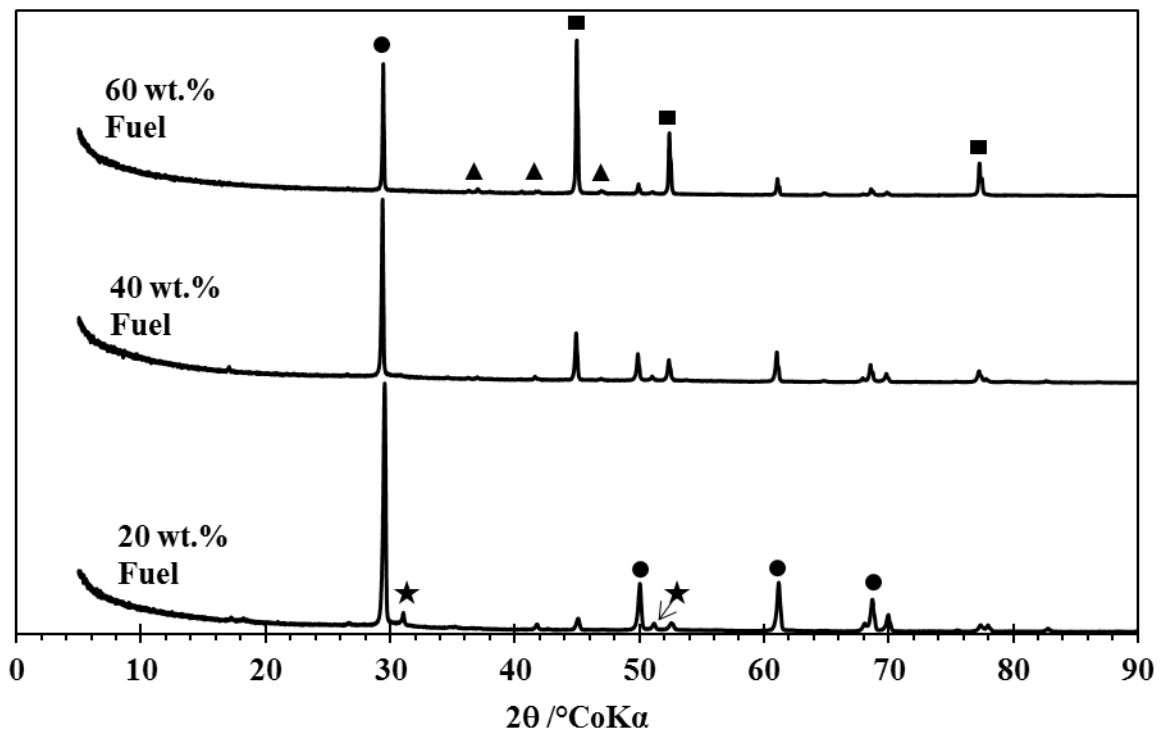


Figure 45: XRD analysis results for reaction products at various fuel loadings. Peaks are identified as follows: ● - Aluminium fluoride, ■ - Aluminium, ★ - Graphite, ▲ - Aluminium carbide

From the XRD results, one can clearly see a decrease in the four primary aluminium fluoride peaks with an increase in fuel loading. This indicates a decrease in the formation of aluminium fluoride as the fuel loading increases. Also decreasing, is the amount of graphite formed. The graphite peaks are quite clear at the lowest fuel loading, albeit quite small, but are barely noticeable at 40 wt.% fuel and have disappeared altogether by 60 wt.% fuel.

In contrast, the amount of unreacted aluminium is clearly increasing with an increasing fuel loading, as indicated by the drastic increase in the three aluminium peaks that have been identified. The results also show that there is aluminium carbide forming at higher fuel



loadings. The relatively low strength of the peaks is attributed to the fact that some of the aluminium carbide may have decomposed upon incidental contact with water while the bomb calorimeter vessel was being opened.

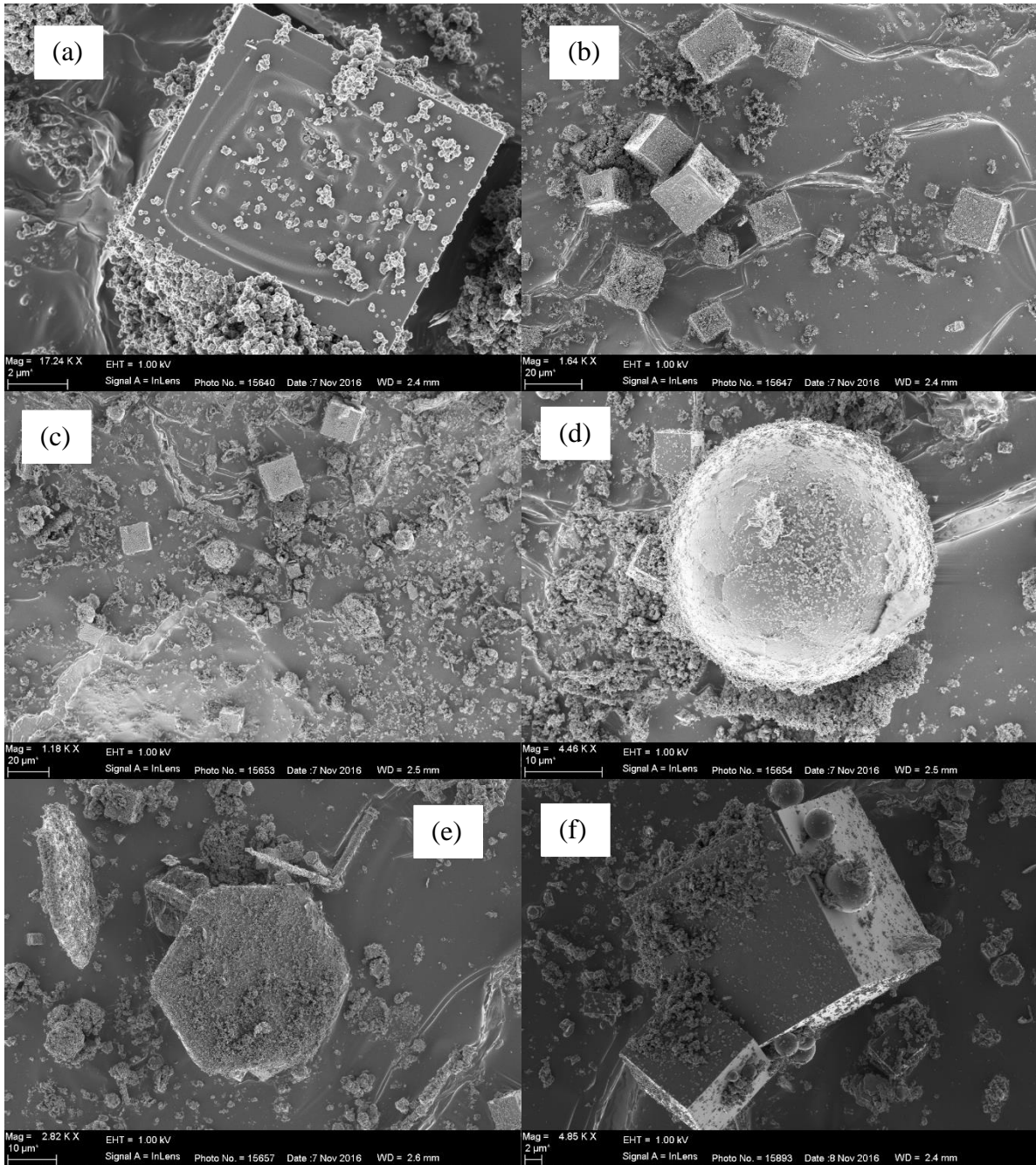


Figure 46: SEM micrographs of ashes collected from bomb calorimeter for FK-800<sup>®</sup>-based compositions. (a-b) 20 wt.% fuel. (c-d) 40 wt.% fuel. (e-f) 60 wt.% fuel.

For the lower fuel loading in Figure 46 (a) and (b), the formation of many cubic crystals can be seen. These crystals range in size from less than 2  $\mu\text{m}$  across to almost 20  $\mu\text{m}$ . Based on the product spectrum predicted in Chapter 8, it was assumed that these crystals were aluminium fluoride. The much smaller particles surrounding the large cubes were assumed to be the carbon fraction which was predicted in Chapter 8.

At the slightly higher fuel loading of 40 wt.% seen in Figure 46 (c) and (d), the same cubic structures appear as the lower fuel loading as well as the carbon particles. However, this fuel loading is marked by the appearance of spherical crystals as well as the cubes described above. These spheres range from less than 2  $\mu\text{m}$  to 10  $\mu\text{m}$  in diameter. It was thought that these spheres may be unreacted aluminium particles.

The highest fuel loading tested, 60 wt.%, can be seen in Figure 46 e and f. Once again the cubic and spherical crystals were found, but there appeared to be a greater number of spheres than were seen at the lower fuel loading. Again these spheres were assumed to be unreacted aluminium particles and these were expected based on the predicted product spectrum as this test was performed in the excess fuel region specified in Chapter 8.

At this fuel loading one can also notice the appearance of thin hexagonal platelets. These crystals were assumed to be aluminium carbide crystals which are naturally hexagonal (Eagleson, 1993). It would also explain why these were only seen at the higher fuel loadings as the formation of the aluminium carbide tends to increase with an increasing fuel loading (up to a point) according to the predicted product spectrum in Chapter 8, and confirmed by the XRD analysis seen in Figure 45. Thus, the higher concentration of aluminium carbide formed from the higher fuel loading was more easily noticed than at lower fuel loadings where the hexagonal crystals were unable to be located.

In order to confirm the compositions of the various crystals observed in Figure 46, SEM-EDS was performed on the same samples. The images taken are shown in Figure 47, and the results obtained shown in Table 24.

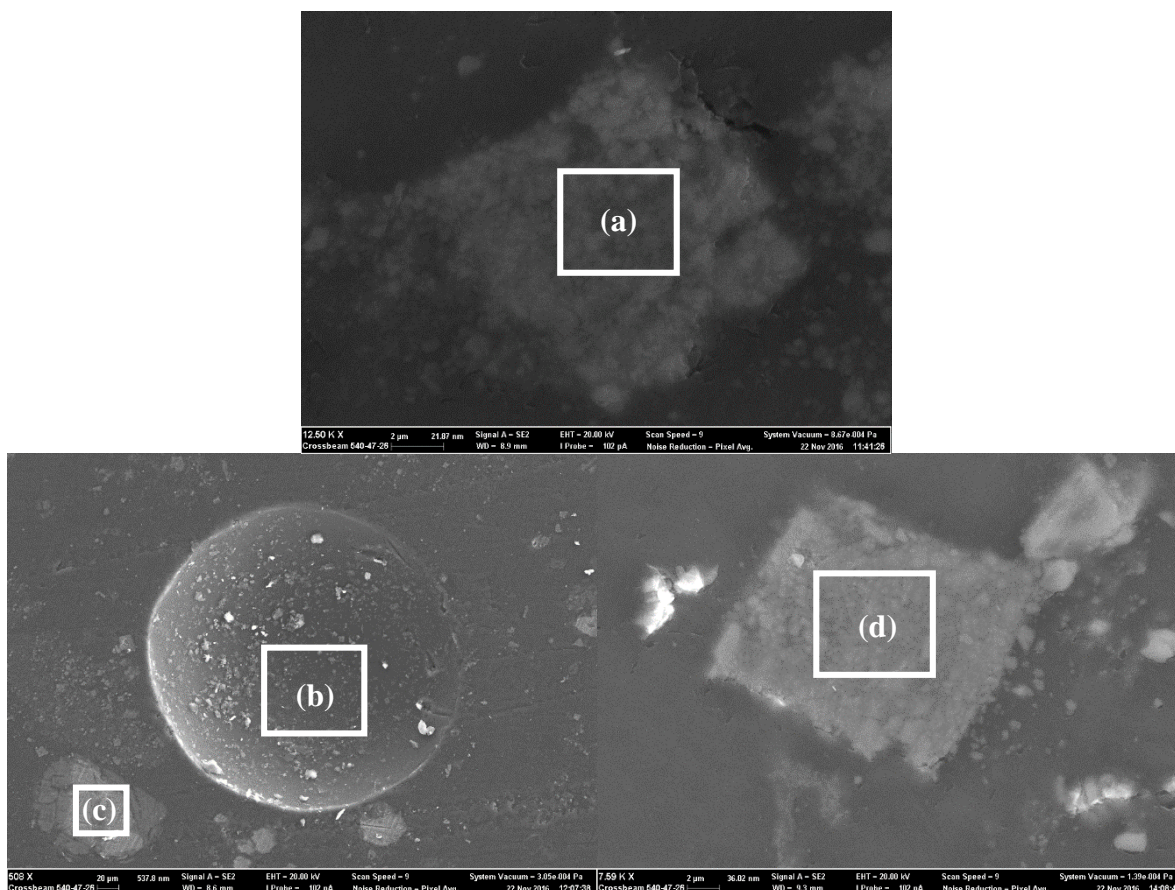


Figure 47: SEM-EDS images showing (a) carbon covered aluminium fluoride (b) spherical aluminium fluoride (c) unreacted aluminium (d) cubic aluminium fluoride particles

Table 24: SEM-EDS results for reaction products

Element	Composition /wt. %			
	(a)	(b)	(c)	(d)
Carbon	25.11	68.39	-	-
Oxygen	1.80	25.50	18.95	-
Fluorine	52.04	1.61	-	63.29
Aluminium	20.58	0.59	79.97	36.71
Chlorine	0.46	0.14	1.08	-

As mentioned in Section 3.5, the composition of the resin from the EDS analysis is approximately 78 wt.% carbon, 13 wt.% oxygen and 9 wt.% chlorine. This is important to take into account as the EDS software will register those elements if the particle is not wholly



exposed. With this in mind, the values obtained for region (a) in Figure 47 were corrected for the resin values and it was determined that an excess amount of carbon was identified. This excess carbon can be attributed to the small particles first seen in Figure 46 (a).

A surprising discovery was the fact that the spherical particles seen in Figure 46 (d) were not aluminium particles as initially thought, but were rather aluminium fluoride crystals that had taken a spherical rather than a cubic shape as seen in Figure 47 (b). This does not discount the fact that there was unreacted aluminium in the residue as proven by the appearance of a piece of unreacted aluminium in Figure 47 (c).

The image in Figure 47 (d) shows a well-exposed aluminium fluoride crystal showing close to the theoretical mass ratio of 32.1 wt.% aluminium to 67.9 wt.% fluorine. This further reinforces the assumption that the cubic structures observed in Figure 46 were aluminium fluoride crystals.

These results prove that aluminium fluoride is the primary product in these reactions with very few other products, with the exception of aluminium carbide at higher fuel loadings, appearing as predicted by the simulations in Chapter 8.

### 9.3 Extrusion trials

Extrusion trials were performed with both unfilled polymers. FK-800<sup>®</sup> was also compounded with magnesium hydroxide.

Both polymers were successfully extruded in their unfilled state. Both were extruded using the single screw extruder described in Section 3.4. In both cases another thermoplastic was extruded before and after the fluoropolymer. This was done to ensure steady-state extrusion conditions were achieved before the more expensive fluoropolymer was processed.

Magnesium hydroxide was added as a model compound to simulate the conditions that would be experienced while processing the final composition.

The magnesium hydroxide was successfully incorporated into the FK-800<sup>®</sup>. Compounding with the Dyneon 31508<sup>®</sup> proved more difficult, and the magnesium hydroxide was unable to be incorporated into the polymer. In order to counter this, LFC-1<sup>®</sup> was added to the Dyneon 31508<sup>®</sup> at 10 wt.%. This would lower the viscosity of the Dyneon 31508<sup>®</sup> during processing

and make it easier to compound the solid particles. The LFC-1<sup>®</sup> wax was successfully compounded with the Dyneon 31508<sup>®</sup> resin using the HAAKE microcompounder.

Further testing would include upscaling to a twin-screw compounder in order to mix this wax-polymer composite with the magnesium hydroxide. The single screw extruder described in Section 3.4 is needed to control the diameter of the filament required for 3D printing. 3D printers are fairly sensitive to changes in the diameter of the filament being used, so this is a very important step. Once fully compounded materials are able to be manufactured into controlled filaments using the single screw extruder, their printability would be tested using an FDM-type 3D printer.

## CHAPTER 10: CONCLUSIONS AND RECOMMENDATIONS

An investigation into the use of fluorinated polymers as oxidisers in extrudable pyrotechnic compositions, as a precursor to future 3D-printable compositions, was conducted. Fluoropolymers are currently used in the energetic materials, but the specific polymers are either not melt processible, or used simply as a binder rather than as the primary oxidising agent. By using an oxidising polymer as the primary oxidiser, oxidising particles will not have to be incorporated into the composition. This will lower the overall solids loading and make the composition easier to process.

### 10.1 PCTFE

Poly(chloro-trifluoroethylene) was investigated as an alternative to PTFE as certain grades may be melt processible. Thermodynamic simulation using EKVI thermodynamic software showed that this polymer, with aluminium as the fuel, may be energetically viable for use as a pyrotechnic composition. The stoichiometric ratio was determined to be at a fuel loading of 24 wt.% with a maximum energy output of  $7.0 \text{ MJ}\cdot\text{kg}^{-1}$ .

Solution casting was attempted but, due to the extremely high chemical resistance of PCTFE, was only marginally successful. The low molecular weight fraction was able to dissolve in the selected solvent whilst the high molecular weight fraction swelled substantially. A mixed composition was achieved, but not in a uniform film as attempted. Open burn tests showed that these compositions do ignite and sustain burning quite easily.

Extrusion trials were performed on the unfilled polymer and were a failure. Multiple runs were attempted and the polymer was unable to be extruded. The polymer was only able to be pulled from the extruder in one run. The polymer was heavily degraded upon exiting the extruder but it had retained some melt strength which allowed it to be pulled from the extruder. Upon cooling the level of degradation became more apparent, with the extruded strand becoming incredibly brittle and having a very porous final structure.

Based on the extrusion trials, it was concluded that PCTFE homopolymer was unsuitable for use in extrudable pyrotechnic compositions and further investigation was not warranted.

## 10.2 Copolymers

### 10.2.1 Energetics

Based on the thermodynamic simulations and open burn tests of the PCTFE it was decided to attempt to use a copolymer of CTFE with better extrusion properties. Two industrially available copolymers were identified, FK-800<sup>®</sup> and Dyneon 31508<sup>®</sup>, both available from 3M<sup>™</sup>. These resins are both copolymers of CTFE with vinylidene fluoride (VDF) but contain different ratios of these two monomers.

Thermodynamic simulations showed that both these polymers may be energetically suitable for use in pyrotechnic compositions. The stoichiometric ratio and maximum energy output for the FK-800<sup>®</sup> resin when using aluminium as the fuel were found to be at a fuel loading of 23 wt.% and a maximum energy output of 7.5 MJ·kg<sup>-1</sup>. Similarly the stoichiometric ratio and maximum energy outputs for the Dyneon 31508<sup>®</sup> resin were found to be at a fuel loading of 22 wt.% and 7.9 MJ·kg<sup>-1</sup>, respectively.

It was thought that the introduction of hydrogen into the system from the VDF content of the polymers may prove to be an issue as it would react with the liberated halogens from the polymers to form poisonous and corrosive hydrofluoric and hydrochloric acids. However, the simulation showed that by using a slightly fuel-rich composition, the formation of these undesirable compounds would be avoided.

Solution casting of both copolymers was much more successful than with the PCTFE homopolymer as both copolymers were able to dissolve entirely in the selected solvents. Uniform pyrotechnic films were cast using this technique and all films were approximately 200 μm thick.

Energetic analyses were performed on the pyrotechnic films. DTA analyses showed that the ignition temperature for all of the FK-800<sup>®</sup>-based compositions was approximately 450 °C and for all of the Dyneon 31508<sup>®</sup>-based compositions was approximately 420 °C. It was known that the processing temperature for both the FK-800<sup>®</sup> and Dyneon 31508<sup>®</sup> resins is approximately 230 °C. Therefore it was decided that the ignition and processing temperatures were far enough apart to allow for the safe processing of these compositions.

Bomb calorimetry results of the FK-800<sup>®</sup>-based compositions showed a close resemblance to the simulated curve. The maximum experimentally determined energy output of the FK-

800<sup>®</sup>-based was  $7.0 \text{ MJ}\cdot\text{kg}^{-1}$  and occurred at a fuel loading of 30 wt.%. The difference between the experimental and simulated results was attributed to the non-ideal conditions of real life as opposed to the ideal conditions and 100 % reaction completion from the simulated environment. The composition containing 15 wt.% fuel failed to ignite on the first attempt for both runs and, as such, it was concluded that 15 wt.% aluminium in FK-800<sup>®</sup> is the lower limit at which reliable ignition and burning may be expected.

The same bomb calorimetry runs were attempted with the Dyneon 31508<sup>®</sup>-based compositions. All runs were attempted twice for two batches of each sample and none were able to be ignited with the exception of one batch. All samples displayed signs of charring where the nichrome wire had maintained contact with the sample, and in some cases the wire had become fused to the film. Thus it was determined that the Dyneon 31508<sup>®</sup>-based compositions are extremely insensitive to ignition by instantaneous heat. This was attributed to the lower heat conductivity of Dyneon 31508<sup>®</sup> when compared to FK-800<sup>®</sup>.

This result, combined with the DTA results, shows that the ignition temperature of the polymer-based compositions is dependent on the rate of heating of the composition as well as the amount of heat put into the system.

### 10.2.2 Product analysis

Reaction products were collected from the bomb calorimeter and subjected to various analyses. XRD and SEM analysis showed that, for the full range of compositions, aluminium fluoride was the primary reaction product, together with graphite at lower fuel loadings. Aluminium carbide was also identified from the compositions with higher fuel loadings.

SEM-EDS analysis showed that the aluminium fluoride formed both cubic and spherical crystals. The presence of unreacted aluminium was also confirmed, but was not the spherical crystals as was thought at first.

### 10.2.3 Extrusion trials

Both copolymers were successfully extruded in their unfilled state. Magnesium hydroxide was successfully compounded with the FK-800<sup>®</sup> but was not able to be compounded with the

Dyneon 31508<sup>®</sup>. LFC-1<sup>®</sup> liquid fluoroelastomer was compounded with the Dyneon 31508<sup>®</sup> in order to reduce its viscosity and improve its processibility. This compounding was successful.

### **10.3 Recommendations**

Further investigation is required into how the addition of solid particles affects the mechanical properties of the polymers. Tensile tests and rheological studies should be performed on the compounded samples.

It is also recommended that the effect of adding the LFC-1<sup>®</sup> fluoroelastomer has on the energetic properties of the composition be investigated further.

Printability tests need to be performed using the magnesium hydroxide-filled model compositions as well as with aluminium-filled active composition.

## REFERENCES

- 3m<sup>(TM)</sup> (2005). 3M Material Safety Data Sheet LFC-1 3M<sup>(TM)</sup> Liquid Fluoroelastomer.
- Agrawal, J. P. (1998). Recent trends in high-energy materials. *Progress in Energy and Combustion Science*, 24, 1-30.
- Akhavan, J. (2011). *The Chemistry of Explosives*, Royal Society of Chemistry, Swindon.
- Aldushin, A. P. & Khaikin, B. I. (1974). Combustion of mixtures forming condensed reaction products. *Combustion, Explosion and Shock Waves*, 10, 273-280.
- Aldushin, A. P., Vol'pert, V. A. & Filipenko, V. P. (1987). Effect of reagent melting on combustion stability for gasless systems. *Combustion, Explosion and Shock Waves*, 23, 408-420.
- Badgujar, D. M., Talawar, M. B., Asthana, S. N. & Mahulikar, P. P. (2008). Advances in science and technology of modern energetic materials: An overview. *Journal of Hazardous Materials*, 151, 289-305.
- Barton, A. F. (1990). *Handbook of Polymer-Liquid Interaction Parameters and Solubility Parameters*, CRC press, Boca Raton.
- Beck, M., Brown, M. & Cawthorne, D. (1984). Pyrotechnic delay composition. *ChemSA*, June 1984, 398-401.
- Berger, B. (2005). Parameters influencing the pyrotechnic reaction. *Propellants, Explosives, Pyrotechnics*, 30, 27-35.
- Blair, L. H., Colakel, A., Vrcelj, R. M., Sinclair, I. & Coles, S. J. (2015). Metal-organic fireworks: MOFs as integrated structural scaffolds for pyrotechnic materials. *Chemical Communications*, 51, 12185-12188.
- Boschet, F. & Ameduri, B. (2013). (Co) polymers of chlorotrifluoroethylene: synthesis, properties, and applications. *Chem. rev.*, 114, 927-980.
- Cadwallader, E. A. (1964). *Flare composition*. Patent number: US3152935 A, assigned to United States of America.
- Chan, S. K., Hsu, N. Y. W. & Oliver, R. (1998). *Process for the preparation of gas-generating compositions*. Patent number: US5756930 A, assigned to Imperial Chemical Industries Plc, Ici Canada Inc.

- Christo, F. C. (1999). *Thermochemistry and kinetics models for magnesium/Teflon/Viton pyrotechnic compositions*. ADA377423. Defence Technical Information Center, Melbourne.
- Clark, B. (2016). *Combustion characterization of nano-particle reactive materials suspended in polymer binders for use in additive manufacturing*. PhD Thesis in Mechanical Engineering, Texas Tech University, Lubbock.
- Colclough, M. E., Desai, H., Millar, R. W., Paul, N. C., Stewart, M. J. & Golding, P. (1994). Energetic polymers as binders in composite propellants and explosives. *Polymers for Advanced Technologies*, 5, 554-560.
- Conkling, J. A. (1985). *Chemistry of Pyrotechnics: Basic Principles and Theory*, Marcel Dekker, Inc., New York, NY.
- Danali, S., Palaiah, R. & Raha, K. (2010). Developments in pyrotechnics (review paper). *Def. Sci. J.*, 60, 152.
- De Yong, L. & Smit, K. (1991). *A theoretical study of the combustion of magnesium/teflon/viton pyrotechnic compositions*. ADA243244. Defence Technical Information Center, Ascot Vale.
- Ding, Y.-H. & Inagaki, S. (2003). Green high energy density material, N<sub>2</sub>H<sub>2</sub>O. *Chemistry Letters*, 32, 304-305.
- Dombe, G., Mehilal, D., Bhongale, C., Singh, P. P. & Bhattacharya, B. (2015). Application of twin screw extrusion for continuous processing of energetic materials. *Central European Journal of Energetic Materials*, 12, 507-522.
- Dugam, A. G., Muttalib, A., Gandhi, H. J., Phawade, P. A., John, A. & Khare, R. R. (1999). Effect of fuel content and particle size distribution of oxidiser on ignition of metal-based pyrotechnic compositions. *Defence Science Journal*, 49, 263-268.
- Dupont<sup>tm</sup>. (2010). *Viton<sup>(R)</sup> data sheets for A, B, and F families* [Online]. Available: [https://www.chemours.com/Viton/en\\_US/data\\_sheets/index.html](https://www.chemours.com/Viton/en_US/data_sheets/index.html) [Accessed 27 October 2015].
- Dyke, P., Coleman, P. & James, R. (1997). Dioxins in ambient air, bonfire night 1994. *Chemosphere*, 34, 1191-1201.
- Eagleson, M. (1993). *Concise Encyclopedia Chemistry*, De Gruyter, New York.



- Ebespacher, M., Klapotke, T. M. & Miro Sabate, C. (2009). Nitrogen-rich alkali metal 5,5[prime or minute]-hydrazinebistetrazolate salts: environmentally friendly compounds in pyrotechnic mixtures. *New Journal of Chemistry*, 33, 517-527.
- Ebnesajjad, S. (2003). *Fluoroplastics, Volume 2: Melt Processible Fluoropolymers-The Definitive User's Guide and Data Book*, William Andrew, Norwich.
- Ellern, H. (1968). *Military and Civilian Pyrotechnics*, Chemical Publishing Company, New York.
- Fleischer, O., Wichmann, H. & Lorenz, W. (1999). Release of polychlorinated dibenzo-p-dioxins and dibenzofurans by setting off fireworks. *Chemosphere*, 39, 925-932.
- Forster, P., Ramaswamy, V., Artaxo, P., Bernsten, T., Betts, R., Fahey, D. W., Haywood, J., Lean, J., Lowe, D. C., Myhre, G., Nganga, J., Prinn, R., Raga, G., Schulz, M. & Van Dorland, R. (2007). Changes in Atmospheric Constituents and in Radiative Forcing. In: Solomon, S., Qin, D., Manning, M., Chen, Z., Marquis, M., Averyt, K. B., M. Tignor & Miller, H. L. (eds.) *Climate Change 2007: The Physical Science Basis. Contribution of Working Group I to the Fourth Assessment Report of the Intergovernmental Panel on Climate Change*. Cambridge University Press, Cambridge, United Kingdom and New York, NY, USA.
- Francis, A. (2007). *Modeling the melt dispersion mechanism for nanoparticle combustion*. MSc Thesis in Mechanical Engineering, Texas Tech University, Lubbock.
- Fronabarger, J. W., Williams, M. D., Sanborn, W. B., Bragg, J. G., Parrish, D. A. & Bichay, M. (2011). DBX-1 – A Lead Free Replacement for Lead Azide. *Propellants, Explos., Pyrotech.*, 36, 541-550.
- Glavier, L., Taton, G., Ducéré, J.-M., Bajot, V., Pinon, S., Calais, T., Estève, A., Djafari Rouhani, M. & Rossi, C. (2015). Nanoenergetics as pressure generator for nontoxic impact primers: Comparison of Al/Bi<sub>2</sub>O<sub>3</sub>, Al/CuO, Al/MoO<sub>3</sub> nanothermites and Al/PTFE. *Combustion and Flame*, 162, 1813-1820.
- Huang, C., Yang, H., Li, Y. & Cheng, Y. (2015). Characterization of Aluminum/Poly(Vinylidene Fluoride) by Thermogravimetric Analysis, Differential Scanning Calorimetry, and Mass Spectrometry. *Anal. Lett.*, 48, 2011-2021.
- Huynh, M. H. V., Hiskey, M. A., Meyer, T. J. & Wetzler, M. (2006). Green primaries: Environmentally friendly energetic complexes. *Proceedings of the National Academy of Sciences*, 103, 5409-5412.

- Ilyushin, M. A., Tselinsky, I. V. & Shugalei, I. V. (2012). Environmentally friendly energetic materials for initiation devices. *Central European Journal of Energetic Materials*, 9, 293-327.
- Jakubko, J. (1999). Combustion of the silicon-red lead system. Temperature of burning, kinetic analysis and mathematical model. *Combustion Science and Technology*, 146, 37-55.
- Jubb, A. M., Mcgillen, M. R., Portmann, R. W., Daniel, J. S. & Burkholder, J. B. (2015). An atmospheric photochemical source of the persistent greenhouse gas CF<sub>4</sub>. *Geophysical Research Letters*, 42, 9505-9511.
- Kappagantula, K. S. (2014). *Combustion experiments of aluminum-fluoropolymer composites. A study of additive influences*. PhD Thesis in Mechanical Engineering, Texas Tech University, Lubbock.
- Kelly, A. L., Brown, E. C. & Coates, P. D. (2006). The effect of screw geometry on melt temperature profile in single screw extrusion. *Polym. Eng. Sci.*, 46, 1706-1714.
- Khaikin, B. I. & Merzhanov, A. G. (1966). Theory of thermal propagation of a chemical reaction front. *Combustion, Explosion and Shock Waves*, 2, 22-27.
- Klapötke, T. M. (2015). *Chemistry of High-Energy Materials*, Walter de Gruyter GmbH & Co KG, Berlin.
- Koch, E.-C. (2007). *Metal-Fluorocarbon Based Energetic Materials*, John Wiley & Sons, Weinheim.
- Kosanke, B. J. & Kosanke, K. L. (2014). Control of Pyrotechnic Burn Rate. *Pyrotechnic Chemistry*. Journal of Pyrotechnics, Inc., Whitewater, CO 81527.
- Kosanke, K. L., Kosanke, B. J. & Jennings-White, C. (2004). *Lecture Notes for Pyrotechnic Chemistry*, Journal of Pyrotechnics, Inc., Whitewater, CO 81527.
- Kosanke, K. L., Kosanke, B. J., Sturman, B. T. & Winokur, R. M. (2012). *Encyclopedic Dictionary of Pyrotechnics (and Related Subjects)*, Journal of Pyrotechnics, Inc., Whitewater, CO 81527.
- Kowalczyk, J. E., Malik, M., Kalyon, D. M., Gevgilili, H., Fair, D. F., Mezger, M. & Fair, M. (2007). Safety in design and manufacturing of extruders used for the continuous processing of energetic formulations. *Journal of Energetic Materials*, 25, 247-271.

- Liu, X., Gao, W., Sun, P., Su, Z., Chen, S., Wei, Q., Xie, G. & Gao, S. (2015). Environmentally friendly high-energy MOFs: crystal structures, thermostability, insensitivity and remarkable detonation performances. *Green Chemistry*, 17, 831-836.
- Margolis, S. B. (1993). A model for condensed combustion synthesis of nonstoichiometric homogeneous solids. *Combustion and Flame*, 93, 1-18.
- Martinez, H., Zheng, Z. & Dolbier Jr, W. R. (2012). Energetic materials containing fluorine. Design, synthesis and testing of furazan-containing energetic materials bearing a pentafluorosulfanyl group. *J. Fluorine Chem.*, 143, 112-122.
- Mccollum, J., Pantoya, M. L. & Iacono, S. T. (2015). Activating aluminum reactivity with fluoropolymer coatings for improved energetic composite combustion. *ACS Appl. Mater. Interfaces*, 7, 18742-18749.
- Morgan, C. G. & Rimmington, C. (2012). *Manufacture of pyrotechnic time delay compositions*. Patent number: US8118956 B2, assigned to AEL Mining Services Ltd.
- Nanda, K. K., Maisels, A., Kruis, F. E., Fissan, H. & Stappert, S. (2003). Higher surface energy of free nanoparticles. *Physical Review Letters*, 91, 106102.
- Nielson, D. B., Truitt, R. M. & Rasmussen, N. (2005). *Low temperature, extrudable, high density reactive materials*. Patent number: US6962634 B2, assigned to Alliant Techsystems Inc.
- Noläng, B. (2007). *Thermochemical calculations using the Ekvi System*. 4<sup>th</sup> Workshop on Pyrotechnic Combustion Mechanisms, Steamboat Springs.
- Osborne, D. T. (2006). *The effects of fuel particle size on the reaction of Al/Teflon mixtures*. MSc Thesis in Mechanical Engineering, Texas Tech University, Lubbock.
- Pantoya, M. L. & Granier, J. J. (2005). Combustion behavior of highly energetic thermites: Nano versus micron composites. *Propellants, Explosives, Pyrotechnics*, 30, 53-62.
- Poret, J. C., Shaw, A. P., Groven, L. J., Chen, G. & Oyler, K. D. (2012). *Environmentally Benign Pyrotechnic Delays*. ADA565275. Defence Technical Information Centre,
- Potgieter, G., Focke, W., Fabbro, O., Labuschagné, G. & Kelly, C. (2016). Fluoroelastomer pyrotechnic time delay compositions. *Journal of Thermal Analysis & Calorimetry*, 126, 1363-1370.

- Puszynski, J. A., Bulian, C. J. & Swiatkiewicz, J. J. (2007). Processing and ignition characteristics of aluminum-bismuth trioxide nanothermite system. *Journal of Propulsion and Power*, 23, 698-706.
- Rider, K. B., Little, B. K., Emery, S. B. & Lindsay, C. M. (2013). Thermal analysis of magnesium/perfluoropolyether pyrolants. *Propellants, Explosives, Pyrotechnics*, 38, 433-440.
- Rose, J. E., Michay, M. & Puszynski, J. (2011). *Non-toxic pyrotechnic delay compositions*. Patent number: US7883593 B1, assigned to The United States of America, US 12/315,488.
- Sabatini, J. J., Koch, E.-C., Poret, J. C., Moretti, J. D. & Harbol, S. M. (2015). Chlorine-free red-burning pyrotechnics. *Angew. Chem., Int. Ed.*, 54, 10968-10970.
- Sego, A. L. (2015). *Additive Manufacturing Initiatives at Sandia National Laboratories*. Sandia National Laboratories (SNL-NM), Albuquerque, NM (United States),
- Shaw, A. P., Poret, J. C., Grau, H. A. & Gilbert, R. A. (2015). Demonstration of the B<sub>4</sub>C/NaIO<sub>4</sub>/PTFE delay in the U.S. Army hand-held signal. *ACS Sustainable Chemistry & Engineering*, 3, 1558-1563.
- Sigma-Aldrich. (2015). *Poly(chlorotrifluoroethylene)* [Online]. Available: <http://www.sigmaaldrich.com/catalog/product/aldrich/454710?lang=en&region=ZA> [Accessed 23 October 2015].
- Singh, A., Soni, P. K., Shekharam, T. & Srivastava, A. (2013). A study on thermal behavior of a poly(VDF-CTFE) copolymers binder for high energy materials. *Journal of Applied Polymer Science*, 127, 1751-1757.
- Steinhauser, G. & Klapötke, T. M. (2008). “Green” pyrotechnics: A chemists' challenge. *Angew. Chem., Int. Ed.*, 47, 3330-3347.
- Steinhauser, G. & Klapötke, T. M. (2010). Using the chemistry of fireworks to engage students in learning basic chemical principles: A lesson in eco-friendly pyrotechnics. *J. Chem. Educ.*, 87, 150-156.
- Steinhauser, G., Sterba, J. H., Foster, M., Grass, F. & Bichler, M. (2008). Heavy metals from pyrotechnics in New Years Eve snow. *Atmospheric Environment*, 42, 8616-8622.
- Talawar, M. B., Sivabalan, R., Mukundan, T., Muthurajan, H., Sikder, A. K., Gandhe, B. R. & Rao, A. S. (2009). Environmentally compatible next generation green energetic materials (GEMs). *Journal of Hazardous Materials*, 161, 589-607.

- Teipel, U. (1999). Production of particles of explosives. *Propellants, Explosives, Pyrotechnics*, 24, 134-139.
- Tsang, D. K. L. (2005). The initiation process inside a detonation delay element. *Int. J. of Appl. Math. and Mech.*, 2, 12-39.
- Usamc (1968). *Theory and Application*, U.S. Army Materiel Command, Washington, D.C. 20315.
- Watson, K. (2007). *Fast reaction of nano-aluminum: A study on fluorination versus oxidation*. MSc Thesis in Mechanical Engineering, Texas Tech University, Lubbock.
- Whitmore, S. A. (2015). *Additive manufacturing as an enabling technology for "green" hybrid spacecraft propulsion*. IEEE, 1-6.
- Whitmore, S. A., Peterson, Z. W. & Eilers, S. D. (2013). Comparing hydroxyl terminated polybutadiene and acrylonitrile butadiene styrene as hybrid rocket fuels. *Journal of Propulsion and Power*, 29, 582-592.
- Wilson, M. A. & Hancox, R. J. (2014). Pyrotechnic Delays and Thermal Sources. *Pyrotechnic Chemistry*. Journal of Pyrotechnics, Inc., Whitewater, CO 81527.
- Yang, D. (2014). *Molecular Weight Determination of KelF--800 (FK--800) Using Multi--Detection Gel Permeation Chromatography (GPC)*. Los Alamos National Laboratory, Los Alamos.